Please cite the Published Version

Paul, Suvendu and Watkinson, Michael (2025) High fidelity optical detection and imaging of the bisulfate ion: Photophysical events, binding mechanisms and applications. Coordination Chemistry Reviews, 541. 216818 ISSN 0010-8545

DOI: https://doi.org/10.1016/j.ccr.2025.216818

Publisher: Elsevier

Version: Accepted Version

High Fidelity Optical Detection and Imaging of the Bisulfate Ion: Photophysical Events, Binding Mechanisms and Applications

Suvendu Paul[1] and Michael Watkinson[2]

[1]Department of Chemistry, University of Kalyani, Kalyani, Nadia, West Bengal-741235, India.
E-mail: paul.suvendu2016@gmail.com

[2]Department of Natural Sciences, Manchester Metropolitan University, Chester Street, Manchester, UK.
Email: m.watkinson@mmu.ac.uk

Abstract:

Bisulfate is a common ingredient in several widely-used commodities such as toothpaste, shampoo and detergent. Whilst it has a number of positive effects on the efficacy of these materials, due to its widespread societal use, it also has an increasingly negative impact on the environment. This has resulted in growing interest in the development of operationally simple systems to detect and quantify this widely used anion. Given the large number of reports that have appeared on its detection to date, this systematic review article focuses on recent developments in such operationally simple colorimetric and fluorescent detection systems for the detection and estimation of bisulfate ions. The small molecule fluorophores utilised for its detection have been categorized according to the signaling moiety and are then discussed accordingly. The key features of recognition phenomena in such systems, including spectroscopic change, naked-eye detection, limit of detection, application in real-world samples and biocompatibility and toxicity in live cell imaging are discussed. The bisulfate ion has multiple features that have been used in its detection, including its high electron deficiency, low pKa, proton donor site, hydrogen bond donor and acceptor sites resulting in an array of chemosensors displaying a wide array of photophysical changes. Hence, a special focus is on the structure-photophysical property relationships and binding mechanisms in these systems. Finally, significant achievements and ongoing challenges in the field are highlighted.

Keywords: Bisulfate Sensing; Colorimetric and Fluorescent Recognition, Ion Sensing; Optical Detection; Naked-eye Detection; Small-Molecule Fluorophore;

1. Introduction

Supramolecular chemistry continues to be an important and popular discipline within contemporary science[1] and has provided solutions to many problems in medicine,[2-3] drug delivery,[4] bioimaging,[5] cancer treatment,[6-7] stimuli-responsive materials,[8-10] halogen bonding and transmembrane ion transport,[11-13] chemical separations and molecular encapsulation technologies,[14-15] 3D printing,[16] organic photovoltaics application,[17] artificial photosynthesis,[18] electrospinning,[19] catalysis,[20] molecular machines,[21-22] ion and molecular sensors[23-28] and it is without question that it has had an immense impact on modern science. Though the term supramolecular chemistry was first established in the 1970s by Jean-Marie Lehn,[29-30] it significance increased significantly following the joint award of the Nobel Prize in chemistry in 1987 to Donald J. Cram, Jean-Marie Lehn and Charles J. Pedersen "for their development and use of molecules with structure-specific interactions of high selectivity";[31] today, termed host-guest interactions. Since then the field of supramolecular luminescent chemosensing of a wide range of analytes has been, and continues to be, an area of considerable activity. Despite there being a wide array of other analytical techniques available, such small molecule systems have proved to be extremely popular. As the field of supramolecular luminescent detection systems for a wide variety of anions continues to evolve at pace, a number of comprehensive reports covering different aspects such as the supramolecular recognition of anions and their applications,[32-34] the role of anion-π interactions in supramolecular anion recognition,[35] the diversity in anion recognition strategies and the role of non-covalent interactions[36] have been published with the most common theme in all of the reports being the use of fluorescent techniques for analyte detection.

It is widely accepted that the first fluorescent chemosensor was reported by F. Goppelsroder in 1867 and since then, almost two centuries later, it remains an area of significant activity.[37-38] Such longevity has undoubtedly established the importance of fluorescent detection in multiple fields including biology, environmental science and medicine.[39-40] Furthermore, small molecule colorimetric and fluorescent sensors display a number of attendant advantages over a range of other recognition techniques, such as ion-electrode methods, ion chromatography, inductively coupled plasma-atomic emission spectroscopy (ICP-AES), inductively coupled plasma-mass spectrometry (ICP-MS) including the small amount of chemical required, almost immediate response, high selectivity and sensitivity, color changes that are distinguishable by the naked-eye, the capability of *in vitro* as well as *in vivo* detection and due to their low cost and operational simplicity they are particularly to analyte detection in real-world environments.[41-44] Several excellent review articles have been published on the fluorescent detection of anions[45-46] and a number have focussed on specific analytes, including fluoride (F^-),[47-53] iodide (I^-),[54] hypochlorite (OCl^-),[55] cyanide (CN^-),[56-57] phosphate (PO_4^{3-}),[58-59] dihydrogen phosphate ($H_2PO_4^-$),[60] pyrophosphate ($P_2O_7^{4-}$),[61-62] sulfate (SO_4^{2-})[63] and nitrate (NO_3^-),[64] however, to date no comprehensive review article on the fluorescent recognition of the HSO_4^- ion has appeared. Qian *et al.* published a review article in 2017 on the optical detection of the HSO_4^- ion.[65] Very recently, Paul *et al.* published a review article on the fluorescent detection of the HSO_4^- ion that covers the very specific area of hydrogen bonding-driven optical detection of the HSO_4^- ion.[66] To our knowledge, there is no full-length review article on the small-molecule-based fluorescent detection of the HSO_4^- ion. This article therefore attempts to provide a comprehensive report on the small molecule-based fluorescent detection of HSO_4^- ion and is divided into several sections based on the binding and/or fluorophore moieties.

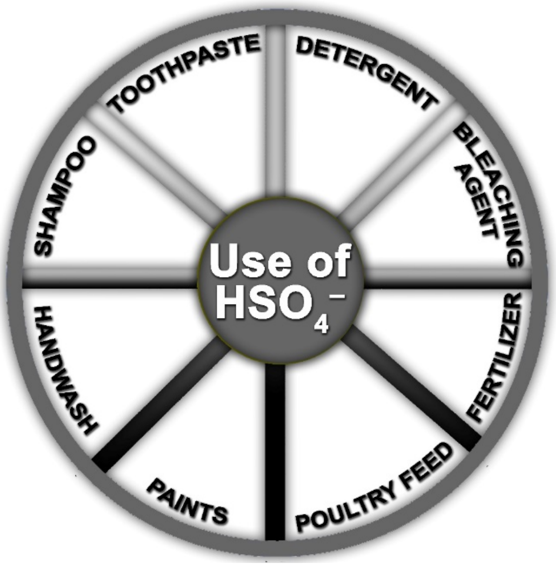

Figure 1: Graphical presentation of the major uses of HSO_4^- salts in contemporary life.

2. Scope and challenges

2.1 Impact of HSO_4^- ion on the environment and health

Of the very many important anions, the bisulfate ion demands extra attention due to its specific and significant role in the environment, agriculture, and biology.[65] The HSO_4^- ion is one of the vital macronutrients in cells and one of the most abundant anions in human plasma.[67] The HSO_4^- ion plays

a crucial role in several events, including biosynthesis and detoxification of various endogenous and exogenous species.[68] On the other hand, HSO_4^- ion is an important constituent in agricultural fertilizers and a significant constituent of nuclear fuel waste.[69] Naturally, the HSO_4^- ion is an unavoidable contaminant of water and soil and pollutes the environment via the production of toxic sulfate ions by dissociation under conditions of high pH.[70-71] The HSO_4^- ion also affects irritation of the eyes and skin and in extreme cases it can cause respiratory paralysis.[70-71] In addition, some common metal salts of bisulfate (e.g. $NaHSO_4$) play important catalytic roles in numerous chemical reactions like catalytic condensation and dehydration reactions and are also widely used as poultry feed and in bleaching agents, paints, cleaning products, shampoos and detergents (**Figure 1**).[72]
Spears *et al.* established that the inclusion of sodium bisulfate in the diet of cats maintains the acidity of their urine above 6.6 but in the longer term, it proved harmful to their health as struvite crystals formed. A few hours after meal their kidneys secreted alkaline ions to neutralise the struvite at the expense of gastric acid released for digestion. Sodium bisulfate can be used as an acidifier to maintain the pH of urine and the effect is almost identical for both sodium bisulfate and phosphoric acid.[73] The above discussion highlights the concern about the dual-directional role of HSO_4^- ion and for the healthy survival of human beings, selective and sensitive detection of HSO_4^- ion in real-life and real samples is highly desirable.

2.2 Different binding motifs and mechanisms of HSO_4^- ion sensing

Fluorescent chemosensors have played an important role in the selective recognition of the HSO_4^- ion, including at low concentration levels. However, for real-life recognition of any analyte, it is crucial to detect the anion in a 100 % aqueous medium[74] and this is a critical challenge for its detection due to its very high Gibbs free energy of hydration ($\Delta G_h = -1080$ kJ mol^{-1}).[75] Another major challenge for the fluorescent sensing of HSO_4^- ion is the inability of many systems to distinguish it from the isostructural, tetrahedral $H_2PO_4^-$ ion.[67] Despite these challenges, a substantial number of fluorescent chemosensors for the recognition of the HSO_4^- ion have been developed by a number of scientific groups during the last couple of decades, including our own.[65-66] In these ongoing developments various types of chemosensors containing different binding and/or signaling moieties including amide, amine, thiourea, urea, guanidine, phenolic hydroxyl groups, pyrrole, indole, coumarin, pyrene, rhodamine, BODIPY, benzimidazole, benzothiazole, pyridine, phthalimide, Schiff bases, quinazoline and metal complexes of some of these moieties.[65-66] In this review article, the chemosensors have been categorized according to the active binding and/or signaling moiety, and the basic principles underlying the selective binding behavior of a particular moiety-based chemosensor towards the HSO_4^- ion are discussed.

It is critical to focus on the unique structural aspects of the HSO_4^- ion when designing selective chemosensors. The anion contains an acidic hydrogen atom which can act as a proton source as well as a hydrogen bond donor. On the other hand, the oxygen atoms of the anion have the potential to act as hydrogen bond acceptors. Therefore, a combination of hydrogen bonding and proton transfer could play a crucial role in the fluorescent detection of the HSO_4^- ion. Besides, since the anion is also charged and contains both electron donor as well as acceptor centers, it can also cause considerable deviations in the intramolecular or intermolecular charge/electron transfer characteristics of the probe molecule (**Figure 2**). This opens up the possibility of utilizing an array of different recognition modalities for its detection such as hydrogen bonding, proton transfer either in the ground state or in an excited state either intramolecularly or intermolecularly, electron transfer, chelation-induced enhanced fluorescence (CHEF), charge transfer, coordination with a metal ion, dissociation of a metal complex, through-bond electron transfer (TBET), inner filter effect (IFE) and hydrolysis of Schiff bases.

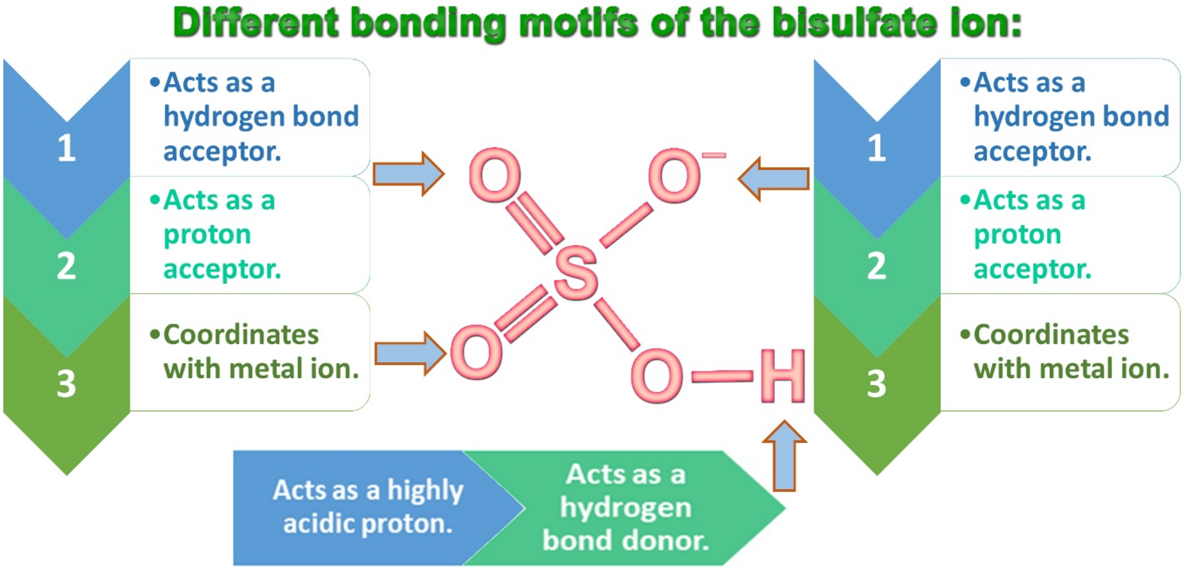

Figure 2: Different binding motifs of the HSO_4^- ion.

2.3 The role of DFT calculations in exploring the mechanisms of HSO_4^- ion sensing

Density functional theory (DFT) is a quantum mechanical method that has been widely used in theoretical electronic structure calculations of molecules and many-body materials.[76] Among the four major theoretical methods, *ab initio*, semiempirical, molecular mechanics, and DFT, the last one is the most promising, reliable, and well-established method to study the interaction of small molecule-based fluorescent probes with the bisulfate ion. This is because the DFT method generates precise results utilizing relatively little computational resources and nominal time.[77] The use of DFT in the determination of binding mechanisms gained pace following the award of the Nobel Prize in Chemistry to Walter Kohn and John A. Pople in 1998 for the development of DFT and computational methods in quantum chemistry.[78] There are now several popular software packages available that have been employed for theoretical calculations using the DFT method and among those, the GAUSSIAN,[79] TURBOMOLE,[80] GAMESS[81-82] and ORCA[83] are amongst the most popular. Detailed discussion on their theoretical background is beyond the scope of this review article as it is well documented in detail elsewhere in the literature. [84-85]

In the case of the colorimetric and fluorescent detection of the HSO_4^- ion, DFT studies are very commonly employed and serve two main purposes. The first is the characterization of the fluorophore molecules when there is no single crystal X-ray structure of the chemical probe molecule. Here, the calculation of simulated IR, ^{1}H NMR spectra, and UV-Vis transitions and comparison with the respective experimentally obtained spectra is a very useful technique to provide additional support to the structure of the chemical probe. The second, and major focus in this area, is the determination of the binding mechanism between the chemical probe and the HSO_4^- ion and the resultant spectroscopic changes that occur and some common features of DFT calculations that have been used in the detection of the HSO_4^- ion are summarized.

In most cases, the HSO_4^- ion is involved in hydrogen bonding (either as an HB donor or acceptor) with the chemosensor, resulting in dissociation of the chemical probe, hydrolytic cleavage, proton transfer in different electronic states, chelation-induced photophysical change, aggregation or disaggregation, intramolecular charge transfer (ICT) or blocking of ICT, photoinduced electron transfer (PET) or inhibition of PET, through bond energy transfer (TBET), host-guest complexation and coordination with a metal ion. In most cases, geometry optimization, binding energy calculation, changes in HOMO-LUMO states and their relative energies upon binding, Natural Bond Orbital (NBO) and Mullikan charges, molecular electrostatic potential (MEP) images, Natural Population Analysis (NPA), simulated UV-Vis transitions and potential energy scan studies are widely used techniques to explore the binding mechanism.[86-87] Which of these techniques is used depends on the nature of the binding sites of the chemosensor and probable molecular level non-covalent interactions with the HSO_4^- ion and are summarized in **Figure 3**.

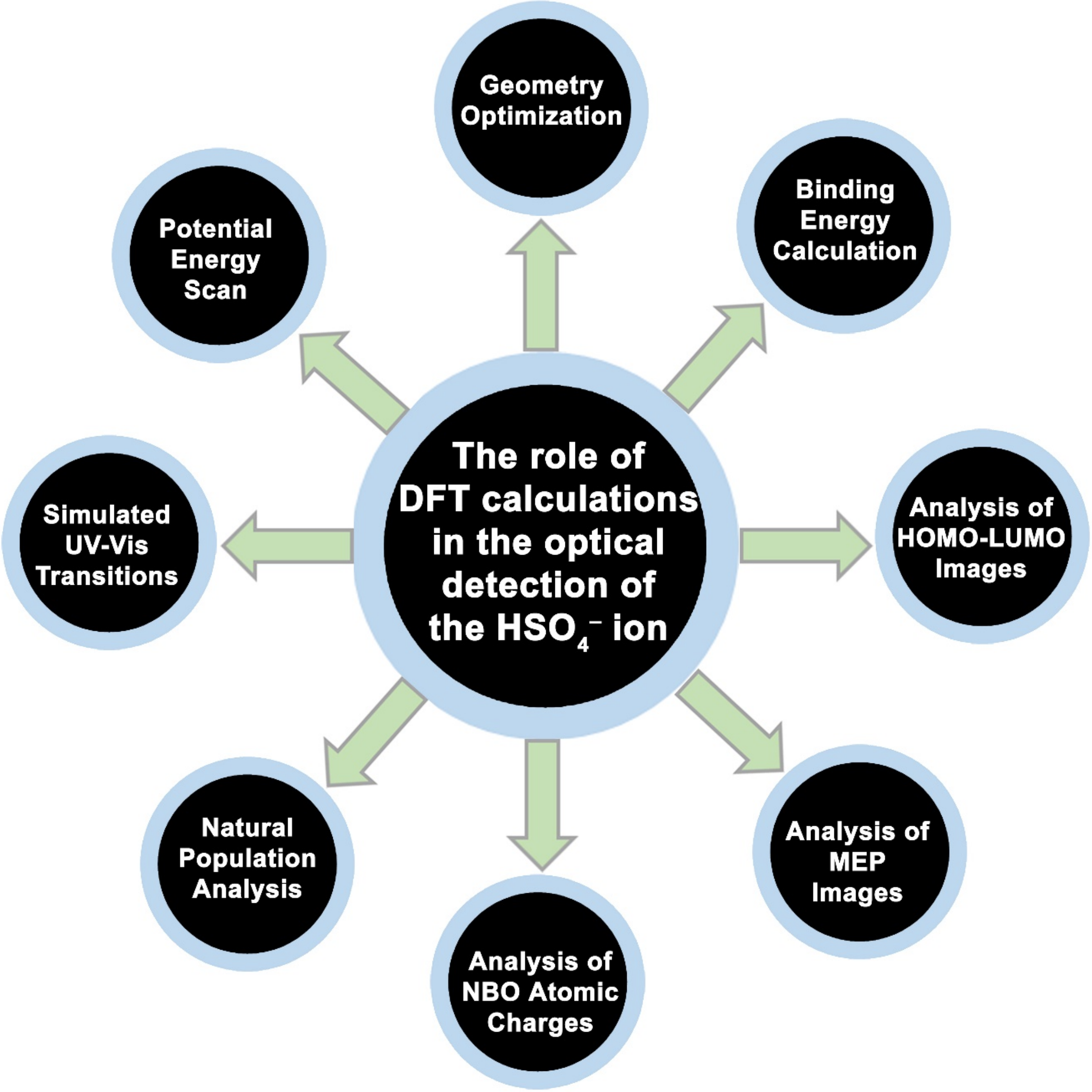

Figure 3: Different types of DFT calculations used in the exploration of the binding mechanism between chemosensors and the HSO_4^- ion.

3. Selective bisulfate detection summarised by class of fluorophores.

3.1. Benzimidazole moiety-based detection.

The benzimidazole moiety is a very popular fluorophore moiety (**Figure 4**) and it has widely been used in the synthesis of functional chemosensors in the detection of a wide variety of analytes.[88] In addition, benzimidazole-pyridine derivatives have a long history of the formation of metal complexes,[89] whilst polycyclic benzimidazole derivatives have also been widely used in optical lasers, optoelectronics, organic luminophores, medicinal chemistry, and drug discovery.[90]

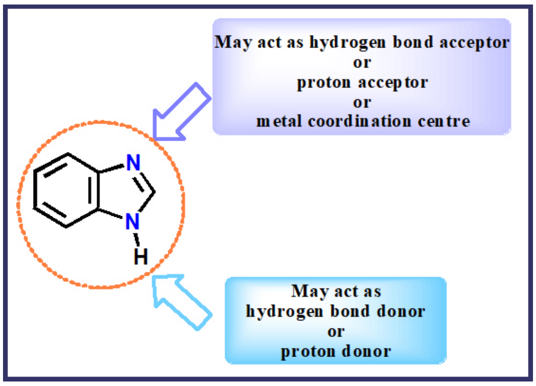

Figure 4: The core structure and different possible binding motifs of the benzimidazole moiety.

Fluorescent recognition of anions by organic fluorophores is very common, but the use of integrated organic-inorganic moieties in chemosensors is very rare, however, in 2011, Alfonso *et al.* reported such a system (**1**, **Scheme 1**) that was able to recognize Hg^{2+} and HSO_4^- ions independently by redox and fluorescent titration.[91] The ferrocene-benzobisimidazole derivative exhibited a sharp increase of emission intensity at 405 nm with a red shift observed in the presence of the HSO_4^- ion. **1** was also highly selective and sensitive (LOD= 1.57 µM) towards the HSO_4^- ion over other potential competitor anions tested, including $H_2PO_4^-$. The HSO_4^- ion protonated the probe and the deprotonated ion was then involved in hydrogen bonding in a chelate fashion, forming a 1:1 complex and displaying the CHEF phenomenon. Such dual-mode detection (redox and fluorescent) of the HSO_4^- ion by an organic-inorganic integrated fluorophore inducing the proton transfer followed by hydrogen bonding was a truly innovative illustration of fundamental chemistry but its wider application in sensing was somewhat limited by its use in ethanol.

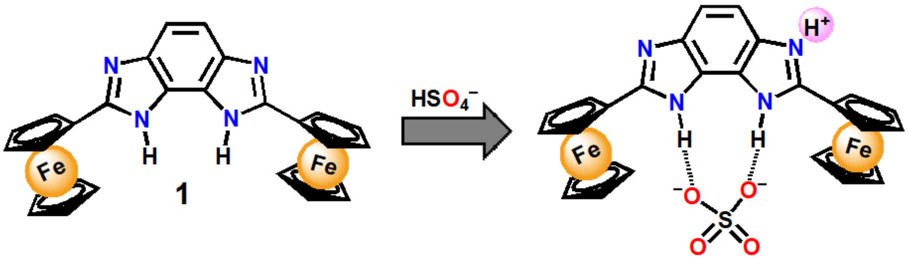

Scheme 1: The proposed binding mechanism of **1** with HSO_4^- ion.

In the next year, three analogous benzimidazole derivatives (**2-4**, **Scheme 2**) were developed and their multiple ion recognition was explored.[92] The probes recognized Cr^{3+} and the probe-Cr^{3+} complex recognized F^- and HSO_4^- ions in different ways. In the presence of the HSO_4^- ion, the emission band of the **2**-Cr^{3+} complex at 420 nm sharply reduced and the 475 nm band was enhanced in a HEPES buffered medium. The HSO_4^- ion was involved in coordination with the metal complex and as a result, altered the internal charge transfer behavior, and the HSO_4^- ion could be detected up to 1.58 µM concentrations. However, the fluoride ion caused displacement of the cation and consequent fluorescent "turn on" response at 420 nm. Nonetheless, the detection of multiple ions via distinguishable fluorescent responses of the same fluorophore was an intriguing and useful aspect of the work.

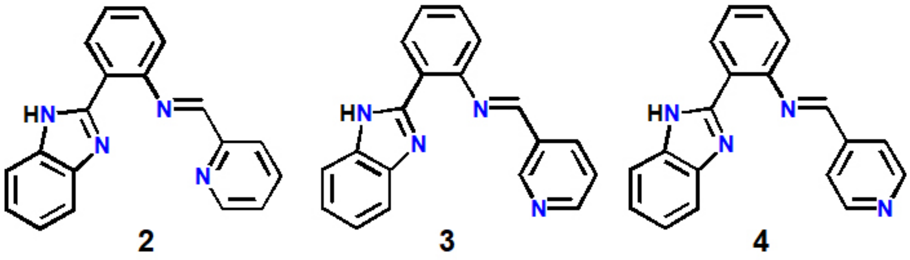

Scheme 2: The molecular structures of the benzimidazole-based HSO_4^- ion chemosensors **2-4**.

Subsequently, three homologous tweezer-shaped benzimidazolium-based fluorescent probes (**5-7**, **Scheme 3**) were utilized in the recognition of both HSO_4^- and $H_2PO_4^-$ anions.[93] In MeCN medium, **5** recognized the $H_2PO_4^-$ ion via a ratiometric red shift of the emission band whereas HSO_4^- was recognized via fluorescence quenching. Strong and multiple hydrogen bonding between HSO_4^-/$H_2PO_4^-$ with **5** enabled the recognition. The presence of both benzimidazole and urea moieties in **5** enabled improved selectivity and sensitivity over the other two probes, **6** and **7**, containing either one of the binding moieties. Such discrimination of two tetrahedral anions was very rare in the literature at this time, but the study was somewhat limited by the requirement for organic media and the switch-off response to bisulfate.

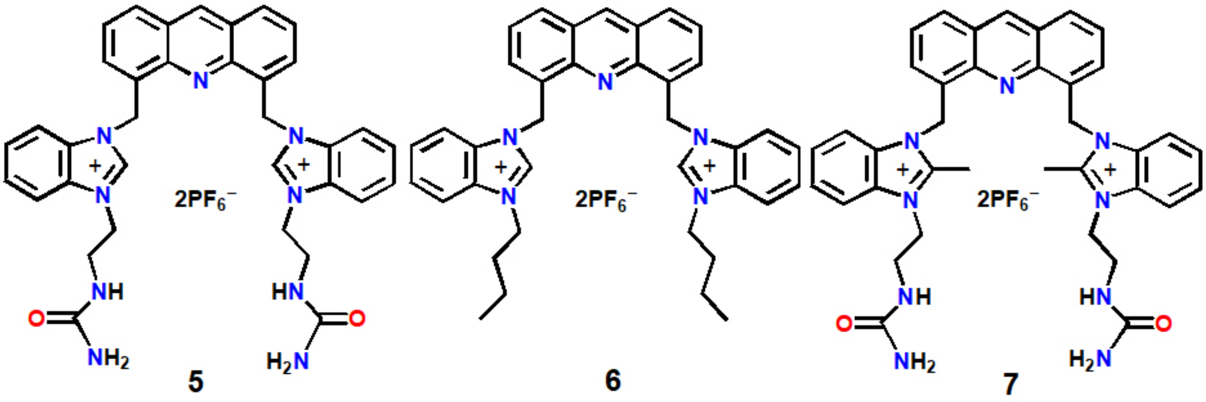

Scheme 3: The molecular structure of the benzimidazole-based HSO_4^- ion chemosensors **5-7**.

In 2014, Mukherjee *et al.* developed a pair of benzimidazole-quinazoline assembled chemosensors (**8-9**, **Scheme 4**) that ratiometrically recognized the HSO_4^- ion at nanomolar concentrations (LOD= 18.08 nM for **8** and 14.11 nM for **9**) in ethanol-water (1:5; v/v) medium.[94] Both **8** and **9** were involved in hydrogen bonding interactions with the HSO_4^- ion and inhibited PET from the benzimidazole to the substituted phenyl moiety. The fluorimetric response of the two probes towards HSO_4^- was different with the alteration of the substitution of the phenyl ring found to tune the fluorescence signal. Chemosensor **9** displayed a switching of its fluorescent signal from a single wavelength to an extremely useful ratiometric response (430 to 485 nm), but **8** displayed a significant multi-fold enhancement of emission intensity at a single wavelength (485 nm) (**Figure 5**). Interestingly, the very short response time (15-20 s) and insignificant toxicity of the probes within a human cervical cancer cell line for up to 8 hours was very promising and demonstrated the efficacy of the probes despite the use of ethanolic solvent.

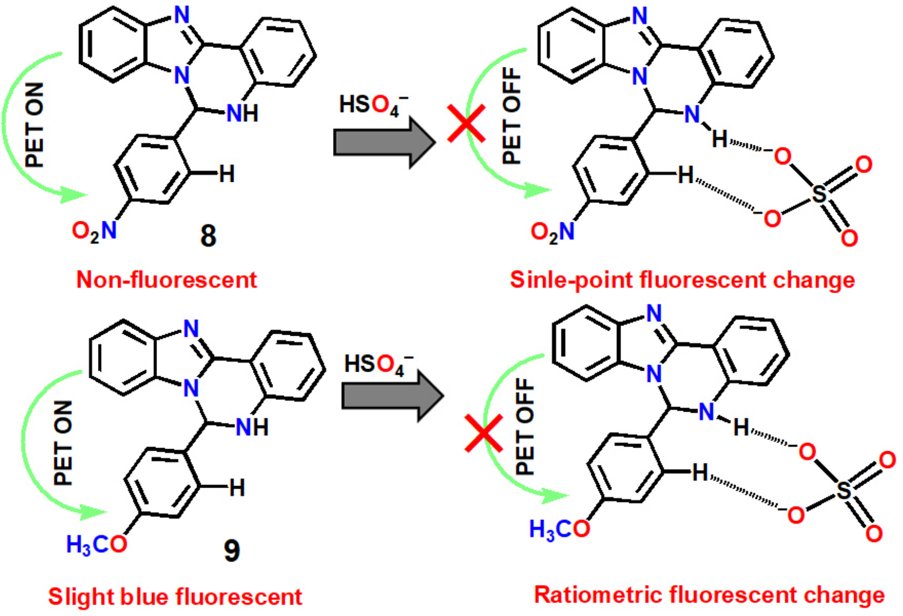

Scheme 4: The proposed binding mechanism of **8** and **9** with the HSO_4^- ion along with respective fluorescent changes.

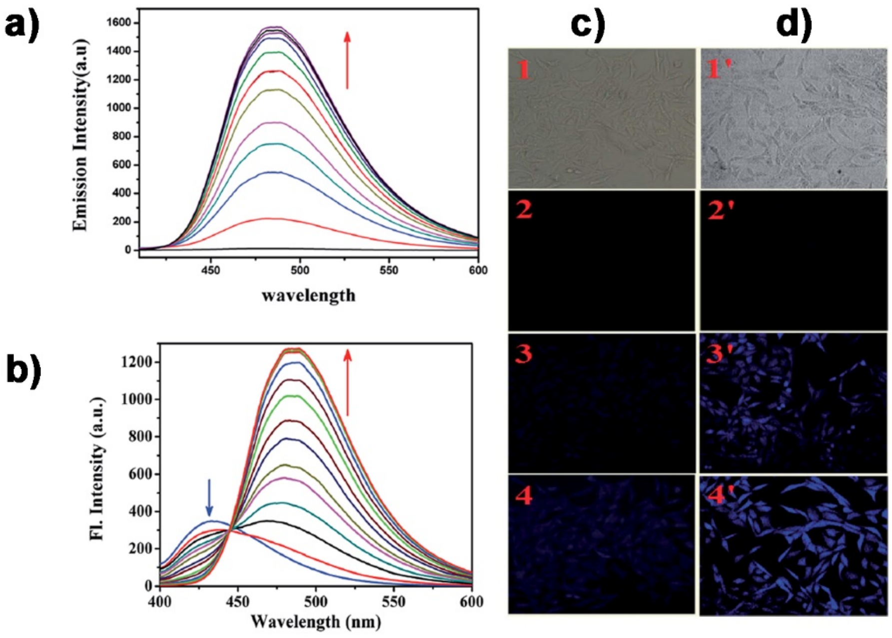

Figure 5: Changes of the fluorescence spectra of **8** (a) and **9** (b) with the gradual addition of the HSO_4^- ion; the fluorescence images of HeLa cells in the presence of the probes, **8** (c) and **9** (d) in the absence (1 for **8** and 1’ for **9**) and presence of HSO_4^- ion at 0 µM (2 for **8** and 2’ for **9**), 5 µM (3 for **8** and 3’ for **9**), 10 µM (4 for **8** and 4’ for **9**) (Reproduced with permission from Ref 94. Copyright 2014, Royal Society of Chemistry).

Later, another water-soluble benzimidazole-based fluorescent probe containing a seven-membered ring (**10**, **Figure 5**) was developed, characterized and shown to display selective and HSO_4^- ion-sensitive (LOD= 5.5 × 10^{-7} M) fluorescent detection behavior.[95] In HEPES buffered water-ethanol (98:2; v/v; pH= 7.4) mixed solvent, **10** displayed ratiometric switching of fluorescent response from a weak band at 430 nm (ϕ= 0.12) to a strong emission band at 483 nm (ϕ= 0.45) in the presence of the HSO_4^- ion. The change of fluorescence response was attributed to intermolecular hydrogen bonding driven CHEF and PET effects. The binding mechanism was also well evidenced by a ^{1}H NMR spectroscopic study and DFT calculations. In addition, 1:1 binding stoichiometry with an association constant, K_a = 4.13 × 10^6 M^{-1} was also reported. The detection event was also confirmed within the HeLa cell with considerable color changes in cellular fluorescent imaging being observed (**Figure 5**). Such instances of the detection of HSO_4^- ion using an essentially water-soluble probe were very useful and rare in the literature at this time.

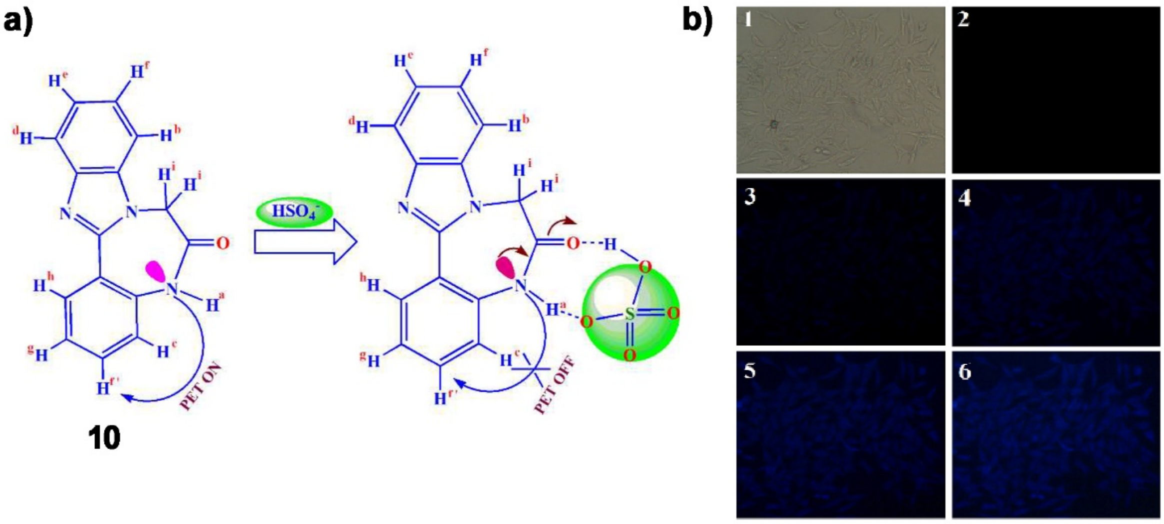

Figure 6: Probable binding mechanism and changes in the PET process of **10** upon binding with the HSO_4^- ion (a); the fluorescence images of the probe, **10** within HeLa cells in the absence and presence of HSO_4^- ion at different time frames (1: phase contras; 2: 0 µM; 3: 3 µM; 4: 5 µM; 5: 7 µM and 6: 10 µM of HSO_4^- ion) (Reproduced with permission from Ref 95. Copyright 2014, Royal Society of Chemistry).

It is very common for an anion to be involved in the primary coordination sphere of a metal complex or replace the metal ion. In 2015, Chattopadhyay *et al.*, developed a benzimidazole-based non-fluorescent Cu(II) complex (**11**, **Scheme 5**) that recognized the HSO_4^- ion via a different and most uncommon intermolecular hydrogen bond aided CHEF mechanism that preserved the metal coordination.[96] The non-toxic and biocompatible probe selectively and sensitively recognized (LOD= 3.18 × 10^{-7} M) the HSO_4^- ion through an "off-on" fluorescent switching mechanism in HEPES buffered medium. In addition, **11** displayed a distinguishable color change under exposure to both sunlight and UV light. The non-cytotoxic probe was also able to image the HSO_4^- ion within model cancer cells. The report of a chemosensor for the HSO_4^- ion with such interesting characteristics was rare and innovative at the time.

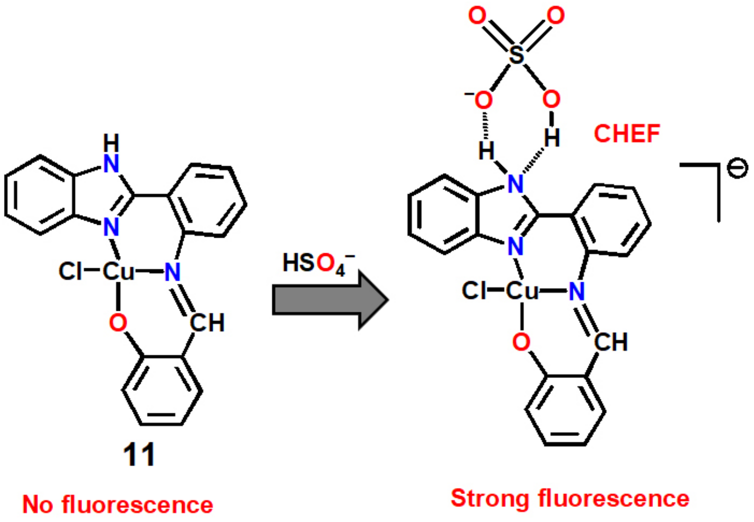

Scheme 5: The proposed binding mechanism of **11** with the HSO$_4^-$ ion in water-DMSO mixed solvent.

In 2019 Das *et al.* developed a styryl-benzimidazole conjugated chemosensor (**12**, **Scheme 6**) that colorimetrically recognized HSO$_4^-$in MeOH medium.[97] In its presence, the absorption band of **12** at 394 nm gradually diminished with the simultaneous appearance of a new red-shifted band at 527 nm along with an extremely visual color change from yellow to dark red. The recognition event was triggered by ICT-induced intramolecular hydrogen bonding. Compound **12** was also able to detect Cu^{2+} and Al^{3+} ions with different distinguishable visual color changes. Interestingly, **12** achieved the micromolar scale detection limit (LOD= 7.96 µM) and a paper-strip-based portable system was devised for naked-eye recognition of HSO$_4^-$ ion in real life.

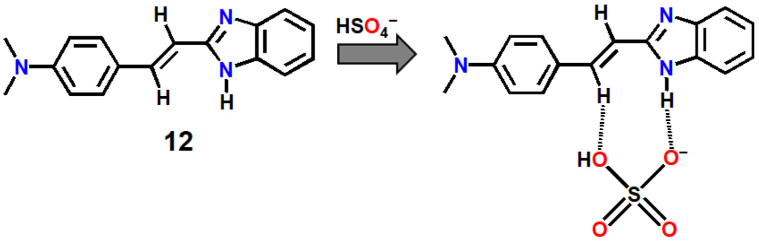

Scheme 6: The proposed binding mechanism of **12** with the HSO$_4^-$ ion in methanol.

Later, Bains *et al.* developed a benzimidazole-thiourea integrated chemosensor (**13**, **Figure 7**) that recognized the HSO$_4^-$ ion colorimetrically and fluorimetrically in pure aqueous medium for the first time.[98] Upon binding with the HSO$_4^-$ ion, **13** displayed a ratiometric blue shift of the absorption band from 311 to even higher energy 261 nm with a prominent isosbestic point at 294 nm. Subsequently, the fluorescence emission band was also ratiometrically shifted from 455 nm to 379 nm with a well-centered isoemissive point at 430 nm (λ_{ex}= 310 nm). The intermolecular hydrogen bonding interaction between the NH proton of the thiourea and the CH proton of the benzimidazolium moiety of **13** (hydrogen bond donor) and the HSO$_4^-$ ion (hydrogen bond acceptor) initiated such ratiometric spectroscopic changes. The selective and highly sensitive (LOD= 5.0 nM) binding of the anion caused aggregation which was confirmed by the DLS data and SEM images (**Figure 7**). In addition, the probe was employed in the detection of HSO$_4^-$ in real water samples with impressive results. Ratiometric detection was most advantageous and the ratiometric detection of the HSO$_4^-$ ion particularly in an aqueous medium remains very rare even to the present day.

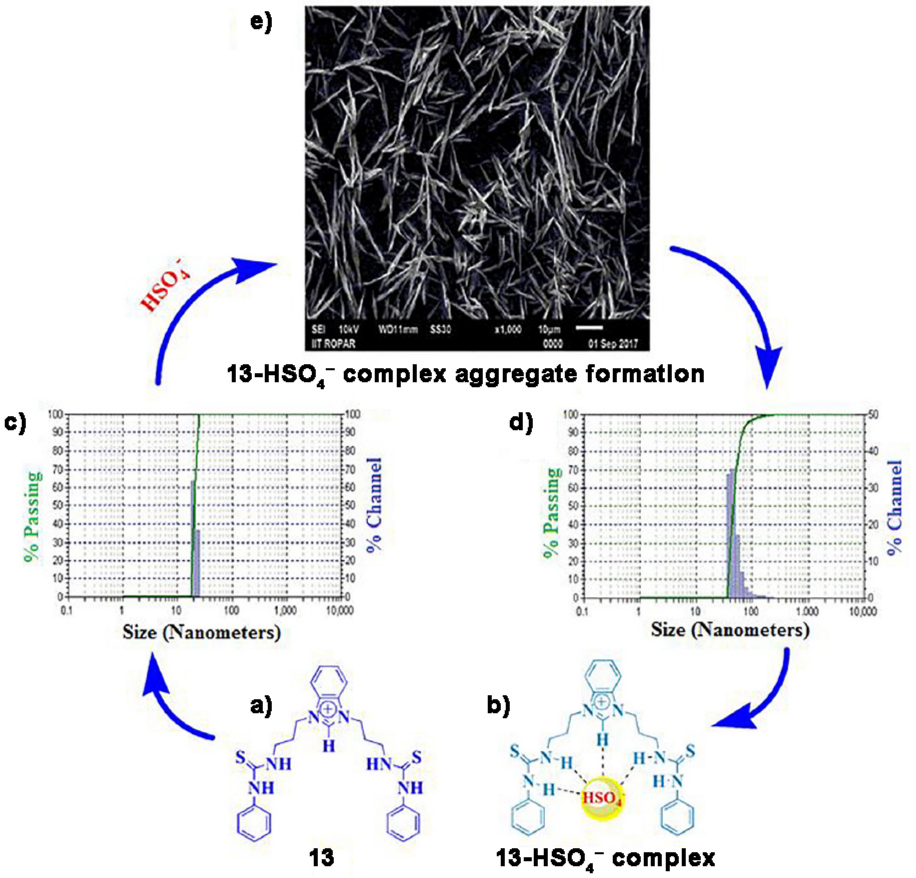

Figure 7: The molecular structure of **13** (a) the proposed molecular structure of the **13**-HSO$_4^-$ complex (b); the DLS diameter image of **13** (c) and of the **13**-HSO$_4^-$ complex (d); the SEM image of the **13**-HSO$_4^-$ complex (e) (Reprinted with permission from Ref 98. Copyright 2019, Elsevier).

Recently, an ESIPT-active benzimidazole-based Schiff base derivative (**14**, **Scheme 7**) selectively recognized Al^{3+} and HSO$_4^-$ ions in a mixed water-methanol mixed solvent.[99] The probe had two different proton transfer sites involving two -OH moieties as hydrogen bond donors as well as one imine nitrogen (-C=N) and one benzimidazole nitrogen as two hydrogen bond acceptors. The ICT active probe displayed a "turn on" fluorescent response at 390 nm in the presence of the HSO$_4^-$ ion (λ_{ex}= 340 nm). Compound **14** was very sensitive to the HSO$_4^-$ ion showing observable response down to nanomolar concentrations (LOD= 23 nM). The binding mechanism between the probe and the HSO$_4^-$ ion was well justified by ^{1}H NMR analysis. Interestingly, **14** could be employed in the real-life detection of the HSO$_4^-$ ion and the fluorescent responses employed in the decoration of an opto-chemical keypad lock.

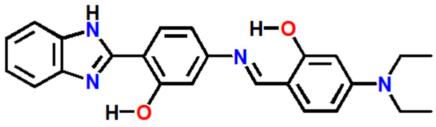

14

Scheme 7: The molecular structure of the benzimidazole-based HSO$_4^-$ ion chemosensor **14**.

Very recently, Moral *et al.* reported a pair of benzimidazole-urea assembled fluorescent probes (**15** and **16**, **Scheme 8**) with different functional groups that displayed very distinct and different fluorescent behavior in the presence of the HSO_4^- ion.[100] Interestingly, **15** displayed aggregation-induced emission (AIE) but **16** exhibited aggregation-caused quenching (ACQ) behavior. Both the probes were very efficient in detecting the HSO_4^- ion up to the micromolar scale in a 100 % aqueous medium with very high binding affinities ($K_a \approx 10^8$ M^{-1}).

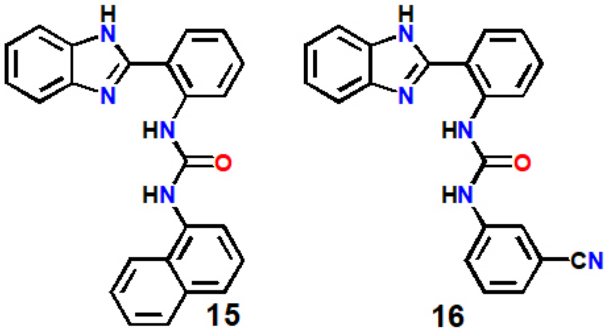

Scheme 8: The molecular structure of the benzimidazole-based HSO_4^- ion chemosensors **15** and **16**.

Based on the above discussion, it can be concluded that the binding of bisulfate with benzimidazole-based chemosensors results from hydrogen bonding interactions with the ion which in turn alter the electronic and charge transfer behavior of the chemosensor resulting in easily detected colorimetric and fluorescent responses represented by **Figure 8** below.

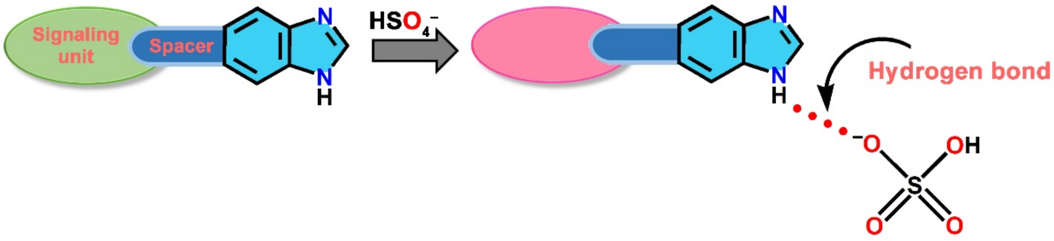

Figure 8: The general mode of binding of benzimidazole-based chemosensors with the HSO_4^- ion.

3.2. Benzothiazole moiety-based detection.

Benzothiazole has been widely used as a sensing unit in an array of chemosensors in the colorimetric and fluorescent detection and imaging of ions, biomolecules, and other important analytes.[101] In addition, benzothiazole derivatives have been extensively utilized in the diagnosis of several diseases and disorders by fluorescent imaging of several analytes.[102] However, the discussion here will focus on the detection and/or imaging of the HSO_4^- ion.

In 2013, Bhardwaj *et al.* reported a pair of benzothiazole derivatives, one of which (**17**, **Scheme 9**), acted as a chemosensor of Fe^{3+} and HSO_4^- ions through different spectroscopic signatures.[103] **17** recognized the HSO_4^- ion via a ratiometric shift of absorption maxima, whereas it detected the Fe^{3+} ion via fluorescence enhancement. In a TRIS buffered CH_3CN/H_2O (8/2, v/v, pH= 7.6) medium, the introduction of HSO_4^- decreased the absorbance of **17** at 310 and 450 nm, which was accompanied by the simultaneous promotion of a new band at 365 nm. Compound **17** was shown to form a 1:1 complex with $HSO_4^-$and achieved a 5.4 µM detection limit. The probe, containing both a hydrogen bond donor hydroxyl group as well as a/two hydrogen bond acceptor nitrogen atom, favored the selective binding of the bisulfate, over which other analytes (F^-, Cl^-, Br^-, I^-, NO_3^-, CN^-, ClO_4^-, AcO^- and

PO$_4^{3-}$).

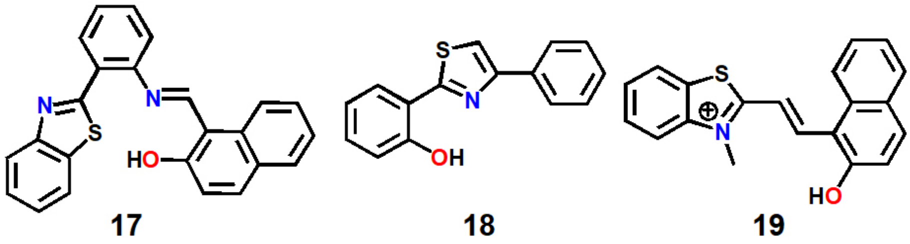

Scheme 9: The molecular structure of the benzothiazole-based HSO$_4^-$ ion chemosensors **17-19**.

Later, three analogous hydroxyphenylthiazole derivatives of which one analog (**18**, **Scheme 9**) was employed in the selective and sensitive sequence-specific fluorescent recognition of Ga^{3+} followed by HSO$_4^-$ in MeCN.[104] The ESIPT active probe displayed two weak emission bands (ϕ= 0.0059) at 375 and 504 nm due to enol and keto tautomers, respectively. With the addition of Ga^{3+}, **18** displayed the development of an emission band at 430 nm (ϕ= 0.0653) due to the inhibition of the ESIPT phenomenon. Subsequently, in the presence of HSO$_4^-$, the emission band of the 1:1 **18**-Ga^{3+} complex sharply declined due to decomplexation and consequent restoration of the ESIPT behavior providing highly selective detection of the ion. Whilst most HSO$_4^-$ ion chemosensors interact with the analyte via hydrogen bonding, this **18**-Ga^{3+} complex interacted via electrostatic interaction.

A benzothiazole-based substituted spiropyran derivative (**19**, **Scheme 9**) was employed in the visual detection of HSO$_4^-$with a distinct color change from pink to yellow being observed in water (**Figure 9**).[105] The anion-induced conversion of **19** from the J-aggregate to H-aggregate which was then converted to the closed spiropyran form upon irradiation with visible light. This facilitated a ratiometric change in absorption maxima upon formation of the **19**-HSO$_4^-$ complex and the system was deployed in a filter paper-based real-life application (**Figure 9**). Interestingly the hydroxy group was involved in hydrogen bonding with the anion whilst the positive charge on the benzothiazolinium moiety was involved in electrostatic interaction leading to such highly selective recognition behavior. Interestingly, this was the first report of a visible light-responsive spiropyran-built reversible chemosensor for the HSO$_4^-$ ion.

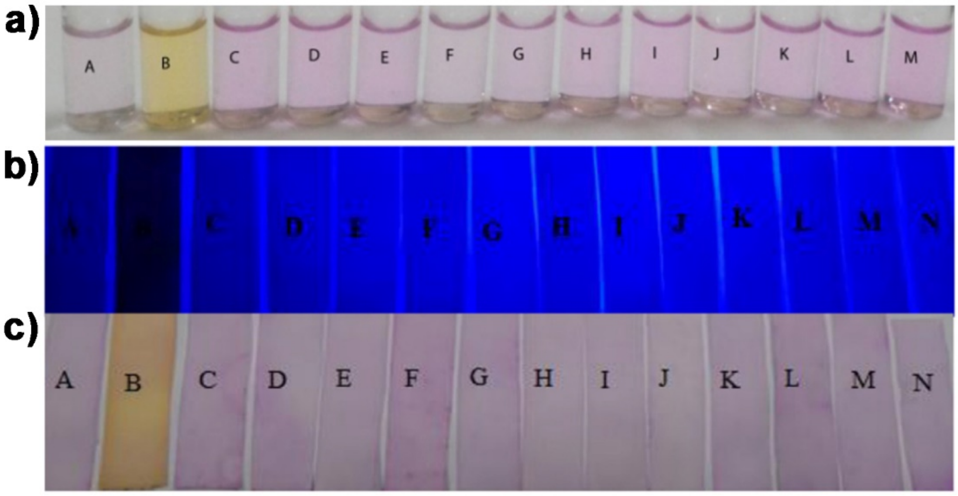

Figure 9: The color change of **19** in the presence of different anions in solution phase (a), test strip under UV light (b) and test strip under sunlight (c). The cuvette or test strip marked with “A” and “B” denote **19** and **19**-HSO$_4^-$respectively and the rest denote other competitive anions. (Reproduced with

permission from Ref 105. Copyright 2017, Wiley).

Subsequently, another benzothiazole-based Schiff base (**20**, **Scheme 10**) fluorometrically recognized two anions (HSO_4^- and I^-) in the solution phase as well as in living nematodes by two different mechanisms.[106] Compound **20** recognized HSO_4^- by promotion of the emission intensity at 468 nm triggered by HSO_4^--induced hydrolytic imine cleavage and subsequent inhibition of the PET process (**Scheme 10**). In contrast, I^- displayed heavy atom quenching of the emission due to the formation of an ICT complex and the system represents a rare example of a chemosensor that can recognize two different anions independently by chromogenic and fluorimetric responses.

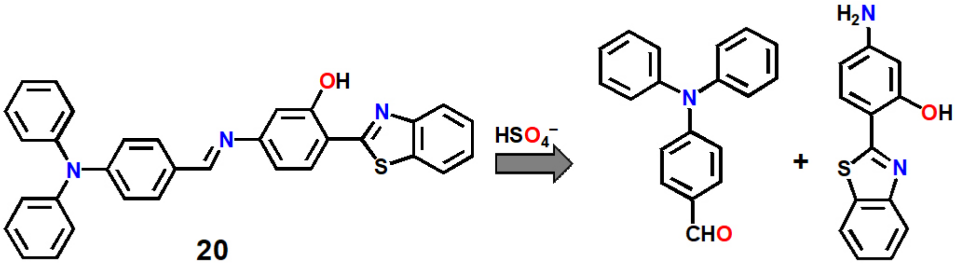

Scheme 10: The proposed mechanism of action of **20** with HSO_4^- ion.

Recently, another fluorophore of benzothiazolinic (**21**, **Scheme 11**) was developed and employed as its halide salt for the fluorescent detection of HSO_4^- by naked-eye color change (purple to yellow) accompanied by a hypsochromic change in both absorption and emission bands.[107] In MeCN-H_2O (1:1; v/v) mixed solvent, **21** selectively recognized HSO_4^-over other anions driven by the formation of an ion-induced H-aggregate leading to the marked color change. ^{1}H NMR spectral analysis and DFT study established the substitution of bromide ion by HSO_4^- ion due to the formation of intermolecular, bifurcated hydrogen bonds with **21 (Scheme 11**).

Very recently, the same group developed another benzothiazolinic spiropyran derivative (**22**, **Scheme 11**) which also recognized HSO_4^-in an aqueous medium with very high selectivity and sensitivity (LOD= 1.58 μM).[108]

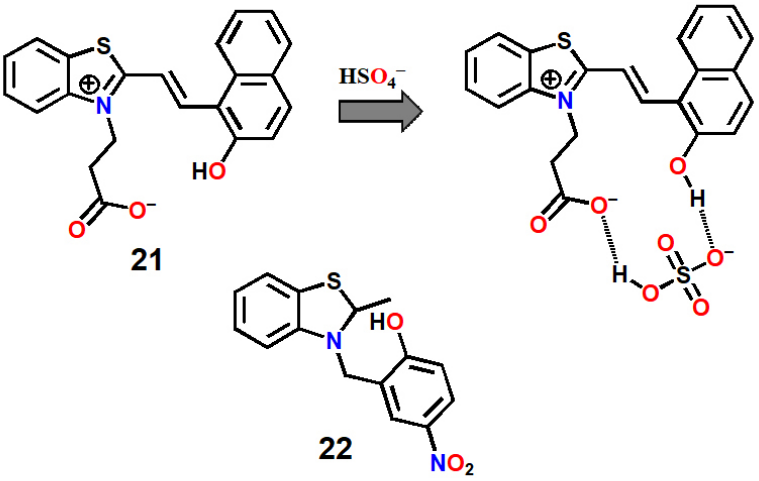

Scheme 11: The proposed binding mechanism of **21** with the HSO_4^- ion and the molecular structure of **22**.

It is very difficult to draw a generalized binding mechanism for benzothiazole-based fluorescent detection of the HSO_4^- ion. In most cases, the nitrogen atom of the benzothiazole is involved in hydrogen bonding with the HSO_4^- ion, but the number of probes developed is very low. This presents an exciting opportunity for future chemists to develop novel benzothiazole-based fluorescent probes for the detection of HSO_4^-.

3.3. BODIPY moiety-based detection.

BODIPY derivatives have a long history of being used as fluorescent indicators,[109] NIR dyes,[110-111] as well as in bioimaging and chemosensing applications,[112-113] optoelectric applications,[114] as photosensitizers for photodynamic therapy[115-117] and photo-redox catalysis.[118-119] Despite their extensive range of applications there are only a few BODIPY dyes that have been employed in the fluorescent detection of HSO_4^- ions.

A BODIPY-indole assembled dye (**23**, **Scheme 12**) was applied in the optical detection of F^- and HSO_4^- ions in both non-aqueous (MeCN) as well as semi-aqueous medium (MeCN-H_2O).[120] The HSO_4^- anion was found to reduce the ICT band of the probe at 324 nm with simultaneous and ratiometric development of a new band at 382 nm. Although the absorption responses of **23** were similar in the presence of both F^- and HSO_4^- ions, the emission responses were completely different. The introduction of F^- ion caused quenching of the emission band whereas the HSO_4^- ion resulted in an increase in emission intensity centered at 512 nm and the PET-driven weak emission band of **23** (ϕ= 0.07) became a strong green fluorescence in the presence of HSO_4^-. The changes were attributed to hydrogen bond-induced inhibition of PET from the imine nitrogen and indole moieties to the excited BODIPY moiety.

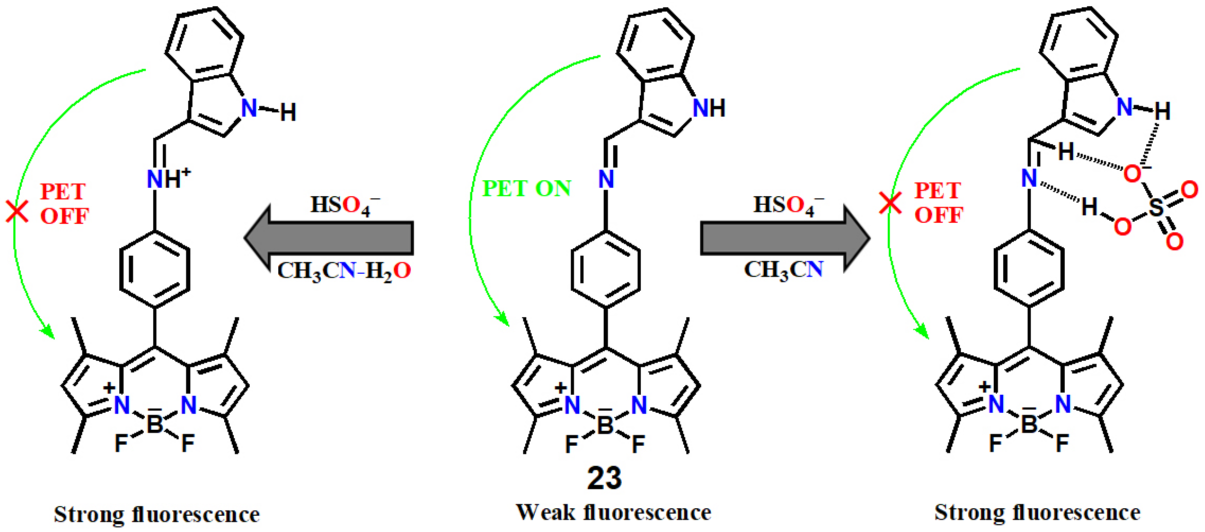

Scheme 12: The proposed binding mechanism of **23** with the HSO_4^- ion.

Subsequently, another hydrazone-based BODIPY derivative (**24**, **Scheme 13**) was successfully utilized in the dual mode relay detection of F^- followed by HSO_4^- ions in MeCN medium.[121] In the presence of the F^- ion, **24** displayed a new red-shifted absorption band at 560 nm with a simultaneous decrease of a charge transfer band at 399 nm resulting in a yellow-to-purple color change that could be readily observed by the naked eye. In contrast, the F^- ion was found to quench the emission band of **24** at 518 nm, which was attributed to the deprotonation of the NH group. Subsequent addition of HSO_4^- as a "recovering agent" reversed the spectroscopic responses in both absorption and emission bands allowing **24** to act as an "on-off-on" molecular switch which was exploited in the development of a molecular keypad lock.

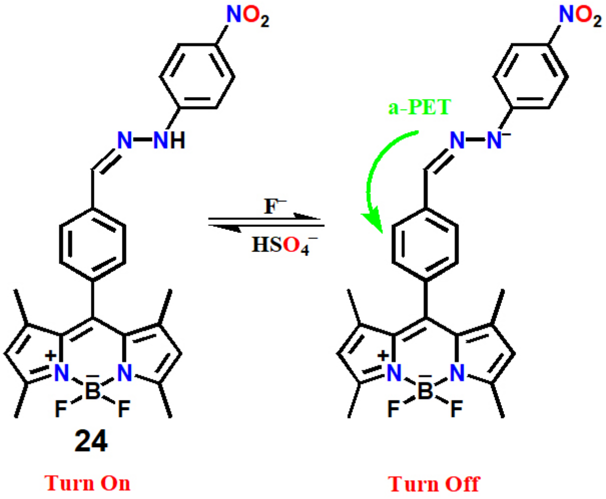

Scheme 13: The proposed mechanism of action of **24** with the HSO_4^- ion.

A Schiff base BODIPY derivative (**25**, **Scheme 14**) was then employed in the dual mode recognition of the HSO_4^- ion.[122] Upon interaction with HSO_4^-, **25** showed a ratiometric red shift of absorption band from 497 to 523 nm with simultaneous color change from pink to yellow. During a fluorescence titration, HSO_4^-gradually induced a strong green fluorescence emission response at 544 nm driven by imine hydrolysis in **25**. Additionally, the detection event was facilitated by cell permeability and poor auto-fluorescence of biological cells.

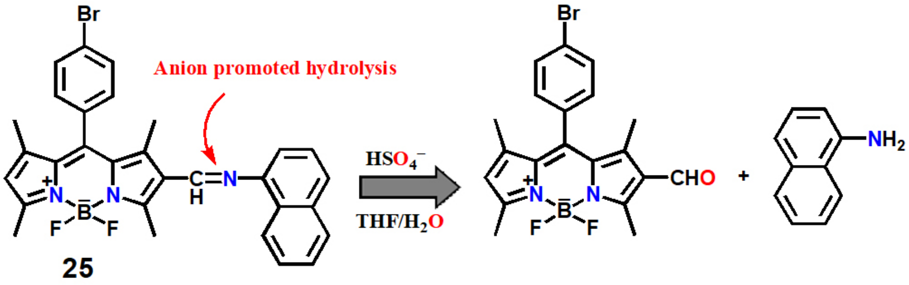

Scheme 14: The proposed mechanism of action of **25** with the HSO_4^- ion.

A pair of azaindole-based BODIPY derivatives (**26-27**, **Scheme 15**) were then developed via a Knoevenagel reaction and employed in the "turn off" fluorescent sensing of the HSO_4^- ion in MeCN.[123] The high-intensity emission bands of **26** and **27** at 655 nm and 677 nm respectively were significantly quenched in the presence of HSO_4^-. Additionally, 1:1 binding stoichiometry and micromolar concentration detection limits were also reported. Remarkably, the chemotherapeutic character of the probe was also interesting.

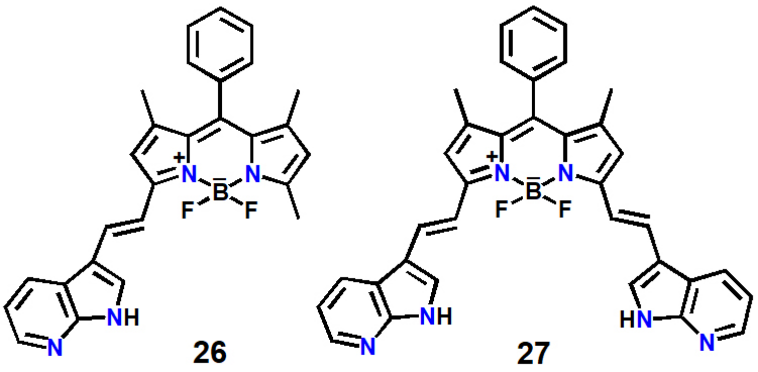

Scheme 15: The molecular structure of the BODIPY-based HSO_4^- ion chemosensors **26** and **27**.

Despite the long history and extensive applications of BODIPY derivatives in chemosensing, to date, there are only four reports of BODIPY-based HSO_4^- ion chemosensors that have appeared offering future opportunities for further development of such systems to image the HSO_4^- ion.

3.4. Coumarin moiety-based detection.

During the last two decades, many examples of coumarin-integrated scaffolds have been developed for the fluorescent detection of different cations, anions, and biomolecules.[124-126] However, there are only a few coumarin scaffold-based supramolecular chemosensors for the detection of the HSO_4^- ion.[127-130]

In 2009, Kim *et al.* synthesized three analogous fluorophores of which the coumarin-based fluorescent probe (**28**, **Scheme 16**) selectively and sensitively recognized HSO_4^- through a “turn on” response.[127] Upon the addition of HSO_4^-, the emission band of **28** at 485 nm was sharply enhanced in MeCN:H_2O:(1:1; v/v) and the detection of the anion was governed by a PET mechanism.

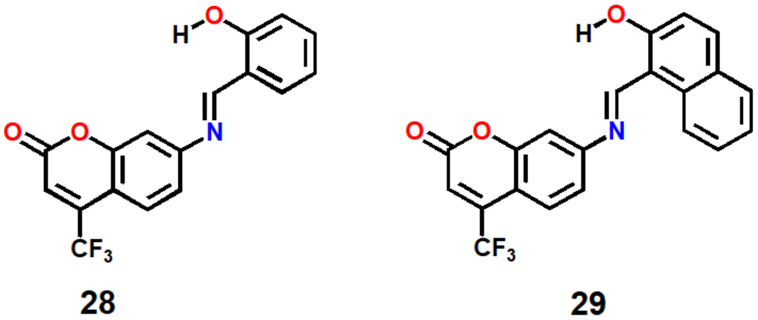

Scheme 16: The molecular structure of the coumarin-based HSO_4^- ion chemosensors **28** and **29**.

The proposed mechanism of this study[127] was revisited by Kumar *et al.*[128] during the course of an investigation with a structurally similar probe (**29**, **Scheme 16**) where it was established that hydrogen bonding was not the underlying mechanism of interaction with the anion. Rather, hydrolysis of the Schiff base played a vital role with the mechanism being well-justified through analysis of the ^1H NMR titration results in a deuterated solvent.

Another coumarin-based fluorescent probe (**30**, **Scheme 17**) recognized Zn^{2+} and HSO_4^- ions independently in a semi-aqueous medium (MeCN-H_2O; 1:1; v/v).[129] In the presence of HSO_4^-, the emission intensity of **30** at 376 nm was considerably enhanced denoting “turn on” recognition. Imine

30 was also able to detect HSO_4^- at concentrations as low as 274 nM and was proposed to be involved in hydrogen-bonded complex formation with the anion.

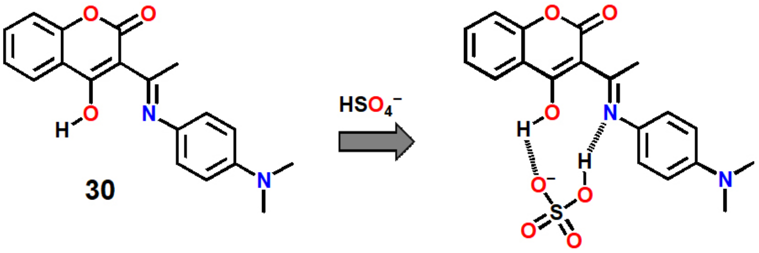

Scheme 17: The proposed binding mechanism of **30** with the HSO_4^- ion.

From the outset of the optical detection of HSO_4^- ion, very little attention was paid to the HSO_4^--SO_4^{2-} deprotonation-protonation mechanism. In 2019, Nair *et al.* mechanochemically synthesized a pair of coumarin derivatives, coumarin-integrated glycine and coumarin-integrated alanine (**31** and **32** respectively, **Scheme 18)** to investigate this hitherto overlooked issue.[130] Both the probes were employed in picomolar scale (LOD= 50 and 100 pM for **31** and **32** respectively) reversible fluorescent detection of HSO_4^-in pure aqueous medium at neutral pH. Also, the hydrogen bonding mechanism between the probes and HSO_4^- was well justified through the use of DFT studies. Interestingly, the optical sensing phenomenon was employed in the detection and estimation of HSO_4^- in real samples including digestible plant foods cabbage, broccoli, carrot, and mustard seeds, as well as drug and urine samples.

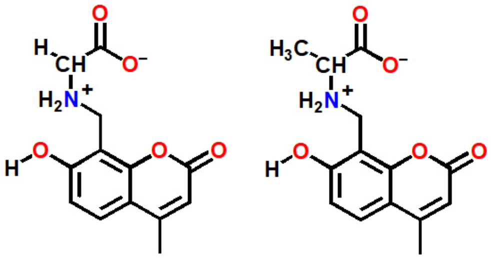

Scheme 18: The molecular structure of the coumarin-based HSO_4^- ion chemosensors **31** and **32**.

Recently, Deng *et al.* designed a coumarin-based Schiff base derivative (**33**, **Figure 10a**) that recognized the HSO_4^- ion via naked-eye color change under sunlight (yellow to colorless) as well as under UV light (dark blue to orange) in semi-aqueous medium (EtOH-H_2O; 9:1; v/v).[131] Interestingly, the probe recognized the HSO_4^- ion down to sub-micromolar levels (LOD= 4.63×10^{-7} M). Analysis of ^1H NMR and HRMS spectral data revealed that the HSO_4^- ion induced the hydrolytic cleavage of the imine bond resulting in such a prominent color change-based detection event. Furthermore, a paper strip-based HSO_4^- ion detection technique was successfully demonstrated (**Figure 10b**). In addition, to explore its real-life applicability, the anion was recovered from different spiked water samples and also recognized within zebrafish through fluorescence imaging (**Figure 10c**).

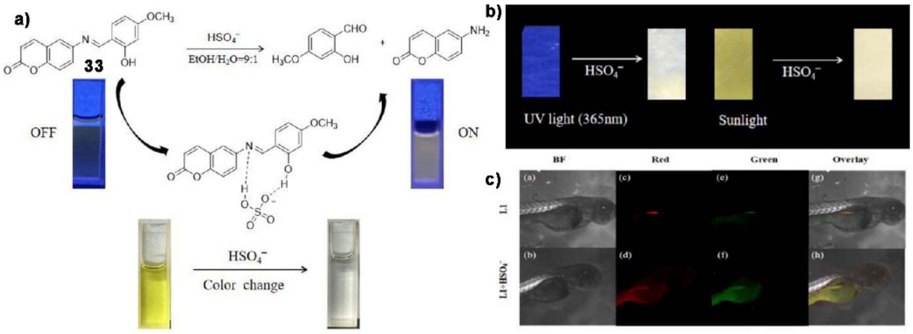

Figure 10: The proposed binding mechanism of **33** with HSO_4^- along with respective naked-eye color changes under daylight and UV light (a); Color changes on paper strips (b) and recognition of HSO_4^- ion within zebrafish by fluorescence imaging. (Reproduced with permission from Ref 131. Copyright 2023, Elsevier).

From the above discussion, it could be stated that all these coumarin-based fluorescent probes involved hydrogen bonding with the HSO_4^- ion and displayed “turn on” fluorescent responses for the selective and sensitive detection of the anion. In addition, almost all the coumarin derivatives contain either a Schiff base unit or a phenolic hydroxy group, or both. There are only four reports on coumarin-based fluorescent chemosensors for HSO_4^- ion and consequently, there is enormous scope to explore this field further.

3.5. Indole moiety-based detection.

Indole-based receptors have a long history of metal-binding properties and it is also an important precursor in the synthesis of novel drug molecules.[132-133] Here, the crucial role of indole-based fluorophores in the detection of the HSO_4^- ion is discussed.

In 2011, Mallick *et al.* reported the first indole-based chemosensor for HSO_4^-, which was an “off-the-shelf” chemosensor requiring no synthetic effort (**34**, **Scheme 19**). The system was also found to be able to detect F^- anions independently by tuning the solvent composition and exploring the acid-base behavior of the probe.[134] Indole **34** recognized the HSO_4^- ion selectively in semi-aqueous medium (MeCN-H_2O; 5:1; v/v) by activating one channel or site of **34** by protonating the pyridinic nitrogen, whilst it detected F^- in pure MeCN by activating the other channel to give a rare dual channel detection of two anions by a single probe molecule.

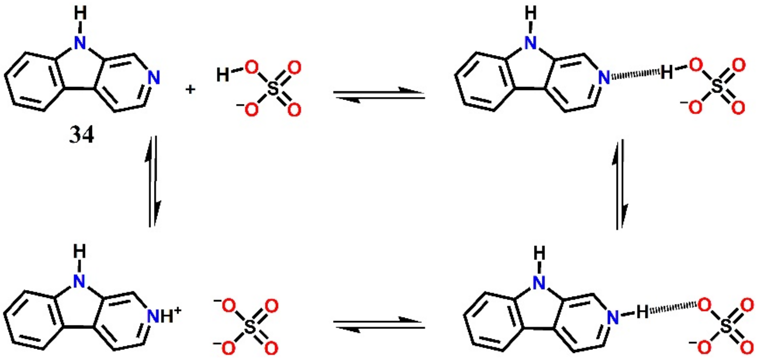

Scheme 19: The proposed binding mechanism of **34** with the HSO_4^- ion.

A few years later, Paul *et al.* utilized the same probe molecule (**34**, **Scheme 19**) in sequence-specific relay recognition of HSO_4^- followed by the F^- anion in a $MeCN-H_2O$ (5:1; v/v) mixed solvent via monitoring of the ratiometric and reversible absorption and emission spectral responses.[135] Interestingly, an opto-chemical molecular keypad lock was sketched (**Figure 11**), and the binding mechanism of **34** and HSO_4^- ion was well-explored by evaluating the DFT calculations (**Scheme 19**). Interestingly, in a different study, Paul *et al.* colorimetrically and fluorimetrically recognized picric acid using the same "off-the-shelf" fluorophore.[136]

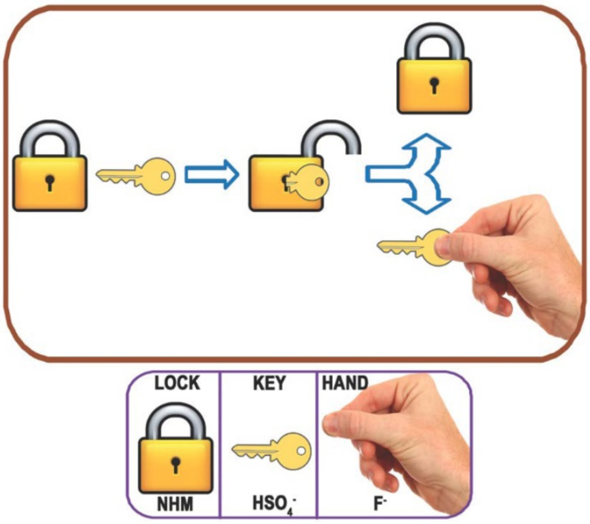

Figure 11: The design of a molecular opto-chemical keypad lock where the probe (**34** or norharmane) acted as the lock, the HSO_4^- ion acted as the key and fluoride acted as hand to unlock the lock. (Reprinted with permission from Ref 135. Copyright 2016, Wiley).

Later, among a set of four analogous styrylindolium derivatives two (**35-36**, **Scheme 20**) were successfully employed in ratiometric optical detection of the HSO_4^- ion in H_2O-EtOH (1:1; v/v) medium.[137] Upon interaction with HSO_4^-, the probes exhibited ratiometric shifts of both absorption and emission bands along with color change under sunlight and UV irradiation (**Figure 12**). The HSO_4^- ion was involved in intermolecular hydrogen bonding with the probes, thereby forming head-to-tail fashion H-aggregates.

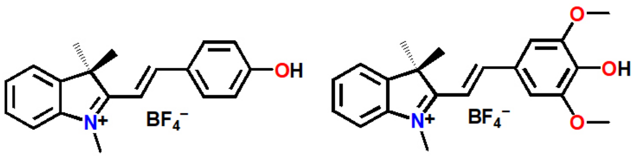

35 **36**

Scheme 20: The molecular structure of the indole-based HSO_4^- ion chemosensors **35** and **36**.

Figure 12: The naked-eye color changes of **35** (a and b) and **36** (c and d) in the presence of different anions (6th cuvette for HSO_4^-) under daylight and sunlight respectively. (Reprinted with permission from Ref 137. Copyright 2013, Royal Society of Chemistry).

Afterward, a series of 2,2'-bis(indolyl)methane and 2-alkylated indole derivatives were developed and employed in the selective and sensitive colorimetric detection of HSO_4^- and F^- by Bayindir and Saracoglu.[138] In the presence of both anions, red-shifted absorption bands accompanied by distinguishable and prominent chromogenic color changes of some probes were noted. Moreover, the binding mechanisms were also well-justified through a ^1H NMR spectroscopic titration study with both anions involved in hydrogen bonding with the N-H protons of the probes.

Subsequently, a pair of tetrapodal and hexapodal indole derivatives (**37-38**, **Scheme 21**) were employed in the recognition of the HSO_4^- ion via a chromogenic color change phenomenon.[139] Unlike other anions, HSO_4^- exhibited a significant red shift of absorption band and consequent visual color change from yellow to red for **37** and from pale yellow to pink for **38** (**Figure 13**) and such prominent color changes could be utilized in on-spot recognition of the anion. However, the fluorescence emission behavior of the two probes in the presence of the anion was different. Upon binding with HSO_4^-, **37** displayed quenching of the emission band at 353 nm but **38** displayed an increase in the emission maximum at 380 nm. Both the probes were involved in hydrogen bonding with the HSO_4^- ion and subsequent through-bond energy transfer phenomenon resulted in the vivid visual color changes. The binding mechanism was well explored and supported through ^1H NMR titration experiments and extensive DFT calculations.

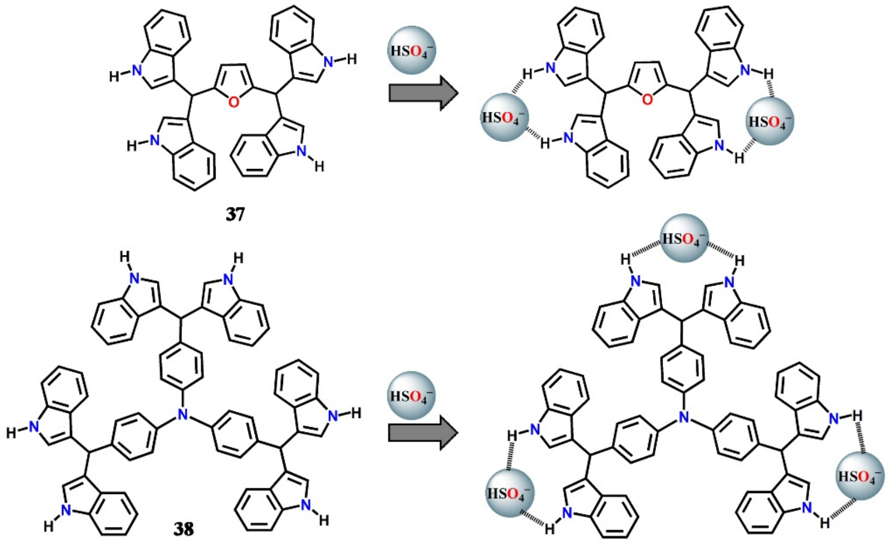

Scheme 21: The proposed binding mechanism of **37** and **38** with the HSO_4^- ion.

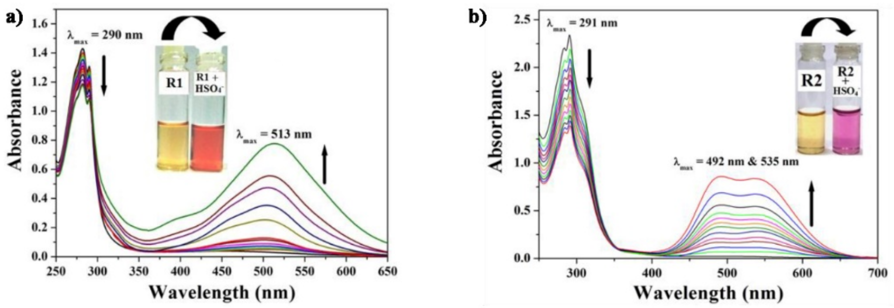

Figure 13: UV-visible absorption spectral changes of **37** (a) and **38** (b) with the gradual addition of the HSO_4^- ion along with chromogenic color changes (**R1**≈ 37 and **R2**≈ 38). (Reprinted with permission from Ref 139. Copyright 2015, Elsevier).

In further progress, three indole-based receptors (**39-41**, **Scheme 22**) were employed in colorimetric and fluorescent recognition of HSO_4^- and CN^- ions in a semi-aqueous medium (MeCN-H_2O; 1:1; v/v).[140] Among the three, one was a tripodal probe (**41**) and the other two (**39** and **40**) were dipodal. The tripodal probe, **41** recognized both HSO_4^- and CN^- ions independently whereas the two dipodal probes behaved differently; one (**40**) selectively recognized HSO_4^- and the other one (**39**) recognized CN^- ion. Both **40** and **41** were capable of detecting HSO_4^- up to the nanomolar scale. Extensive DFT calculations revealed that multiple hydrogen bonds between the probes and the HSO_4^- ion initiated such spectroscopic changes.

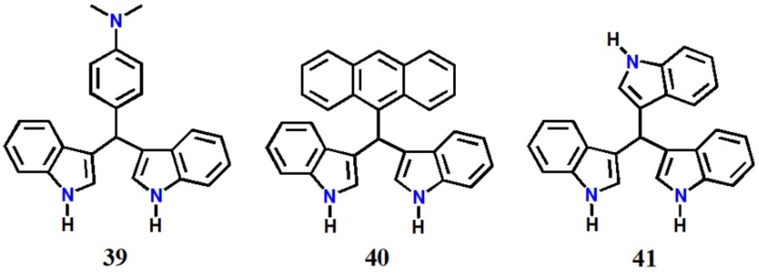

Scheme 22: The molecular structure of the indole-based HSO_4^- ion chemosensors **39**-**41**.

Detection of any analyte in 100% aqueous medium is challenging and but highly desirable due to real-world sensing applications. In 2016, Samanta *et al.* developed an indole-based fluorogenic probe (**42**, **Scheme 23**) that recognized HSO_4^- and SO_4^{2-} ions via a "turn on" fluorescent response in pure aqueous medium;[141] The probe also recognized the SO_3^{2-} ion via a similar fluorescent response. The weakly fluorescent **42** exhibited strong blueish-green fluorescence (λ_{em}= 442 nm) in the presence of $SO_3^{2-}$and greenish-yellow fluorescence (λ_{em}= 511 nm) upon interaction with both HSO_4^- and SO_4^{2-} ions. It was well justified that the exceptionally high hydration energy of SO_4^{2-} disfavoured the solubility of **42** and consequently facilitated the aggregation and switched on the fluorescence response. Moreover, the ppm scale detection limit for HSO_4^- and appreciable biocompatibility of **42** was impressive.

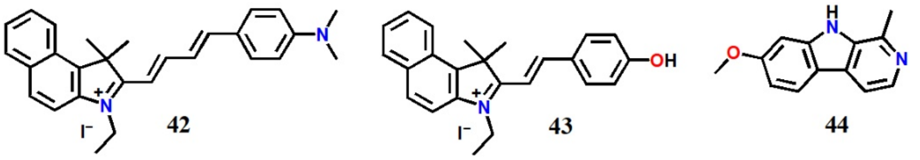

Scheme 23: The molecular structure of the indole-based HSO_4^- ion chemosensors **42-44**.

Later, another hydroxystyryl and benzo[e]indolium integrated chemosensor (**43**, **Scheme 23**) was designed that selectively and simultaneously recognized SO_3^{2-}/HSO_3^- and HSO_4^- ions via monitoring of different emission channels.[142] The weak emission band of **43** at 580 nm (λ_{ex}= 420 nm) was significantly promoted upon interaction with $NaHSO_4$. But, in the presence of the SO_3^{2-} ion, **43** displayed substantial emission enhancement at 455 nm (λ_{ex}= 320 nm). In addition, the absorption band of **43** at 562 nm declined significantly with the simultaneous promotion of a new absorption band at 463 nm due to the inclusion of the HSO_4^- ion, and the expected visual color change from red to yellow was noted. Formation of a 1:1 **43**-HSO_4^- complex together with an impressive 1.3 nM detection limit for HSO_4^- was also reported with the detection of the multiple anions guided by the principle of ion-induced rotation-displaced H-aggregates. Moreover, **43** was shown to be capable of imaging bisulfate ions within HeLa cells.

To date, the application of fluorescent signals in the design of opto-chemical logic gates, molecular keypad locks, and resettable passwords is achieved through the bespoke synthesis of chemosensors. In 2017 Majumdar *et al.* reported that the commercially available fluorescent probe, harmine (**44**, **Scheme 23**)[143] exhibited a ratiometric change of emission maxima in the presence of fluoride in polar aprotic MeCN medium and displayed a ratiometric shift of emission maxima only in the presence of HSO_4^- ion in MeCN-H_2O (5:1; v/v). Notably, this solvent-dependent fluorescent recognition behavior was successfully applied in the development of unusual but useful opto-chemical logic gates (**Figure 14**).

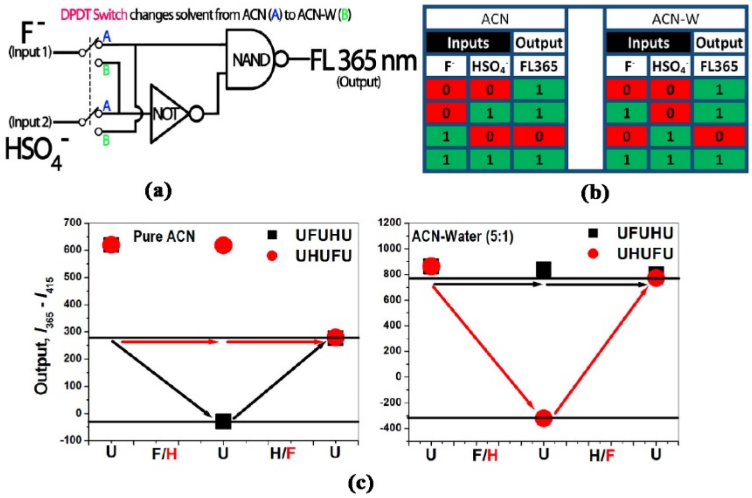

ACN			ACN-W		
Inputs		Output	Inputs		Output
F⁻	HSO₄	FL365	F⁻	HSO₄	FL365
0	0	1	0	0	1
0	1	1	1	0	1
1	0	0	0	1	0
1	1	1	1	1	1

Figure 14: The design of opto-chemical logic gate (a), truth table (b) and password trajectories (c) based on the sequential addition of fluoride and bisulfate ions within the solution of **44** in MeCN and MeCN-water solvents. (Reprinted with permission from Ref 143. Copyright 2017, Springer).

Thereafter, Bayindir and Lafzi reported a pair of oxindole derivatives (**45-46**, **Scheme 24**) that recognized the HSO_4^- ion fluorometrically via a "turn-on" response in HEPES buffered (pH= 7.4) semi-aqueous medium (MeCN-H_2O; 7:3; v/v).[144] When excited at 371 nm, the poorly emissive **45** (ϕ= 0.02) exhibited a fluorescence response at 486 nm (ϕ= 0.27) upon binding with HSO_4^-. Experimental and theoretical arguments revealed the formation of multiple bifurcated hydrogen bonds between **45** and HSO_4^-. Additionally, 1:1 binding stoichiometry and up to 8.9 µM detection limit were also determined.

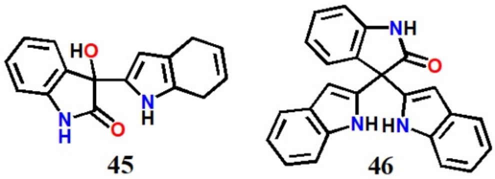

Scheme 24: The molecular structure of the indole-based HSO_4^- ion chemosensors **45** and **46**.

Later, Paul *et al.* designed and synthesized a trio of analogous oxidized bisindolyl methane derivatives (**47-49**, **Scheme 25**) and explored their dual mode independent ratiometric optical recognition behavior toward two anions, HSO_4^- and CN^-.[145] In pure aqueous medium, a prominent and distinguishable color change of **47** in the presence of HSO_4^- (from orange to red) and CN^- (from orange to yellow) was worthy of real-life application. Additionally, **47** achieved a remarkable ppb detection limit (LOD= 8.7 and 6.2 ppb for HSO_4^- and CN^- respectively) without any mutual interference. Moreover, the ion-induced tuning of the ICT behavior of **47** was also explored using the DFT study to reveal the interaction mechanism (**Figure 15**). The effect of the substitution of electron-withdrawing and donating groups on analogs of **47** (**48** and **49** respectively) on the anion binding behavior was explored and explained rationally through experimental observations and DFT calculations.

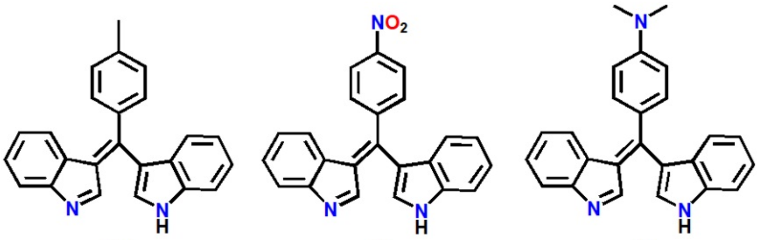

47 **48** **49**

Scheme 25: The molecular structure of the indole-based HSO_4^- ion chemosensors **47-49**.

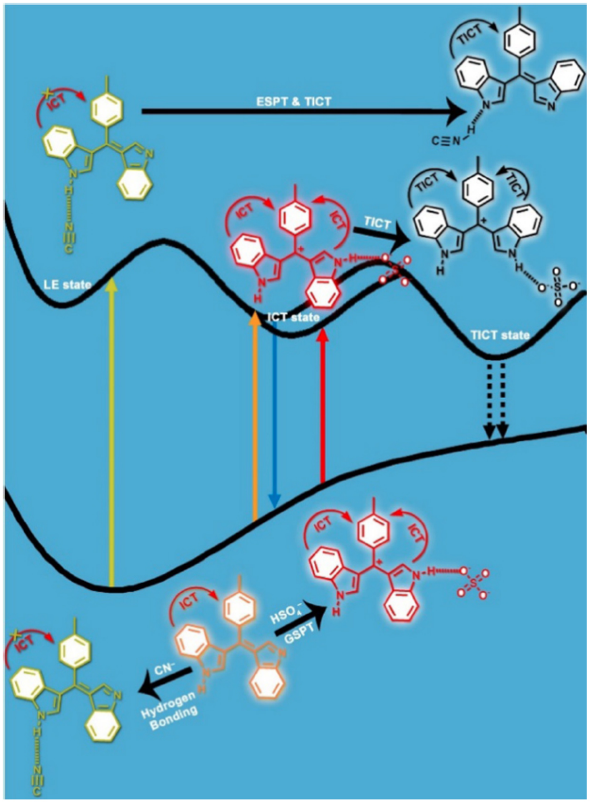

Figure 15: The proposed binding mechanism of **47** with the HSO_4^- ion along with different photoprocesses in the energy profile diagram. (Reprinted with permission from Ref 145. Copyright 2022, Royal Society of Chemistry).

In summary, indole-based receptors have been widely utilized in the detection of the HSO_4^- ion. Here, both bespoke synthesized receptors as well as commercially available chemosensors have been utilized efficiently. Most of the indole derivatives utilize hydrogen bonding interactions with the HSO_4^- ion, which can represented in generalized form in **Figure 16**. Interestingly, several indole derivatives display sharp chromogenic color changes upon interaction with the HSO_4^- ion, which may prove to be a beneficial feature for the simple real-world visual detection of the anion without the need for expensive instrumentation. In addition, several different opto-chemical logic devices, passwords, and trajectories have been prepared for application in modern security devices.

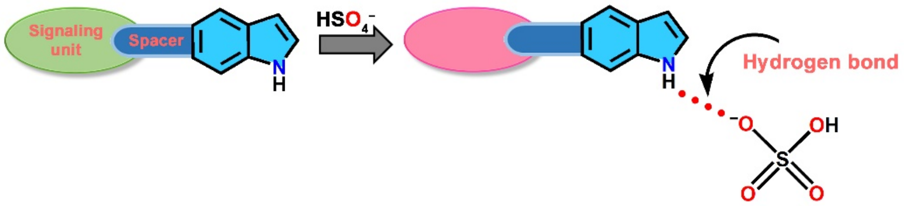

Figure 16: The general mode of binding of the indole-based chemosensors with the HSO$_4^-$ ion.

3.6. Macrocycle moiety based detection.

There are several macrocyclic entities like smaragdyrin and sapphyrin derivatives,[146] oligopyrroles,[147] porphyrin scaffolds,[148] cyclam, calixarenes, cyclodextrins, aza crown ether derivatives,[149] cyclic BODIPY derivatives,[150] cucurbit[n]urils,[151] calixoxa and calixthiasmaragdrins derivatives, calix[n]arenes, and pillar[n]arenes,[152-155] which have a long history of diverse applications in catalysis, as nonlinear optical materials, drug delivery, ion-responsive transmembrane channels, photodynamic therapy sensitizers, molecular machines, information storage technology, and fluorescent chemosensors.[146-157] Such macrocyclic and interlocked derivatives have been widely used in the selective and sensitive recognition of anions. In the following section, the exploration of such macrocyclic derivatives that have been utilized in the fluorescent detection of the HSO$_4^-$ ion is discussed.

In 2008, Shen *et al.* developed three metal complexes of a xanthone-crown ether derivative among which the Mg^{2+} complex (**50**, **Scheme 26**) acted as a colorimetric and fluorescent chemosensor for the HSO$_4^-$ ion with excellent selectivity and sensitivity in MeCN.[158] Upon interaction with the HSO$_4^-$ ion, **50** displayed a blue shift of its absorption band from 380 to 340 nm with a new band also appearing at 430 nm and consequent chromogenic color change from colorless to yellow. In contrast, the ion caused significant quenching of the emission band of **50** at 450 nm (λ_{ex}= 320 nm). However, the H$_2$PO$_4^-$ ion also caused a similar type of quenching. Further studies revealed that the HSO$_4^-$ ion was more strongly bound with the xanthone-crown ether than the Mg^{2+} ion and replaced the cation, resulting in a red-shifted absorption band and chromogenic color change (**Scheme 26**). Notably, the xanthone-crown ether derivative could be employed in the extraction of Mg^{2+} ions by HSO$_4^-$ ion.

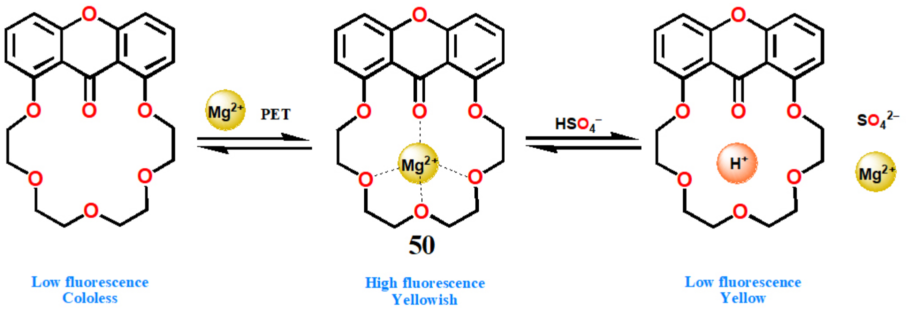

Scheme 26: The binding mechanism between **50** and the HSO$_4^-$ ion.

In 2011, a new and unique strategy was reported by Tripathi and Pandey in which detection of the HSO$_4^-$ ion was achieved via sol-gel conversion.[159] In this report, a pair of bile acid derivatives were synthesized (**51-52**, **Figure 17**) and the anion recognition behavior was explored. In CHCl$_3$-DMSO (1:5; v/v) mixed solvent, probe, **51**, formed a stable gel exclusively in the presence of the HSO$_4^-$ ion (**Figure 17**) through the imidazolium and amide moieties interacting strongly with the HSO$_4^-$ ion through hydrogen bonding interaction. The hydrogen bond-induced aggregation and consequent sol-gel conversion in the presence of (TBA$^+$ HSO$_4^-$) was confirmed from the upfield shift of peaks of the amide-NH and aryl-CH protons of **51** in its ^{1}H NMR spectrum along with SEM and TEM images. The other analogous probe, **52**, containing a pyridine unit displayed affinity towards the HSO_4^- ion but did not exhibit the sol-gel transformation behavior. Additionally, **52** displayed poor selectivity with the $H_2PO_4^-$ ion. These two factors reduced its potential use as a chemosensor for HSO_4^- ion. Notably, such HSO_4^- ion-induced sol-gel conversion might be used as a unique and novel strategy for the exclusive visual recognition of the anion.

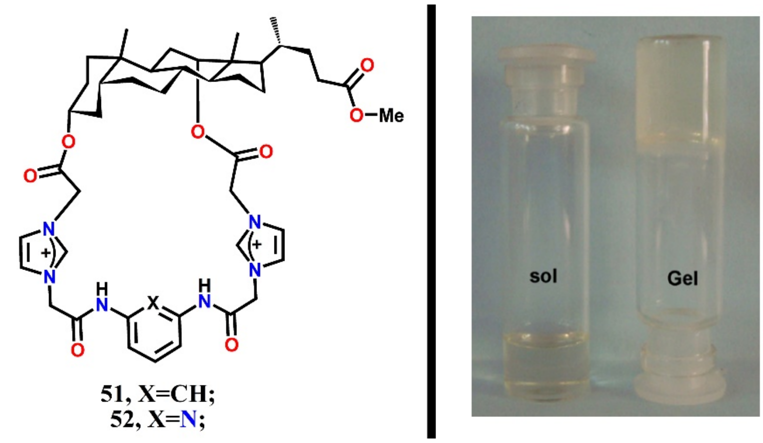

51, X=CH;
52, X=N;

Figure 17: Molecular structure of probes, **51** and **52** (left); image of HSO_4^- ion induced sol-gel conversion of **51** in $CHCl_3$-DMSO (5:1; v/v) mixed solvent (right). (Reprinted with permission from Ref 159. Copyright 2011, Elsevier).

In the following year, a sugar-azacrown ether derivative (**53**, **Scheme 27**) was successfully deployed in the selective fluorescent detection of HSO_4^-in MeOH.[160] The probe only showed a "turn on" fluorescence response in the presence of the HSO_4^- ion with a 1:1 binding stoichiometry and 1.39 × 10^{-6} M detection limit. Strong hydrogen bonding between the probe and the HSO_4^- ion within its inner cavity increased rigidity and the consequent "turn-on" fluorescent response (**Scheme 27**). Such host-guest complexation of the bisulfate ion is very rare in the literature.

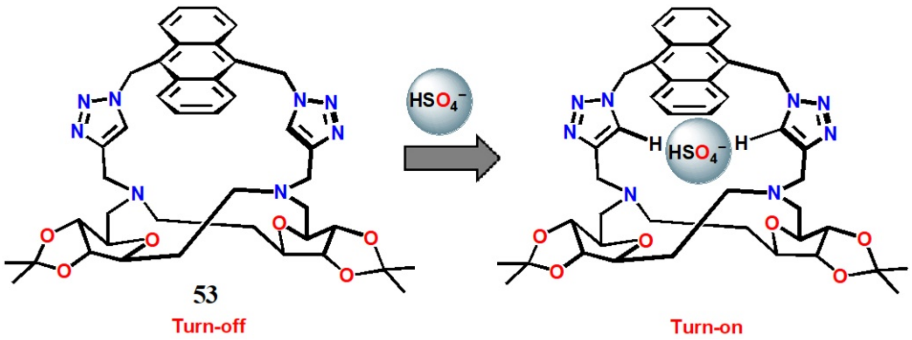

Scheme 27: Proposed binding mechanism between **53** and the HSO_4^- ion.

In the same year, Liu *et al.* synthesized a ditopic macromolecule integrating two bisindole moieties and a bis-benzocrown ether scaffold (**54**, **Scheme 28**) that recognized the HSO_4^- ion in a cooperative manner.[161] The probe was also very effective at detecting F^-/ K^+ ions and the F^--K^+ ion pair in DMSO. The probe efficiently recognized HSO_4^- ion in the presence of K^+ ion via naked-eye color change. The addition of HSO_4^- ion to the ditopic probe did not show any color change but in the presence of the K^+ ion, it displayed a naked-eye detectable color change to orange. This occurred due to the hydrogen bonding interaction between the molecule, **54** and two HSO_4^- ions (**Scheme 28**).

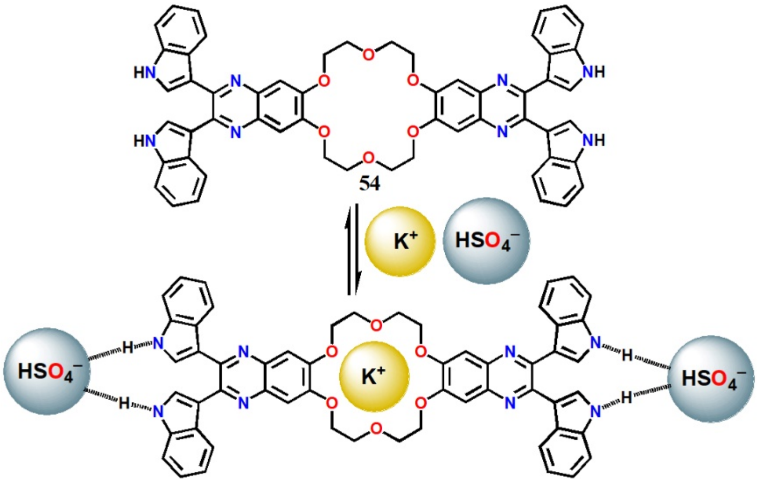

Scheme 28: Proposed binding mechanism between **54**, K^+ and the HSO_4^- ion.

In 2013, Song *et al.* designed and synthesized a cyclic benzo-bisimidazole derivative (**55**, **Scheme 29**) which acted as a fluorescent probe that recognized the HSO_4^- ion selectively and sensitively in HEPES buffered MeCN (9:1; v/v; HEPES buffer: MeCN; pH= 7.4) medium.[162] Here, the HSO_4^- ion bound with the probe in such a manner that it enhanced the hydrogen bond donor ability of the aryl C-H group and enhanced the rigidity of the architecture of the two benzobisimidazole groups. Such specific binding of the HSO_4^- ion facilitated the rare optical detection of the anion using a cyclic probe. The formation of multiple hydrogen bonds of HSO_4^- ion within the pocket of cyclic benzo-bisimidazole was further explored by the absorption, fluorescence, and ^{1}H NMR spectroscopic studies.

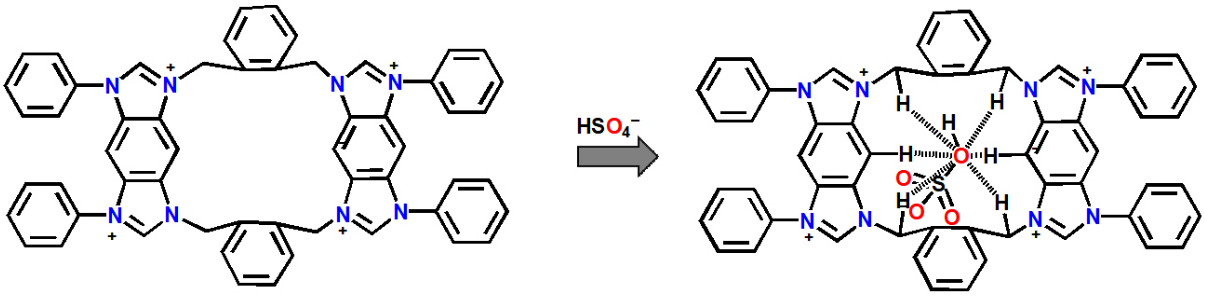

55

Scheme 29: Proposed binding mechanism between **55** and the HSO_4^- ion.

Later, Chatterjee *et al.* developed a series of calixoxa and calixthiasmaragdrins derivatives that were characterized by several spectroscopic techniques including HR-MS, 1D and 2D NMR spectroscopy, absorption studies, and XRD structure.[163] Interestingly, one calixthiasmaragdrin (**56**, **Scheme 30**) displayed selective chemosensory responses towards the HSO_4^- ion in chloroform. The addition of the HSO_4^- ion to a solution of **56** induced a red shift of the absorption band from 445 nm to 476 nm; the Q-type absorption band of **56** also disappeared upon binding. Detection was also easily visualized by the naked eye through a color change from green to yellow and the 1:1 binding stoichiometry due to the formation of hydrogen bonding driven host-guest complex explored.

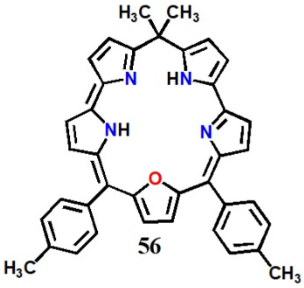

56

Scheme 30: The structure of chemosensor **56**.

In 2016, another macrocyclic fluorescent probe (**57**, **Scheme 31**) containing one calix[4]arene and four benzothiazole units that selectively recognized Cu^{2+}, S^{2-} and HSO_4^- ions in a MeCN-H_2O (4:1; v/v) mixed solvent.[164] Unlike other anions, in the presence of the HSO_4^- ion **57** displayed a ratiometric shift of its absorption band from 462 nm to 365 nm, which was accompanied by a yellow to colorless naked-eye detectable color change and also a nearly 10-fold increase of fluorescence intensity (λ_{ex}= 365 nm; λ_{em}= 542 nm). In the presence of the HSO_4^- ion, the fluorescence enhancement originated due to the hydrolytic cleavage of the imine bond of **57** and the generation of its component aldehyde and trisamine derivatives (**Scheme 31**). This hydrolytic dissociation was further confirmed by FTIR spectral analysis and ^1H NMR titration studies. Notably, **57** was able to detect the HSO_4^- ion up to 9.79×10^{-7} M^{-1}.

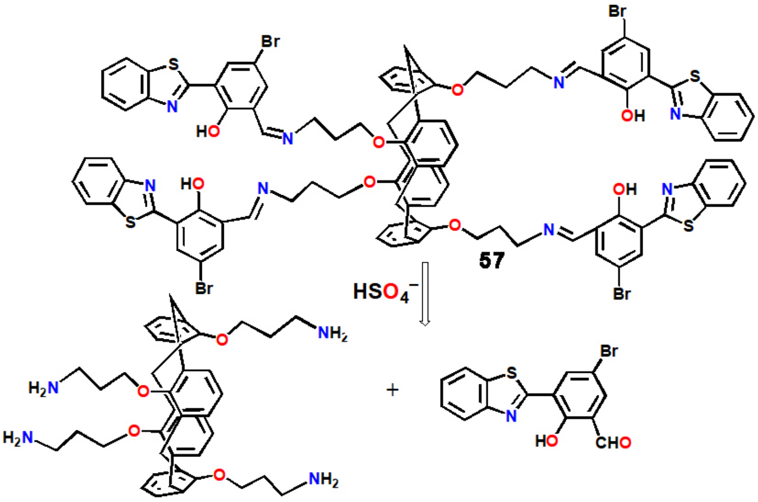

Scheme 31: Proposed binding mechanism between **57** and the HSO_4^- ion.

Later, a pendant-like tetra-aza macrocyclic fluorophore (**58**, **Scheme 32**) was synthesized which efficiently detected the Hg^{2+} ion via a "turn off" fluorescence response due to chelation enhanced quenching (CHEQ). However, **58** was able to recognize the HSO_4^- ion via a "turn on" fluorescence response.[165] In the HEPES buffered MeCN medium, the HSO_4^- ion initiated significant enhancement of fluorescence intensity of the probe at 490 nm, which facilitated high fidelity fluorescent detection of the anion (LOD= 7.0 μM). Such spectroscopic changes were driven by the formation of intermolecular hydrogen bonding between the probe and anion and the subsequent CHEF effect and the non-toxic probe was able to detect the HSO_4^- ion in model living systems via fluorescence imaging.

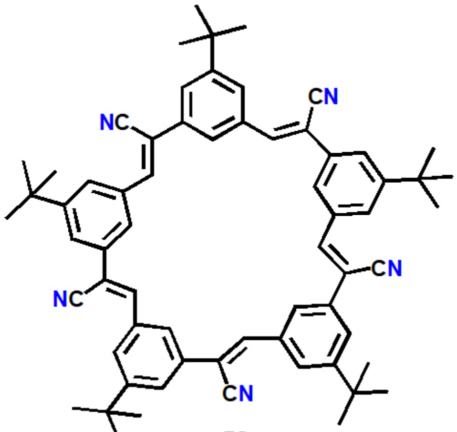

58

Scheme 32: Molecular structure of **58**.

Shin *et al.* then developed a fluorescent probe (**59**, **Scheme 33**) by combining three moieties, tolan, aza-crown ether, and urea, and explored its cooperative ion-pair ($Na^+HSO_4^-$) receptor behavior in MeCN.[166] In MeCN, **59** displayed its characteristic absorption bands at 317 and 342 nm which changed slightly in the presence of the Na^+ ion but changed significantly in the presence of both Na^+ and HSO_4^- ions. In fact, the Na^+ ion binding affinity was found to be stronger in the presence of the HSO_4^- ion. The 1:1 binding stoichiometry between **59** and the $Na^+HSO_4^-$ ion-pair was also confirmed with the emission band of **59** sharply quenched, driven by the photoinduced electron transfer (PET) process. In addition, a 16 μM detection limit was also confirmed and a reversible fluorescent response opto-chemical logic gate was also designed. A structurally similar derivative (**60**, **Scheme 33**) was reported containing an aza-12-crown-4 base.[167] As expected it also displayed ion-pair receptor phenomenon for the Li^+-HSO_4^- ion-pair in DCM with the formation of hydrogen bonding interactions between the receptor and HSO_4^-confirmed from analysis of ^1H NMR titration and DFT studies.

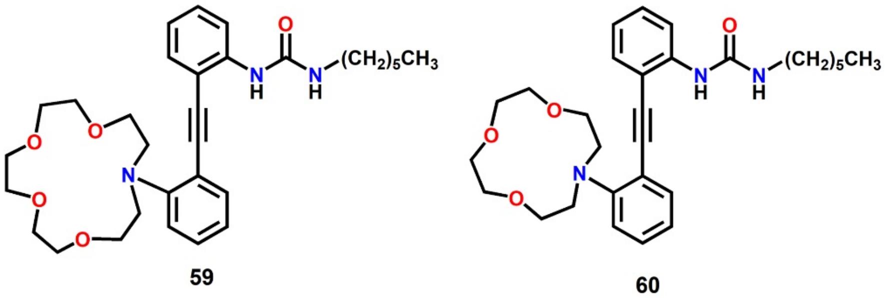

59

60

Scheme 33: Molecular structure of **59** and **60**.

The next year a bis-benzimidazolium conjugated *N*-heterocyclic Ag(I) based macrometallocycle (**61**, **Scheme 34**) was developed and employed in the selective and sensitive detection of HSO_4^- in CH_2Cl_2-DMSO (99:1; v/v) medium.[168] Upon addition of the HSO_4^- ion, the probe displayed enhancement of an absorption band in the range of 250-400 nm and a sharp increase of the emission band at 363 nm. A 1:2 (Probe: HSO_4^-) binding stoichiometry and 7.5 nM detection limit were also confirmed with the two hydrogen sulfate ions situated outside of the macrocyclic sphere via interactions between the metal and oxygen of the anion together with CH••••O hydrogen bonds. The weak fluorescence of the free probe due to PET quenching of the azobenzene form was turned off by binding of the HSO_4^- ions resulting in the "turn on" fluorescence response.

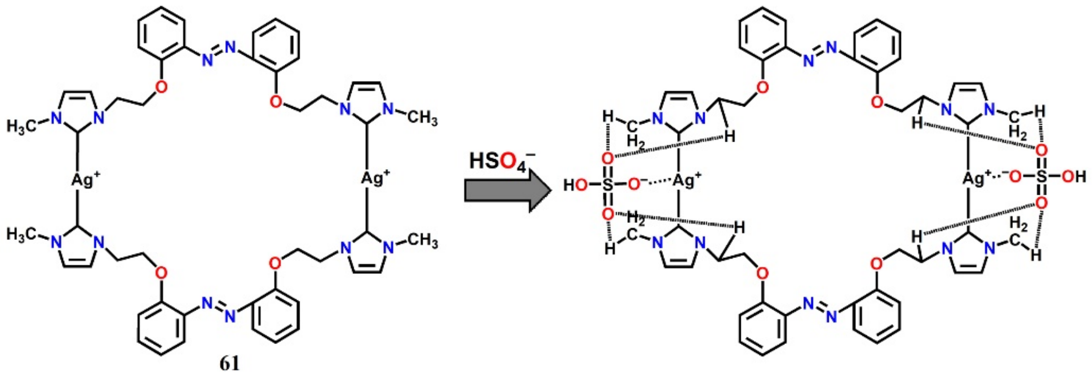

Scheme 34: Proposed binding mechanism between **61** and the HSO_4^- ion.

In 2020, Sethupathi *et al.* synthesized a macrocyclic probe (**62**, **Scheme 35**) by assembling bromosalicyladehyde and azamacrocyclic moieties which acted as an “off-on” fluorescent sensor for the HSO_4^- ion and an “on-off” fluorescent sensor for Hg^{2+} in HEPES buffered MeCN.[169] The probe formed a 1:1 complex with HSO_4^-via chelation and displayed a chelation-enhanced fluorescence response. The binding constant of the complex was very high (5.58×10^5 M^{-1}) and the micromolar scale detection limit (LOD = 7 µM). The probe was non-toxic and biocompatible and it was successfully employed in live cell imaging in breast cancer cells. A time-correlated single-photon counting (TCSPC) study revealed the significant enhancement of lifetime from 0.47 to 1.02 ns upon hydrogen bonding promoted chelation and subsequent promotion of rigidity of the probe.

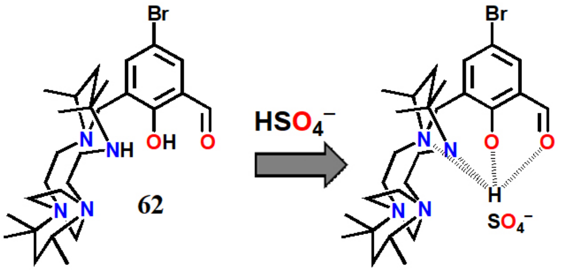

Scheme 35: Proposed binding mechanism between **62** and the HSO_4^- ion.

Recently, a novel pyrene-ester- calix[4]triazolium integrated fluorescent sensor (**63**, **Scheme 36**) was developed and employed for the selective detection of the HSO_4^- ion via the formation of a 1:1 stoichiometric sensor- HSO_4^- complex.[170] The selectivity for the HSO_4^- ion of the probe was developed due to the perfect spatial orientation of the anion allowing it to be involved in hydrogen bonding with the probe molecule. The fluorescence ‘turn on’ response of the probe was observed due to the restriction of oxidative PET phenomenon from pyrene to triazolium moiety of the probe. This artifact was well explored and argued through a well-organized DFT study.

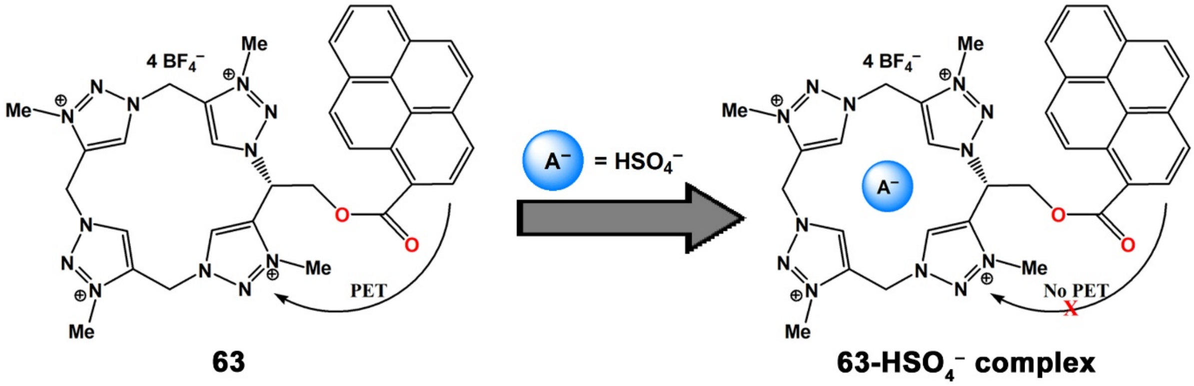

Scheme 36: Proposed binding mechanism between **63** and the HSO_4^- ion.

In this section, the fluorescent probes are composed of an extremely diverse range of binding motifs and fluorophores, and a wide range of derivatives has been utilized to achieve the selective and sensitive detection of the HSO_4^- ion. Most of the probes rely on a host-guest binding strategy, although some of the chemosensors not only recognized the HSO_4^- ion but also acted as ion-pair receptors; in some cases, the chemosensors could be used to extract a particular metal ion. Moreover, in addition to the solution phase detection by chromogenic color change, a sol-gel conversion technique was also utilized for its detection. In some cases, bio-imaging of HSO_4^- ion was also performed with the chemosensors displaying low toxicity and good biocompatibility. Interestingly, in most cases, the chemosensor was involved in multiple and strong hydrogen bonding interactions with the HSO_4^- ion. Therefore, a generalized mechanism for the detection of the HSO_4^- ion by macrocyclic ligands is presented in **Figure 18**.

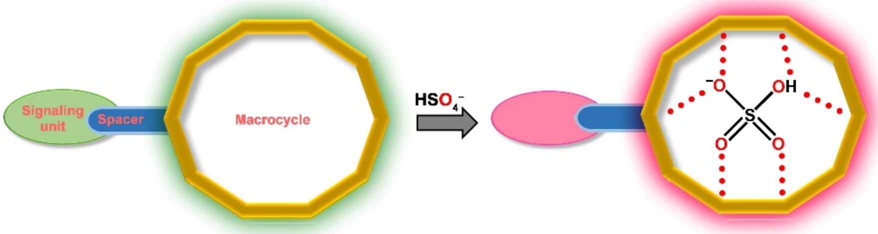

Figure 18: The general mode of binding of the macrocycle-based chemosensors with the HSO_4^- ion.

3.7. Pyridine moiety-based detection.

The pyridine moiety has widely been used in the synthesis of several fluorophore derivatives, which have been used for a variety of purposes,[171-172] including in thermotropic mesogens,[173] clinical applications as drugs and food,[174] perovskite solar cells and organic light-emitting diodes.[175] However, pyridine-based ligands have been extensively utilized in the synthesis of interlocked molecules and the detection and imaging of different analytes.[176-177]

In 2011 three analogous fluorophores, integrating pyridine-furan and pyrimidine moieties (**64-66**, **Scheme 37**), displayed excellent chemosensory response towards the HSO_4^- ion in polar protic medium ($CHCl_3$-MeOH; 9:1; v/v)[178] and all three probes displayed strong fluorescence quenching in its presence. Notably, in addition to other common anions, the isostructural $H_2PO_4^-$ was unable to impart any significant changes in the fluorescence behavior of the probes. Chemosensor **64** was involved in bifurcated hydrogen bonding with two HSO_4^- ions at the two ends of the fluorophore leading to the observed spectroscopic changes that facilitated its selective chemosensory behavior (**Scheme 37**).

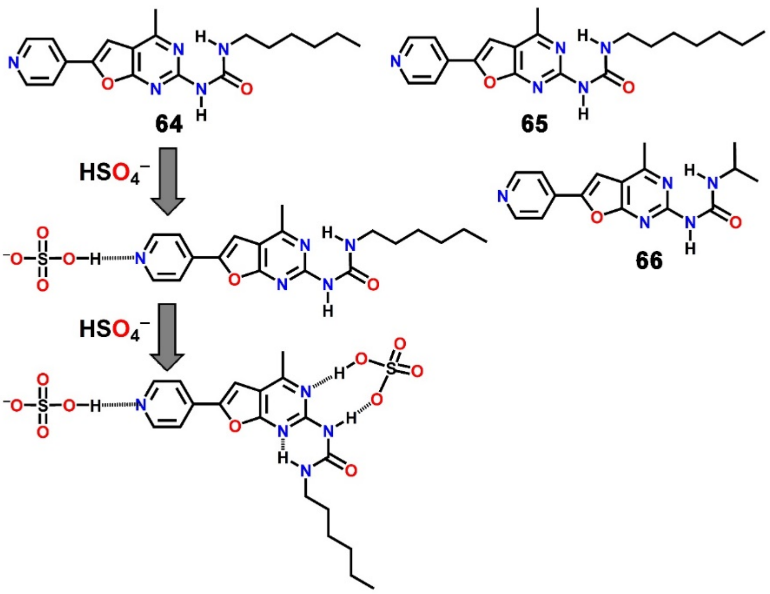

Scheme 37: Molecular structure of chemosensors **64**-**66** and proposed binding mechanism between **64** and the HSO_4^- ion.

Small molecule organic fluorophore-based chemosensors for the HSO_4^- ion are increasingly common, but the application of organic fluorophore-based nanoparticles in the detection of HSO_4^- is very rare. Dipodal aminephenol-pyridine assembled organic fluorophore-based nanoparticles **(67**, **Scheme 38)** were found to be very effective in the selective and low-concentration detection of HSO_4^- (LOD= 0.25 μM) in an aqueous medium.[179] The chemosensor exhibited a ratiometric shift of absorption maxima from 314 to 342 nm with a prominent isosbestic point and distinguishable naked-eye color change upon analyte binding. The probe also displayed a red shift of its emission maximum only in the presence of HSO_4^- of the anions tested. The probe was involved in multiple and bifurcated intermolecular hydrogen bonding with the ion (**Scheme 38**) and the 1:1 probe-HSO_4^- complex stoichiometry was well supported through DFT calculations. Interestingly, the iso-structural $H_2PO_4^-$ ion failed to accommodate within the small cavity of the dipodal probe to facilitate a recognition event.

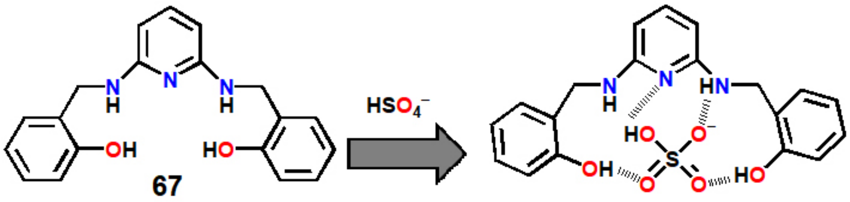

Scheme 38: Proposed binding mechanism between **67** and the HSO_4^- ion.

Thereafter, another fluorescent organic nanoparticle of the tripodal pyridine-naphthalene derivative (**68**, **Scheme 39**) was successfully employed in the optical detection of HSO_4^- in DMF-H_2O (1:99; v/v) medium.[180] The nano-aggregate of the probe showed extensive quenching of emission maximum at 450 nm upon interaction with the HSO_4^- ion over other anions tested and achieved a micromolar scale detection limit (LOD= 1.12 μM). Such strong quenching of the nano-aggregate of the probe molecule occurred due to a "PET switch on" phenomenon and formed a stable complex with a very high binding constant of 6.68×10^7 M^{-1}. The chemosensor system was also very effective in the precise estimation of HSO_4^- concentration in real samples.

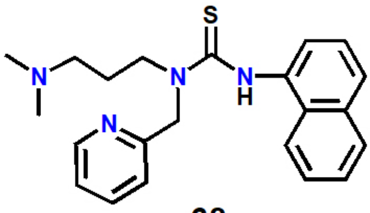

68

Scheme 39: Molecular structure of chemosensor **68**.

In 2015, Wan *et al.* developed a ferrocene-pyridine assembled derivative (**69**, **Scheme 40**) that acted as a Pb^{2+}-HSO_4^- ion pair sensor fluorometrically facilitated by a clear color change phenomenon in MeCN.[181] In the presence of Pb^{2+}, **69** displayed considerable promotion of its emission intensity at 420 nm (λ_{ex}= 350 nm). In the presence of Zn^{2+}, similar fluorometric changes were also observed but not to the same extent. Subsequently, the HSO_4^- ion further promoted the emission intensity of both the complexes, **69**-Pb^{2+} and **69**-Zn^{2+}, whereas the other anions tested quenched the emission intensity. From ^{1}H NMR titration and DFT data analysis, it was proposed that binding of the metal ion inhibited the PET process of the probe and that the HSO_4^- ion was involved in multiple hydrogen bonding interactions with the metal complex. In addition, the electrochemical behavior of the probe was also analyzed in the absence and presence of the ion pair.

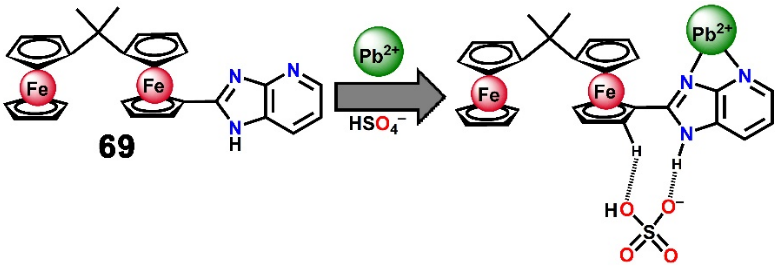

Scheme 40: Proposed binding mechanism between **69** and the HSO_4^- ion.

An isonicotiamide based fluorescent probe (**70**, **Scheme 41**) was then designed and developed and it was successfully employed in the highly selective fluorescent detection of Zn^{2+} and HSO_4^- ions independently in semi-aqueous medium (MeCN-H_2O; 1:1; v/v).[182] The weakly fluorescent **70** became highly fluorescent, with an emission maximum at 425 nm upon binding with the HSO_4^- ion, forming a 1:1 probe-anion complex able to detect the ion down to the sub-nanomolar scale (LOD= 0.95 nM). The "turn on" fluorescence response was driven by intermolecular hydrogen bonding between the probe and the HSO_4^- ion (**Scheme 41**). In addition, **70** was effective in imaging the anion and Zn^{2+} within HeLa cells (**Figure 19**) and the fluorescence responses were intelligently utilized in designing opto-chemical logic gates.

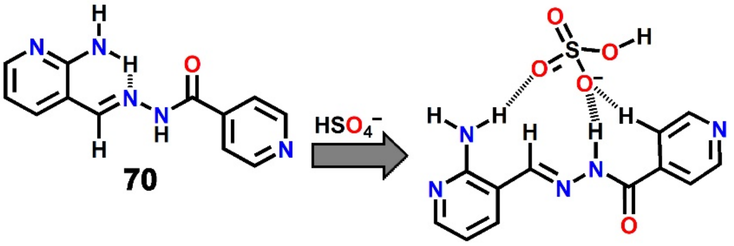

Scheme 41: Proposed binding mechanism between **70** and the HSO_4^- ion.

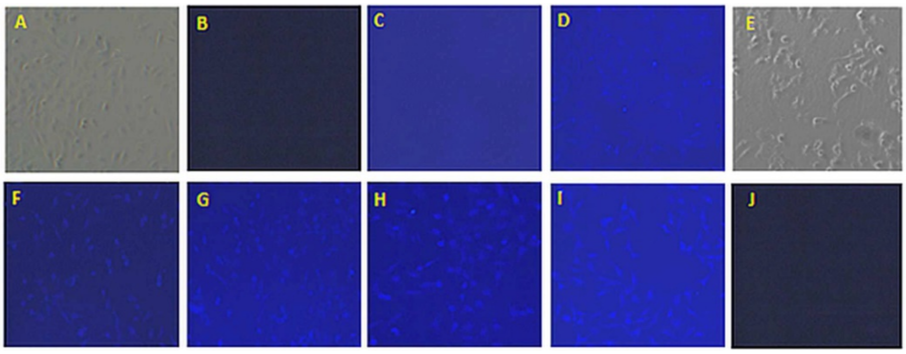

Figure 19: Fluorescence imaging of **70** within HeLa cells in the absence and presence of the HSO_4^- ion (Top) and Zn^{2+} (Bottom) under different conditions, (A: Phase contrast; B: Under UV filter; C: With receptor **70;** D: **70** for 2 hours and HSO_4^- (25 µM) for 1 hour; E: Phase contrast image treated with Zn^{2+} (25 µM) only; F: **70** for 2 hours and Zn^{2+} (2.5 µM) for 1 hour; G: **70** for 2 hours and Zn^{2+} (5 µM) for 1 hour; H: **70** for 2 hours and Zn^{2+} (10 µM) for 1 hour; I: **70** for 2 hours and Zn^{2+} (25 µM) for 1 hour; J: Cells treated with Zn^{2+} (25 µM) only). (Reprinted with permission from Ref 182. Copyright 2016, Royal Society of Chemistry).

Granados *et al.* developed a pyridine-ruthenium complex and the sequence-specific chemosensory responses of AcO^- followed by the HSO_4^- ion was efficiently explored in MeCN-H_2O mixed solvent (2:8; v/v).[183] The emission intensity was strongly quenched in the presence of the acetate ion and subsequently recovered in the presence of the HSO_4^- ion driven by the PET phenomenon and both anions could be imaged within living cells (**Figure 20**); the PET-driven fluorescent "on-off" responses were well justified by analyzing DFT data.

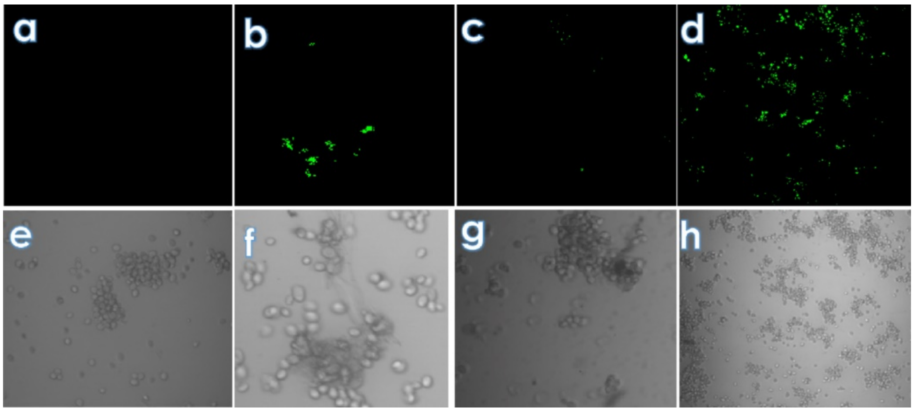

Figure 20: Confocal images of saccharomyces cerevisiae cells in the presence of Ru^{3+}complex; Ru-complex-acetate; Ru-complex + acetate + HSO_4^- under UV and visible light. (Reprinted with permission from Ref 183. Copyright 2018, Elsevier).

Very recently, Fernandes and Dey developed a pyrene-pyridine integrated pH-sensitive donor-acceptor type fluorescent probe (**71**, **Figure 21**) that formed a nanoscale aggregate in an aqueous environment.[184] Interestingly, **71** displayed TICT behavior in a non-polar organic solvent but surprisingly exhibited TICT and AIE behavior in water (**Figure 21**). The probe displayed a naked-eye color change from pale yellow to deep yellow only through interactions with HSO_4^- in an aqueous medium. The HSO_4^- ion was involved in hydrogen bonding with the pyridinic nitrogen atom of **71** and as a consequence, a change in charge transfer behavior and subsequent enhancement of aggregation of the chemosensor were observed. Moreover, a paper-strip-based portable kit was designed for real-life *in situ* monitoring of HSO_4^- in water samples (**Figure 21**) enabling operationally simple state-of-the-art detection of the HSO_4^- ion.

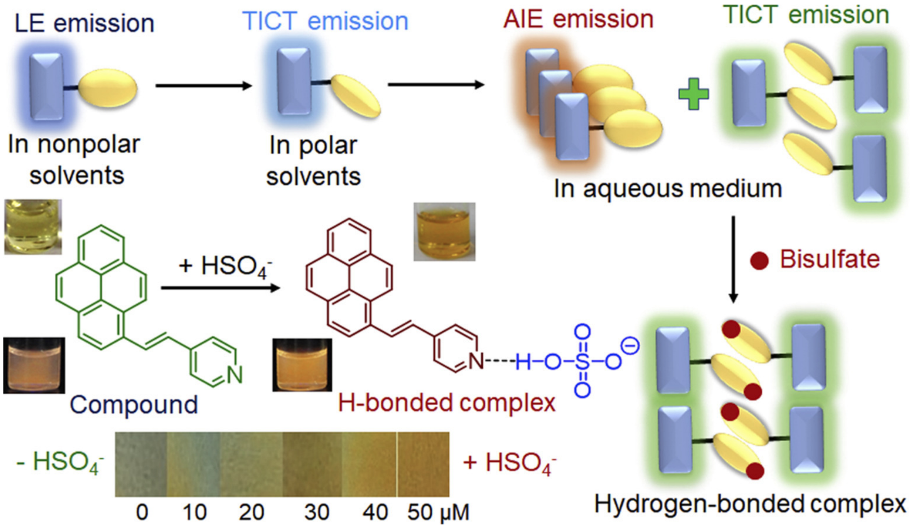

Figure 21: TICT and AIE mechanism of **71** along with the mode of interaction with the HSO_4^- ion and naked-eye color change of the paper-strip wet with the chemosensor solution. (Reprinted with permission from Ref 184. Copyright 2023, Elsevier).

Very recently, Fernandes *et al.* consecutively reported two different pyridine-end HSO_4^- ion sensors in two different reports.[185,186] In the first report, a pyridine-end oligo *p*-phenylenevinylene derivative (**72**, **Scheme 42**) was developed that consecutively recognized HSO_4^- ion followed by fluoride ion both chromogenically and fluorimetrically in a sequence-specific relay technique. In addition to naked-eye color change, the presence of the bisulfate ion initiated the protonation of the probe molecules augmenting the amphiphilic characteristics and resulting in the formation of nanostructures via self-assembly.[185]

In the next report, the group developed a pair of triphenylamine-pyridine based push-pull dyes linked by pyridinic linkage (**73** and **74**, **Scheme 42**) that recognized the HSO_4^- ion in pure water. Intermolecular and bifurcated hydrogen bonding between the probe and HSO_4^- ion enhanced the ICT character of the probe resulting in a notable red-shift of the absorption band. Despite spectroscopic changes, the probe displayed extensive self-assembly behavior after the addition of the HSO_4^- ion. Detection of the HSO_4^- ion in this way in pure water remains very rare and worthy of real-life application.[186]

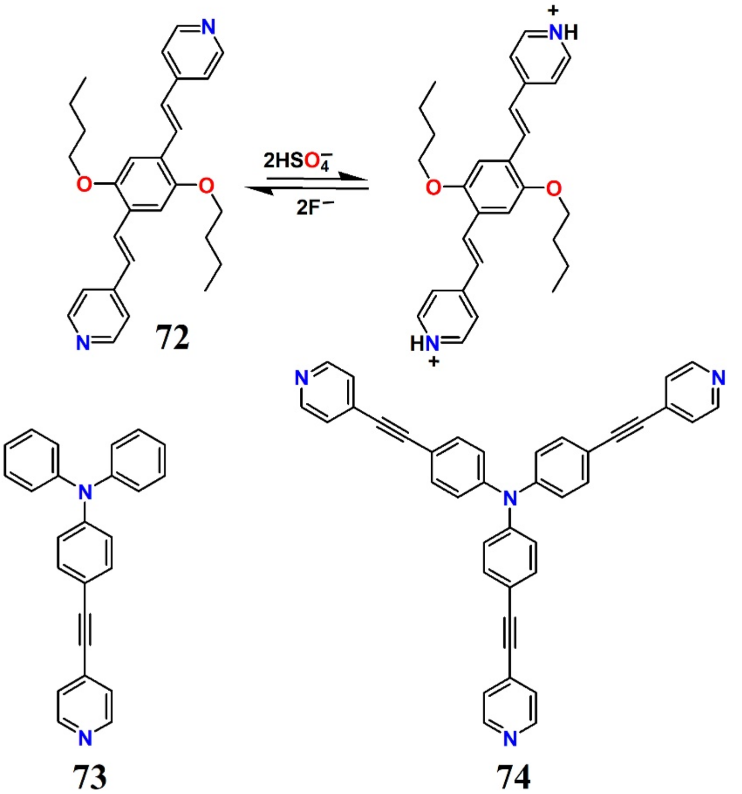

Scheme 42: Proposed binding mechanism between **72** and the HSO_4^- ion and molecular structure of **73** and **74**.

Thus, the pyridine moiety has played a significant role in the detection of the HSO_4^- ion. The basic nature of the pyridinic nitrogen helped chemosensors to be involved in hydrogen bonding or proton transfer with the acidic proton of the anion. Using this particular basic strategy several research groups have developed a series of other fluororphore-integrated pyridine-based colorimetric and fluorescent probes where pyridine acted as a binding unit and the integrated fluorophore acted as the signaling unit as shown in **Figure 22**.

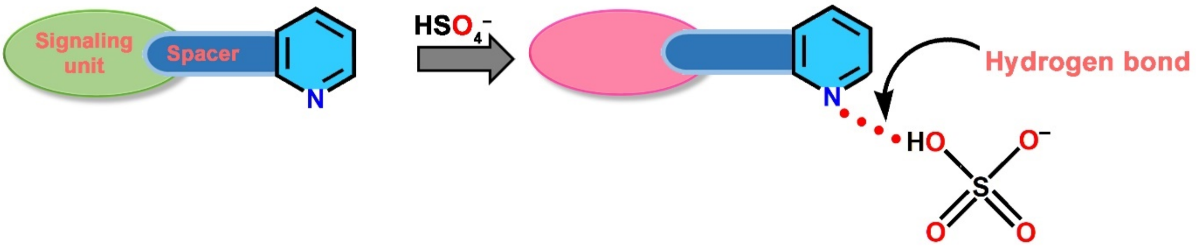

Figure 22: The general mode of binding of pyridine-based chemosensors with the HSO_4^- ion.

3.8. Quinazoline and quinoline moiety-based detection.

Quinazoline and quinoline are very popular bicyclic heterocyclic moieties that have found multiple applications and their derivates have been extensively utilized in various types of drug and biological molecules,[187-188] agricultural fertilizers[189] and fluorescent chemosensors.[190-195] In the following section, the reports on the quinazoline and quinoline-based HSO_4^- ion chemosensors are summarized and their key strengths are highlighted.

In 2012, Alfonso *et al.* synthesized a ferrocene-imidazoquinoxaline assembled chemosensor (**75**, **Scheme 43**) which itself did not show any spectroscopic responses in the presence of the HSO_4^- ion, but its Pb^{2+} and Zn^{2+} metal bound complexes were effective sensors.[190] In the presence of either of the metal ions, **75** displayed a dramatic increase of emission intensity at 475 nm with concomitant enhancement of quantum yield. The probe-metal ion complex formed in 1:1 stoichiometry with the HSO_4^- ion with very high binding constants ($K_a = 7.31 \times 10^7$ M^{-1} for **75**-Pb^{2+} and $K_a = 1.99 \times 10^6$ M^{-1} for **75**-Zn^{2+}). Despite metal coordination, HSO_4^- ion also played an important role in the protonation of the iron atom of the ferrocene moiety and brought such unique spectroscopic changes and it represents a rare example where a HSO_4^- ion chemosensor is composed of a redox unit and a fluorophore unit.

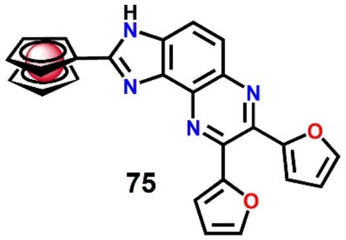
75

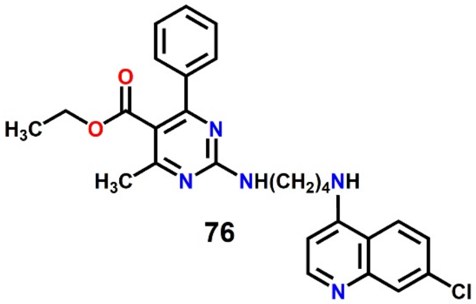
76

Scheme 43: Molecular structure of chemosensors, **75** and **76**.

In 2013, a quinoline-based fluorophore (**76**, **Scheme 43**) recognized the HSO_4^- ion via a "turn off" fluorescence response.[191] The emission band of **76** at 376 nm was sharply quenched upon interaction with the HSO_4^- ion with the probe forming a 1:1 hydrogen-bonded complex. Although such switch-off sensors are less desirable than their switch-on analogs, the quenching was extremely selective towards HSO_4^- and was not impacted by the tetrahedral $H_2PO_4^-$ ion.

A quinazoline-based probe (**77**, **Scheme 44**) recognized the HSO_4^- ion in a HEPES buffered EtOH-H_2O (1:5; v/v) polar protic environment at biological pH.[192] In the presence of the HSO_4^- ion, **77** formed a 1:1 complex via protonation of the quinazoline nitrogen followed by an intermolecular hydrogen bonding induced CHEF phenomenon. Consequently, HSO_4^- ion inhibited PET from the benzimidazole to the *o*-anisyl moiety, thereby enhancing the emission intensity (**Scheme 44**). The detection of the HSO_4^- ion in the semi-aqueous medium, at biological pH, with a nanomolar scale detection limit (LOD= 28.72 nM) and low toxicity of the probe within HeLa cells was an impressive addition to the class of chemosensors.

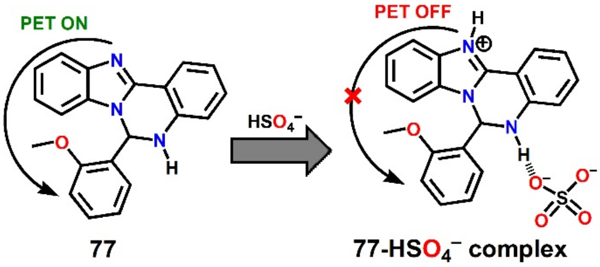

Scheme 44: Binding mechanism and hydrogen bonding motif of **77** with the HSO_4^- ion.

In 2015, a quinazoline-diarylethene based photochromic probe (**78**, **Figure 23**) displayed color-changing phenomena from colorless to purple upon irradiation with UV-light and a reverse color change upon irradiation with visible light (λ >500 nm) in MeCN.[193] The probe acted as a ratiometric fluorescent chemosensor for Cu^{2+} and HSO_4^- ions. With the introduction of HSO_4^- ion, the emission band of the probe at 427 nm reduced in intensity with the simultaneous promotion of a new band at 491 nm. The spectroscopic change was accompanied by a distinct color change from blue to bright cyan due to the formation of 1:1 hydrogen-bonded complexation (**Figure 23**).

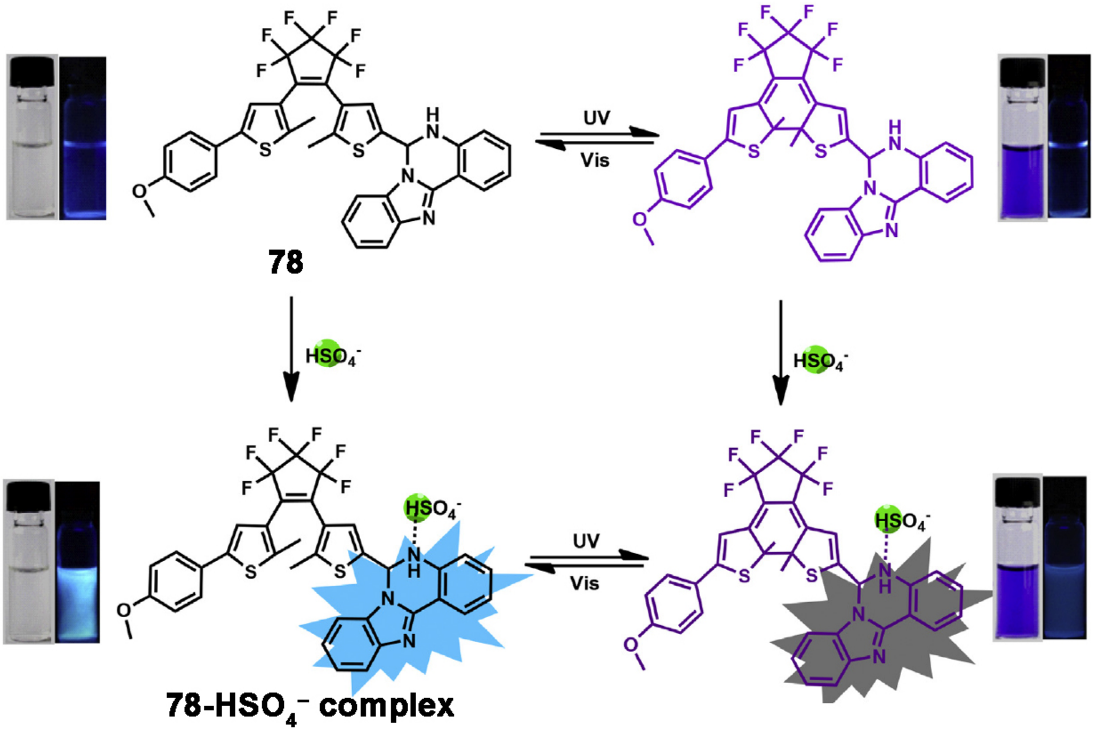

Figure 23: UV-Vis light-driven stimuli-responsive switching of **78** along with the mode of interaction with the HSO_4^- ion and respective color changes under daylight and UV light. (Reprinted with permission from Ref. 193. Copyright 2023, Elsevier).

In 2021, the quinazoline-rhodamine assembled probe (**79**, **Scheme 45**) was reported that recognized the HSO_4^- ion by a visual color change from yellow to pink in MeOH.[194] Upon interaction with the HSO_4^- ion, a new absorption band at 558 nm and a fluorescent "turn on" band at 609 nm were observed due to lactam ring-opening and subsequent extension of conjugation. It was also shown that **79** was able to detect the HSO_4^- ion in solid paper strip and gel form.

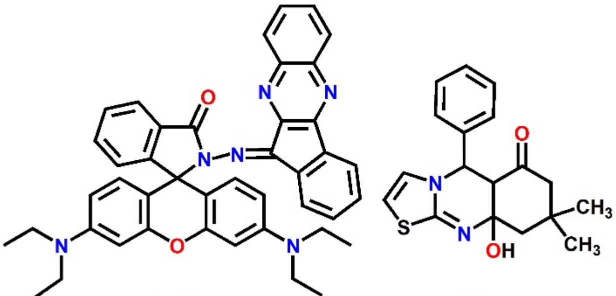

79 **80**

Scheme 45: Molecular structure of the chemosensors, **79** and **80**.

Thereafter, a series of thiazoloquinazoline-based fluorescent probes (**80**, **Scheme 45**) were developed using a one-pot multicomponent relay reaction utilizing microwave radiation methodology.[195] The fluorophores were employed for selective and micromolar scale "turn on" fluorescent detection of the HSO_4^- ion (λ_{ex}= 404 nm, λ_{em}= 460 nm) in polar protic medium (MeOH-H_2O; 20:80; v/v). The recognition of HSO_4^- ion was initiated by the formation of a 1:1 hydrogen-bonded complex and the binding mechanism was well supported by a DFT study.

Thus, there are only a few reports on quinoline and quinazoline-based colorimetric and fluorescent sensors for the detection of the HSO_4^- ion. There therefore remains huge potential to develop new chemosensors based on these motifs. It is difficult to propose a generalized mechanism for the quinoline and quinazoline-based HSO_4^- chemosensors but most bind with a metal ion and then the fluorophore-metal ion complex selectively binds with the HSO_4^- ion involving either hydrogen bonding, coordination with the metal ion or both.

3.9. Rhodamine moiety-based detection.

Rhodamine is a very popular and widely employed fluorophore due to its bright fluorescent emission, high quantum yield and the useful color change that occurs due to the spirolactam ring-opening.[196] Rhodamine-based fluorophores have been extensively used in the detection and imaging of metal ions as well as reactive nitrogen,[197-198] oxygen and sulfur species.[199] Despite this, there are relatively few reports of rhodamine-based chemosensors for the HSO_4^- ion.

Kaur *et al.* developed a rhodamine dye-based organic nanoparticle and coated the organic nanoparticle with a gold nanoparticle.[200] The inorganic-organic hybrid nanoparticle acted as a selective and sensitive (LOD= 37 µM) HSO_4^- sensor in aqueous medium. With the gradual addition of the HSO_4^- ion, the nanohybrid exhibited a sharp enhancement of emission intensity at 555 nm and the fluorescence response persisted even in the presence of other competitive anions denoting almost no interference. Interestingly, the sensor system was able to determine HSO_4^- levels in daily essential commodities like shampoos and detergents.

Felpin *et al.*, developed a rhodamine-based probe covalently linked to a hydrophilic cellulose surface (**81**, **Scheme 46**) that acted as a portable device for the selective detection of HSO_4^-in water.[201] In addition to aqueous phase detection, the device acted as a solid-state sensor. In the aqueous phase, the weak absorption band at 560 nm was strongly promoted with the broadening of the band. Interestingly, the HSO_4^- ion displayed a naked-eye detectable color change from deep pink to pale rose and achieved naked-eye detection in the 0.1-0.5 mM range. Additionally, the sensor device was recyclable and the paper-based device was extremely useful for on-site applications.

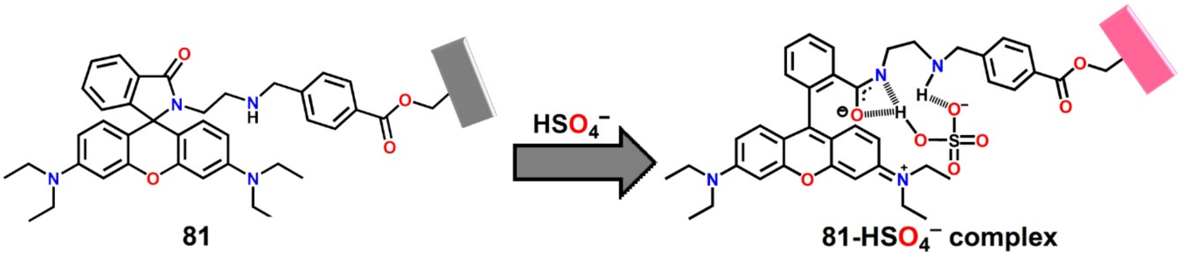

Scheme 46: The HSO_4^- ion binding mechanism of chemosensor **81**.

In 2017, Upadhyay *et al.*, developed an easily synthesizable rhodamine-based fluorescent probe (**82**, **Scheme 47**) that selectively recognized the HSO_4^- ion in aqueous medium with high sensitivity (LOD= 16.70 μM).[202] The weakly fluorescent probe became strongly fluorescent (λ_{ex}= 500 nm; λ_{em}= 544 nm) due to spirolactum ring-opening upon interaction with the HSO_4^- ion. In addition, the sensing event was also facilitated by a significant naked-eye detectable color change from colorless to pink. DFT analysis revealed that the HSO_4^- ion was involved in multiple hydrogen bonds with carbonyl oxygen and hydrazine -NH moieties of the probe (**82**, **Scheme 47**).

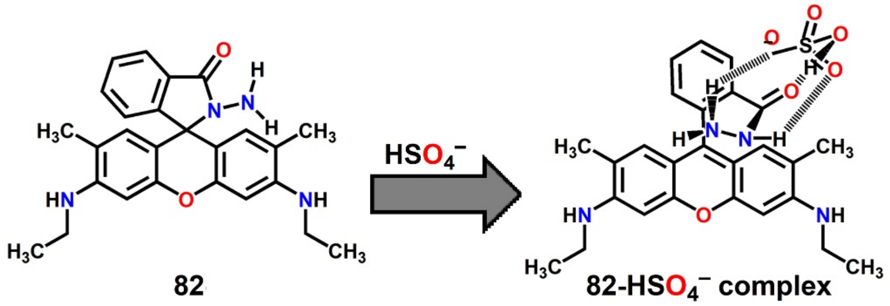

Scheme 47: The HSO_4^- ion binding mechanism of chemosensor **82**.

Despite there being relatively few examples of rhodamine-based HSO_4^- ion chemosensors as the fluorescent probes undergo HSO_4^- ion induced spirolactum ring-opening and consequent sharp naked-eye detectable color changes they represent a potentially useful class of sensor that behavior could be utilized further to develop a more efficient fluorescent probes that could be immobilized on solid-state systems for real-world sensing applications.

3.10. Schiff base ligand detection.

To this point, we have largely attempted to classify bisulfate detecting systems based on the signaling unit but Schiff bases are not as straightforward to classify as they can form part of both the signaling and binding moiety. Nonetheless, Schiff bases have found widespread applications in fluorescent sensing and imaging of cations, anions, biomolecules, pH, and bacteria.[203] Moreover, during the detection of any ion, Schiff bases have been involved in a multitude of strategies and display distinct photophysical changes[204] and have also been applied in the detection of multiple ions in living cells.[205] Unsurprisingly, given their widespread applications in sensing, Schiff bases are also a versatile category of compound that has played a significant role in the detection and imaging of the HSO_4^- ion.

Li *et al.* developed a Schiff base derivative (**83**, **Scheme 48**) containing nitrophenyl, azo benzol and carboxyl groups which displayed a significant naked-eye detectable color change along with absorption spectral changes in the presence of only the HSO_4^- ion in an aqueous medium.[206] The probe formed a very strong complex (K_a = 6.59 × 10^4 M^{-1}) with the anion driven by the formation of multiple bifurcated hydrogen bonds and achieved a detection limitation of 2.0 μM. Moreover, the system was applied in the recognition of the anion on a test strip in aqueous medium.

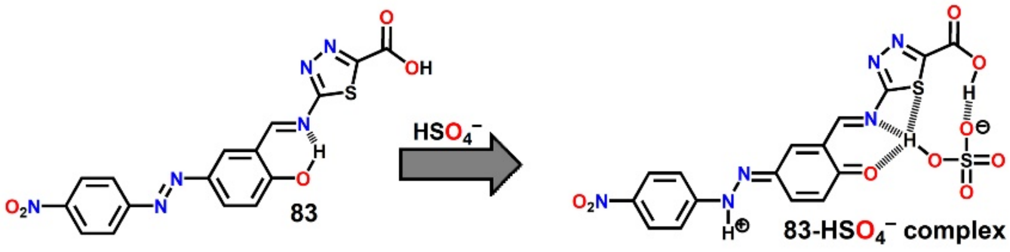

Scheme 48: The HSO_4^- ion binding mechanism of chemosensor **83**.

A Schiff base derivative (**84**, **Scheme 49**) comprised of pyrimidine and naphthalene moieties acted as a fluorescent sensor for Al^{3+} and HSO_4^-/$H_2PO_4^-$ ions in aqueous medium via "off-on-off" responses.[207] Upon binding with the Al^{3+} ion, sharp enhancement of the emission band of the probe was recorded centered at 478 nm and 502 nm due to the hindrance of "*cis-trans*" isomerism along the C=N bond of the probe. Subsequently, HSO_4^-/$H_2PO_4^-$ ions displaced the Al^{3+} ion and again the emission became switched off. Though the probe failed to distinguish between HSO_4^- and $H_2PO_4^-$ ions, it displayed reasonably high sensitivity for bisulfate (LOD= 2.91×10^{-6} M). In addition, the binding mechanism was also supported by a DFT study and the system was applied in opto-chemical logic gates and molecular switches.

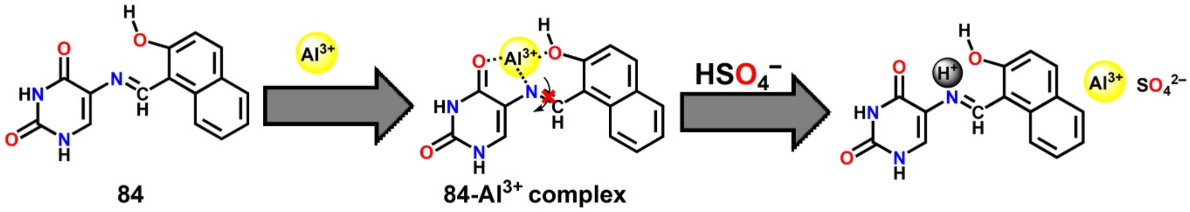

Scheme 49: The HSO_4^- ion binding mechanism of chemosensor **84**.

In 2013, Lin *et al.* synthesized a pair of Schiff base derivatives (**85** and **86**, **Scheme 50**) that were employed in the sub-micromolar scale recognition of HSO_4^-colorimetrically (LOD= 5.12 µM) and fluorometrically (LOD= 0.24 µM) in semi-aqueous medium (MeCN: H_2O; 4:1; v/v).[208] In the presence of the HSO_4^- ion, **85** displayed a rapid chromogenic color change from light pink to gold, which has the potential to be implemented in real-life applications. When excited at 360 nm, a sharp enhancement of the emission band of **85** at 459 nm was observed upon binding with the HSO_4^- ion which resulted in the formation of a 1:1 complex. Both the probes were highly selective towards HSO_4^- over other potential competitors due to HSO_4^- ion-induced hydrolysis of the imines. The hydrolyzed products were isolated and identified by several spectroscopic techniques.

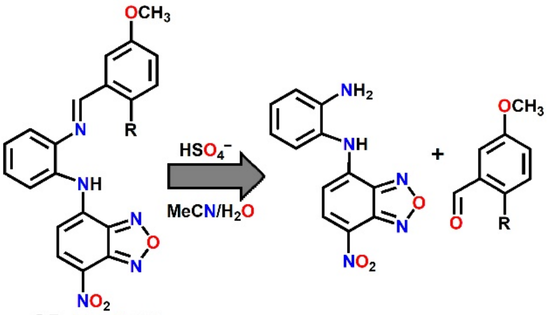

85, R= OCH_3**,**
86, R= H

Scheme 50: The HSO_4^- ion binding mechanism of chemosensors **85** and **86**.

A pair of salicylaldehyde-based Schiff bases (**87** and **88**, **Scheme 51**) that selectively and sensitively recognized Zn^{2+} and HSO_4^- ions (LOD= 1.9×10^{-8} M for **87** and 6.86×10^{-8} M for **88**) independently via ion-induced colorimetric and fluorescent changes.[209] In semi-aqueous medium (MeCN-H_2O; 1:1; v/v), both the ESIPT active probes exhibited keto-enol tautomerism (**Scheme 51**) and ratiometric changes in absorption bands with a sharp enhancement of emission intensity upon interaction with the HSO_4^- ion. Compound **87** was involved in bifurcated hydrogen bonding interactions with the bisulfate ion which caused the observed spectroscopic changes and facilitated the high-fidelity optical detection of the anion.

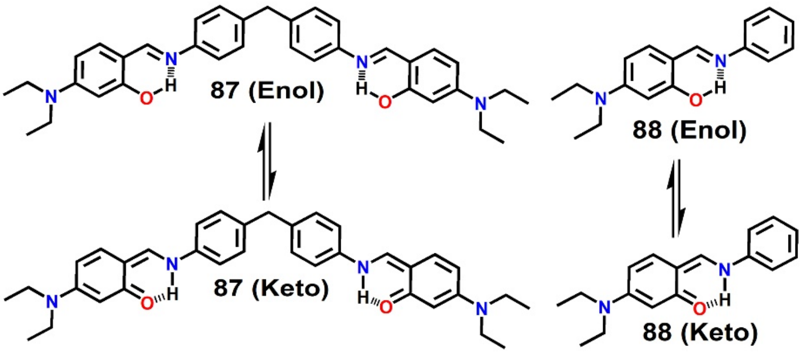

Scheme 51: Keto-enol tautomerism of chemosensors **87** and **88**.

The phenomenon of sequence-specific relay fluorescent detection in which a probe recognizes a cation and the probe-cation ensemble then detects an anion selectively and sensitively is relatively common, however, the reverse order of ion detection is very rare but an example was reported in 2015 by Wang *et al.*[210] The diketopyrrolepyrrole-based Schiff base derivative (**89**, **Scheme 52**) was utilized in the fluorometric recognition of HSO_4^-(LOD= 350 nM) followed by Fe^{3+} (LOD= 140 nM) along with a prominent visible color change. In THF medium, the probe displayed a red/orange to faint yellow color change and "off-on-off" fluorescence responses upon interaction with HSO_4^-followed by Fe^{3+} and the HSO_4^- ion-induced hydrolysis mechanism of the probe was well-supported.

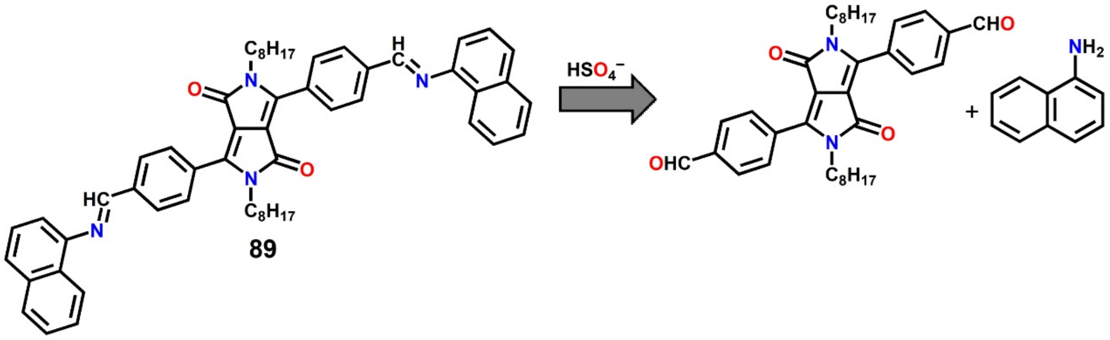

Scheme 52: The HSO$_4^-$ ion binding mechanism of chemosensor **89**.

Most of the HSO$_4^-$ sensors are involved in hydrogen bonding with the anion in aqueous media but suffer from a lack of selectivity. To avoid this issue, Wang *et al.,* developed the pyrrole-substituted Schiff base derivative (**90**, **Scheme 53**) that acted as a reaction-based HSO$_4^-$ sensor and displayed dual-mode responses (chromogenic and fluorogenic).[211] In THF-H$_2$O (8:1; v/v) mixed solvent, the highly intense absorption bands of the probe at 504 and 366 nm diminished upon interaction with the HSO$_4^-$ ion with a prominent visible color change from dark red to orange also being observed. Subsequently, the weak emission bands of **90** at 370 and 597 nm (λ_{ex}= 366 nm) were strongly quenched due to HSO$_4^-$ ion induced hydrolysis of **90** producing an aldehyde and *p*-methoxy aniline. Almost zero interference of competitive anions and an impressive 6.45 × 10^{-9} M detection limit was noted. The binding mechanism was further supported through analysis by ^{1}H NMR spectroscopy.

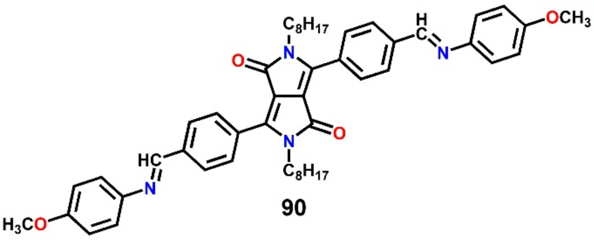

Scheme 53: Molecular structure of chemosensor **90**.

Then Fegade *et al.* developed a tridentate zinc (II) coordinated pyrrole-substituted salicylimine complex (**91**, **Scheme 54**) which was employed in high selectivity optical detection for HSO$_4^-$ ion semi-aqueous medium (MeOH:H$_2$O; 70:30; v/v).[212] The probe displayed a ratiometric shift of absorbance band from 400 to 340 nm due to the formation of a 1:1 complex. Subsequently, the probe displayed sharp quenching of emission intensity at 500 nm initiated by photoinduced electron transfer (PET) and intramolecular charge transfer (ICT) character. The probe achieved a high sensitivity detection with an LOD value of 40 nM.

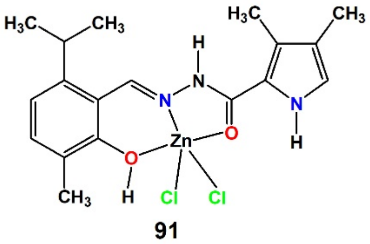

Scheme 54: Molecular structure of chemosensor **91**.

A quinoline-naphthalimide containing Schiff base derivative (**92**, **Scheme 55**) was employed in the fluorescent "turn on" detection of the HSO_4^- ion in a semi-aqueous medium (DMSO-H_2O; 1:1; v/v).[213] The probe exhibited sharp enhancement of emission intensity at 542 nm upon the addition of HSO_4^- and achieved highly selective detection up to 7.79×10^{-7} M. Analysis by ^1H NMR titration revealed that the HSO_4^- ion induced the hydrolysis of the Schiff base imine bond and the hydrolysis products were also identified by ^1H NMR spectroscopy and mass spectrometry.

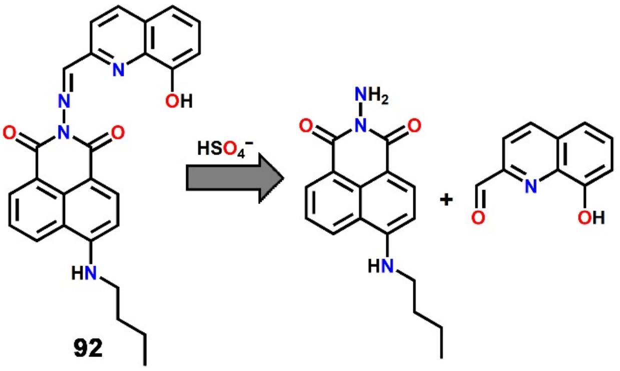

Scheme 55: The HSO_4^- ion binding mechanism of chemosensor **92**.

Later, Goel *et al.* developed another naphthalimide-based Schiff base fluorescent probe (**93**, **Scheme 56**) for the selective detection of both HSO_4^- and Hg^{2+} ions.[214] In the presence of the HSO_4^- ion, the probe underwent ion-induced dissociation and displayed a sharp decrease of absorbance at 380 nm. This was accompanied by the simultaneous development of a red-shifted absorption band at 430 nm, and subsequent enhancement of emission intensity at 530 nm together with a significant increase of quantum efficiency from 0.16 to 0.32. The chemosensor was able to detect the HSO_4^- ion at concentrations as low as 50 nM and interestingly displayed good DNA intercalation properties which were accompanied by an enhancement of emission intensity.

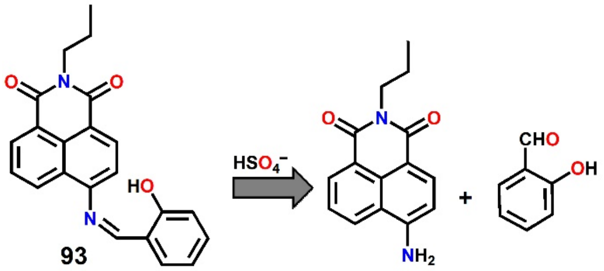

Scheme 56: The HSO_4^- ion binding mechanism of chemosensor **93**.

Later in 2018, Dong *et al.* synthesized a Schiff base by assembling naphthylamine and trifluoromethyl benzaldehyde (**94**, **Scheme 57**) and employed it in the colorimetric and fluorescent "turn on" detection of bisulfate in MeCN-H_2O (3:2; v/v) mixed solvent.[215] In the presence of HSO_4^-, the absorption bands of **94** at 286 nm and 354 nm gradually diminished and a new band at 320 nm developed accompanied by a visible color change from yellow to colorless. Subsequently, the weakly fluorescent **94** (ϕ= 0.04; λ_{ex}= 320 nm; λ_{em}= 425 nm) became highly fluorescent (ϕ= 0.41) in the presence of HSO_4^-. Under UV-light exposure, a color change from dark to blue was also noted. The spectroscopic changes were selective for HSO_4^- ion and achieved a very low detection limit (LOD= 1.44×10^{-7} M) again caused by imine hydrolysis. Interestingly, **94** was also employed in the detection of the HSO_4^- ion in real-world samples with satisfactory results.

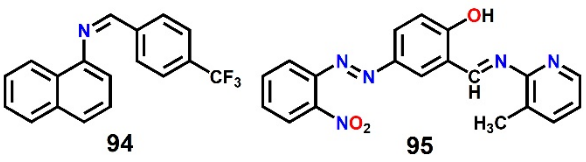

Scheme 57: Molecular structure of chemosensors **94** and **95**.

Subsequently, another methylpyridine and azo group assembled colorimetric probe (**95**, **Scheme 57**) was developed that selectively recognized multiple trivalent cations and HSO_4^- ion by colorimetric and fluorescent changes in DMF/H_2O (4:1, v/v) medium.[216] Interestingly, the probe displayed distinguishable naked-eye color change (yellow to colorless) only in the presence of HSO_4^- ion over other anions. Moreover, a 1.30 µM detection limit was determined and the formation of hydrogen bonding between the anion and **95** was also supported by a ^{1}H NMR titration.

Biswas *et al*. developed a pair of Schiff bases (**96** and **97**, **Scheme 58**) using green chemistry principles and employed both molecules in colorimetric relay detection of fluoride followed by bisulfate ions by tuning "C=N" isomerization, ICT, and proton transfer mechanisms.[217] Both of the probes displayed a ratiometric red shift of absorption bands with the addition of fluoride ion and a reversed spectroscopic response was registered upon the addition of HSO_4^- to the probe-fluoride composite. In addition, 1:1 (probe-anion) binding stoichiometry was also confirmed. The probes also displayed distinguishable and reversible naked-eye color changes upon sequential addition of the anions and the sensing mechanism was well argued through the use of extensive DFT calculations.

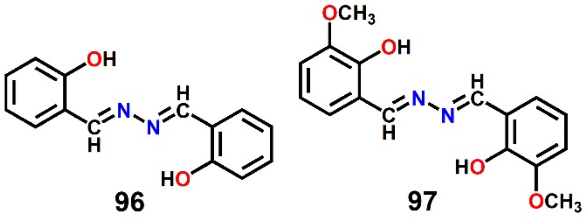

Scheme 58: Molecular structure of chemosensors **96** and **97**.

In 2021, a diarylethene-based Schiff base derivative was reported (**98**, **Figure 24**) which displayed excellent photochromic behavior and was involved in the relay recognition of Zn^{2+} ion followed by $H_2PO_4^-$/HSO_4^- ion colorimetrically.[218] The **98**-Zn^{2+} composite displayed excellent fluorogenic color change due to the quenching of emission intensity at 495 nm in the presence of either of the anions. In addition, the photochromic properties and ion binding mechanism were proposed (**Figure 24**). Interestingly, the **98**-Zn^{2+} composite was able to detect HSO_4^- ion at concentrations as low as 30.4 nM in acetonitrile medium, and the relay recognition of multiple anions was utilized in multiple opto-chemical logic gates.

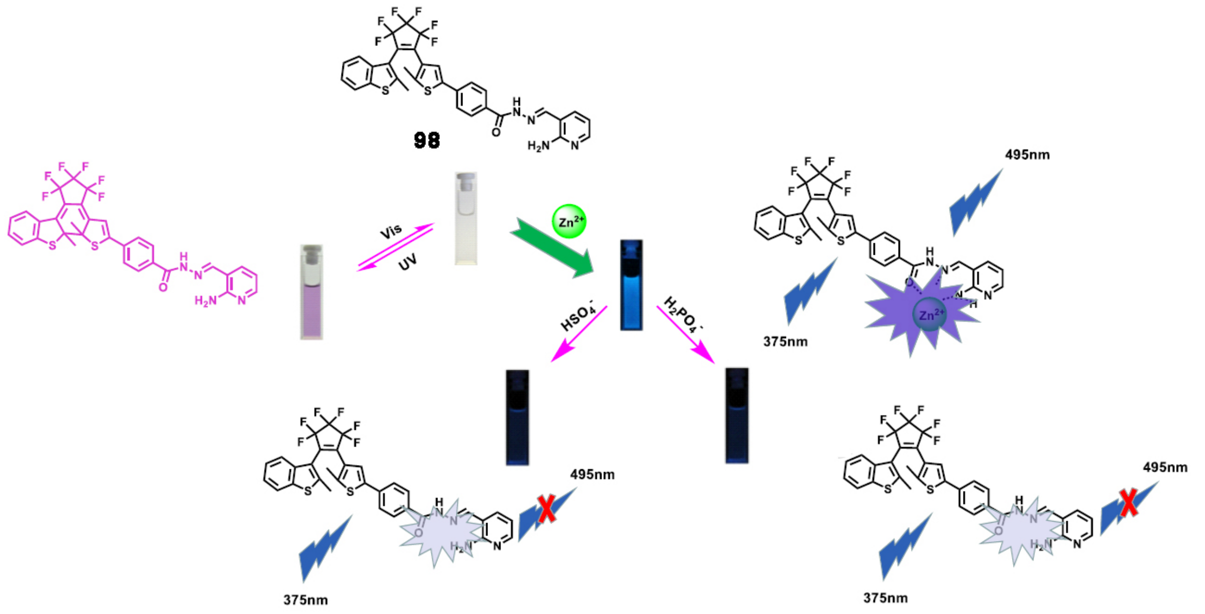

Figure 24: The photochromic behavior of **98** along with the mode of interaction with Zn^{2+} followed by the HSO_4^- ion with relevant color changes under UV light. (Reprinted with permission from Ref. 218. Copyright 2021, Elsevier).

Very recently, a rigid and symmetric bis(salamo)-like Schiff base molecule (**99**, **Scheme 59**) was developed that selectively recognized Cu^{2+}/ HSO_4^- ion colorimetrically and fluorimetrically in semi-aqueous medium (DMF-H_2O; 9/1, v/v, 10 mM HEPES, pH = 7.4).[219] The probe displayed strong binding affinity towards the HSO_4^- ion (K_a= 3.5×10^6 M^{-1}), achieved a limit of detection up to 4.97×10^{-7} M and a limit of quantification of 1.65×10^{-6} M. The binding mechanism was also thoroughly investigated by DFT analysis.

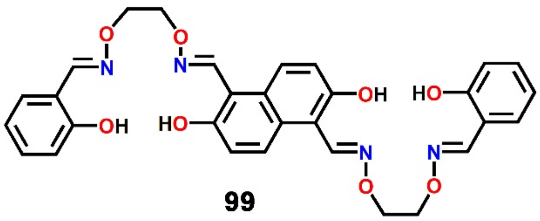

99

Scheme 59: Molecular structure of chemosensor **99**.

The above discussion clearly denoted that Schiff bases have been extensively utilized in the detection and imaging of HSO_4^- ion. Interestingly, very few of the Schiff bases form hydrogen-bonded interactions with the anion with the majority undergoing anion-induced dissociation in non-aqueous or semi-aqueous medium producing the component aldehyde and aromatic amines. Hence, a general sensing mechanism for the detection of the HSO_4^- ion by Schiff bases can be readily depicted (**Figure 25**).

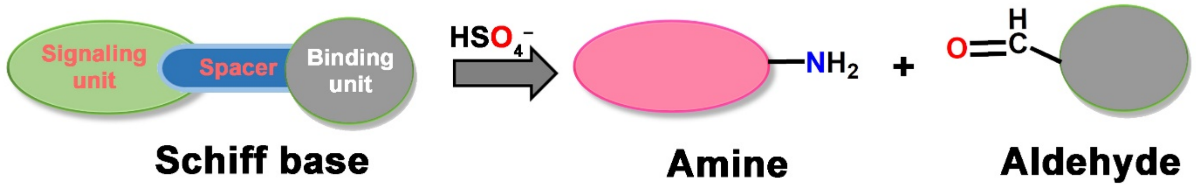

Figure 25: A generalized mechanism for the detection of HSO_4^- ion: HSO_4^- ion induced dissociation of Schiff bases.

3.11. Detection in water.

From the above discussion it is clear that despite the very large number of colorimetric and fluorescent sensors that have been reported, most undergo detection of HSO_4^- ion either in non-aqueous or semi-aqueous medium, with very few able to detect the anion in pure water. Hence, the chemosensors that can recognize the HSO_4^- ion in water are highlighted (**Table 1**).

Table 1: A summary of water-based HSO_4^- chemosensors summarising key structural features, the medium of detection, their binding mechanism, the limit of detection, and any other special features.

Structure of the probe	**Binding mechanism**	**Limit of detection**	**Special feature**	**Ref**
Benzimidazole-thiourea derivative (**13**)	Hydrogen bonding	5.0 nM	Ratiometric spectroscopic change	[98]
Benzimidazole-urea derivatives (**15** and **16**)	AIE and ACQ	1.09 µM for **15** and 0.93 µM for **16**	Different aggregation-induced spectroscopic changes	[100]
Benzothiazole-based substituted spiropyran derivative (**19**)	Hydrogen bonding	780 nM	Anion induced the conversion from the J-aggregate to the H-aggregate	[105]
Coumarin-integrated glycine and coumarin-integrated alanine derivatives (**31** and **32**)	Hydrogen bonding	LOD= 50 & 100 pM for **31** and **32** respectively	Detection and estimation of HSO_4^- in real samples like digestible plant foods drug and urine samples	[130]
Indole derivative (**42**)	AIE	106.0 nM	Detection of HSO_4^- within HeLa cells	[141]
Oxidized bisindolyl methane derivatives (**47**-**49**)	ICT	8.7 ppb for **47**	DFT study on effect of the substitution and sensitivity	[145]
Aminephenol-pyridine derivative (**67**)	Hydrogen bonding	0.25 µM	Formation of fluorescent organic nanoparticles	[179]
Pyrene-pyridine derivative (**71**)	Hydrogen bonding and AIE	Not reported	Portable Paper-strip based detection	[184]
Triphenylamine-pyridine derivatives (**73** and **74**)	Hydrogen bonding and proton transfer	15.1 ppb for **73** and 8.3 ppb for **74**	Formation of fluorescent organic nanoparticles	[186]
Rhodamine derivative covalently bound to a	Hydrogen bonding induced spiro-	11.6 ppm	Paper-based device was designed to act as a solid-state sensor and for on-site application.	[201]

hydrophilic cellulose surface (**81**)	lactam ring opening			

4. Concluding remarks and outlook

The significant role of the HSO_4^- ion in human life and the environment has already been discussed and the colorimetric and fluorescent detection of HSO_4^- ion will doubtless play an important role in identifying future challenges and positive impacts associated with the anion. To the best of our knowledge, all the colorimetric and fluorescent small molecule chemosensors for bisulfate reported to date are summarised herein. Despite the many advances that have been made in the field, a few challenges remain, including:
1) Most of the detection is reported in organic-based solvent systems and there are a few examples where solid phase detection is achieved. The immobilization of chemosensors onto solid surfaces may be a solution to this issue and may result in effective systems for real-life applications. Within this broad field, there are number of strategies that may be adopted, but the use of fluorescent organic nanoparticles may be an area in which significant advances can be made in the future.
2) In several cases, the ambiguity of selectivity between the two anions HSO_4^- and $H_2PO_4^-$ due to their similar tetrahedral structure exists. Whilst this is an ongoing issue for the design and synthesis of anion receptors of increasingly high specificity, there is already a clear roadmap to suggest that this is not an insurmountable problem to overcome.
3) The detection of the analyte in water is very important for on-site and real-world applications for which colorimetric and fluorescent probes are so well-suited. However, the detection of the anion in pure water is challenging due to its relatively high hydration energy. This is a serious drawback of many HSO_4^- chemosensors and an ongoing challenge for chemists to overcome. Nonetheless, the emergence of systems able to operate under such challenging conditions indicates that further solutions should be forthcoming.
4) There is a growing trend of designing opto-chemical logic gates based on the spectroscopic changes brought about by the anion. However, the solution phase changes will not be effective in real-life applications and future information technology unless water-based alternatives can be discovered.
5) For *in vivo* detection and imaging of HSO_4^- ion, the biocompatibility and toxicity of fluorophores are major challenges and there are relatively few reliable and promising chemosensors that display good biocompatibility and low toxicity.
6) Though there are several reports where the HSO_4^- ion has been detected on paper strips coated with a solution of a chromogenic sensor, nanomolar scale detection of HSO_4^- ion is very rare. More particularly, nanomolar-scale detection of the HSO_4^- ion in pure water remains a significant challenge.

These ongoing challenges will no doubt be addressed in due course, and we hope that this article represents an important and comprehensive resource for those working towards this end.

Acknowledgments
The authors acknowledge Dr. Tapas Majumdar, Professor, Department of Chemistry, University of Kalyani, West Bengal, India, for his support and cooperation.

Declaration
"The authors declare no conflict of interest."

5. References

[1] P. A. Gale and J. W. Steed, Supramolecular chemistry: From molecules to nanomaterials, John Wiley

& Sons, **2012**. DOI: 10.1002/9780470661345.

[2] C. B. Rodell, J. E. Mealy and J. A. Burdick, Supramolecular guest-host interactions for the preparation of biomedical materials, *Bioconjugate Chem.*, **2015**, *26*, 2279-2289.

[3] C. M. A. Gangemi, R. Puglisi, A. Pappalardo, G. T. Sfrazzetto, Supramolecular complexes for nanomedicine, *Bioorg. Med. Chem. Lett.*, **2018**, *28*, 3290-3301.

[4] M. J. Webber and R. Langer, Drug delivery by supramolecular design, *Chem. Soc. Rev.*, **2017**, *46*, 6600-6620.

[5] W.-C. Geng, Z. Ye, Z. Zheng, J. Gao, J.-J. Li, M. R. Shah, L. Xiao and D.-S. Guo, Supramolecular bioimaging through signal amplification by combining indicator displacement assay with forster resonance energy transfer, *Angew. Chem. Int. Ed.*, **2021**, *60*, 19614-19619.

[6] J. Zhou, L. Rao, G. Yu, T. R. Cook, X. Chen and F. Huang, Supramolecular cancer nanotheranostics, *Chem. Soc. Rev.*, **2021**, *50*, 2839-2891.

[7] J. Zhou, G. Yu and F. Huang, Supramolecular chemotherapy based on host-guest molecular recognition: A novel strategy in the battle against cancer with a bright future, *Chem. Soc. Rev.*, **2017**, *46*, 7021-7053.

[8] M. Ikeda, Stimuli-responsive supramolecular systems guided by chemical reactions, *Polym. J.*, **2019**, *51*, 371-380.

[9] S. J. D. Lugger, S. J. A. Houben, Y. Foelen, M. G. Debije, A. P. H. J. Schenning and D. J. Mulder, Hydrogen-bonded supramolecular liquid crystal polymers: Smart materials with stimuli-responsive, self-healing, and recyclable properties, *Chem. Rev.*, **2022**, *122*, 4946-4975.

[10] X. Yan, F. Wang, B. Zheng and F. Huang, Stimuli-responsive supramolecular polymeric materials, *Chem. Soc. Rev.*, **2012**, *41*, 6042-6065.

[11] A. V. Jentzsch, D. Emery, J. Mareda, S. K. Nayak, P. Metrangolo, G. Resnati, N. Sakai and S. Matile, Transmembrane anion transport mediated by halogen-bond donors, *Nat. Commun.*, **2012**, *3*, 905, DOI: 10.1038/ncomms1902.

[12] L. E. Bickerton, A. J. Sterling, P. D. Beer, F. Duarte, and M. J. Langton, Transmembrane anion transport mediated by halogen bonding and hydrogen bonding triazole anionophores, *Chem. Sci.*, **2020**, *11*, 4722-4729.

[13] J. T. Davis, P. A. Gale and R. Quesada, Advances in anion transport and supramolecular medicinal chemistry, *Chem. Soc. Rev.*, **2020**, *49*, 6056-6086.

[14] H. Wang, M. Wang, X. Liang, J. Yuan, H. Yang, S. Wang, Y. Ren, H. Wu, F. Pan and Z. Jiang, Organic molecular sieve membranes for chemical separations, *Chem. Soc. Rev.*, **2021**, *50*, 5468-5516.

[15] N. J. Williams, C. A. Seipp, K. A. Garrabrant, R. Custelcean E. Holguin , J. K. Keum, R. J. Ellis and B. A. Moyer, Surprisingly selective sulfate extraction by a simple monofunctional di(imino)guanidinium micelle-forming anion receptor, *Chem. Commun.*, **2018**, *54* , 10048-10051.

[16] A. M. Pekkanen, R. J. Mondschein, C. B. Williams and T. E. Long, 3D printing polymers with supramolecular functionality for biological applications, *Biomacromolecules*, **2017**, *18*, 2669-2687.

[17] G. Giancane, S. Bettini, L. Valli, V. Bracamonte, M. Carraro, M. Bonchio and M. Prato, Supramolecular organic-inorganic domains integrating fullerene-based acceptors with polyoxometalate-bis-pyrene tweezers for organic photovoltaic applications, *J. Mater. Chem. C*, **2021**, *9*, 16290-16297.

[18] T. Keijer, T. Bouwens, J. Hessels and J. N. H. Reek, Supramolecular strategies in artificial photosynthesis, *Chem. Sci.*, **2021**, *12*, 50-70.

[19] H. Che and J. Yuan, Recent advances in electrospinning supramolecular systems, *J. Mater. Chem.*

B, **2022**, *10*, 8-19.

[20] A. Bhattacharyya, S. D. Sarkar and A. Das, Supramolecular engineering and self-assembly strategies in photoredox catalysis, *ACS Catal.*, **2021**, *11*, 710-733.

[21] H. Chen and J. F. Stoddart, From molecular to supramolecular electronics, *Nat. Rev. Mater.*, **2021**, *6*, 804-828.

[22] J. F. Stoddart, Mechanically interlocked molecules (MIMs)-molecular shuttles, switches, and machines, *Angew. Chem. Int. Ed.*, **2017**, *56*, 11094-11125.

[23] T. L. Mako, J. M. Racicot and M. Levine, Supramolecular luminescent sensors, *Chem. Rev.*, **2019**, *119*, 322-477.

[24] N. Busschaert, C. Caltagirone, W. V. Rossom and P. A. Gale, Applications of supramolecular anion recognition, *Chem. Rev.*, **2015**, *115*, 8038-8155.

[25] G.-H. Liu, R. Chen, R.-W. Yang, X.-X. Li and W.-K. Dong, A novel naphthalimide-appended salamo-type fluorescent sensor for continuous “on-off-on” detection of Cu^{2+} and CN^{-} ions, sensing mechanisms and applications, *J. Mol. Struct.*, **2024**, *1309*, 138180.

[26] M.-X. Du, C.-Y. Ma, X.-X. Li, Y.-N. Yue and W.-K. Dong, A new oligo(N,O-donor)-like ratiometric fluorescent probe with FRET effect for dual-channel recognition of $B_4O_7^{2-}$ ions in practical water samples, *Inorg. Chim. Acta*, **2024**, *569*, 122117.

[27] P.-L. Yuan, L. Tong, X.-X. Li, W.-K. Dong and Y. Zhang, A benzimidazole-appended double-armed salamo type fluorescence and colorimetric bifunctional sensor for identification of MnO_4^{-} and its applications in actual water samples, *Spectrochim. Acta, Part A*, **2024**, *315*, 124252.

[28] L.-L Man, S.-Z. Li, J. Zhang, Y. Zhang and W.-K. Dong, A new single-armed salamo-based sensor with aggregation-induced emission characteristic for selective sensing of aluminium ions, *J. Photochem. Photobiol. A*, **2023**, *437*, 114433.

[29] J. M. Lehn, Cryptates: The chemistry of macropolycyclic inclusion complexes, *Acc. Chem. Res.*, **1978**, *11*, 49-57.

[30] G. T. Williams, C. J. E. Haynes, M. Fares, C. Caltagirone, J. R. Hiscock and P. A. Gale, Advances in applied supramolecular technologies, *Chem. Soc. Rev.*, **2021**, *50*, 2737-2763.

[31] F. Huang and E. V. Anslyn, Introduction: Supramolecular chemistry, *Chem. Rev.*, **2015**, *115*, 6999-7000.

[32] P. D. Beer and P. A. Gale, Anion recognition and sensing: The state of the art and future perspectives, *Angew. Chem. Int. Ed.*, **2001**, *40*, 486-516.

[33] N. Busschaert, C. Caltagirone, W. V. Rossom and P. A. Gale, Applications of supramolecular anion recognition, *Chem. Rev.*, **2015**, *115*, 8038-8155.

[34] L. You, D. Zha and E. V. Anslyn, Recent advances in supramolecular analytical chemistry using optical sensing, *Chem. Rev.*, **2015**, *115*, 7840-7892.

[35] D.-X. Wang and M.-X. Wang, Exploring anion−π interactions and their applications in supramolecular chemistry, *Acc. Chem. Res.*, **2020**, *53*, 1364-1380.

[36] P. Molina, F. Zapata and A. Caballero, Anion recognition strategies based on combined noncovalent interactions, *Chem. Rev.*, **2017**, *117*, 9907-9972.

[37] A. W. Czarnik, Fluorescent chemosensors for ion and molecule recognition, American Chemical Society, Washington, DC, **1993**.

[38] D. Wu, A. C. Sedgwick, T. Gunnlaugsson, E. U. Akkaya, J. Yoon and T. D. James, Fluorescent chemosensors: The past, present and future, *Chem. Soc. Rev.*, **2017**, *46*, 7105-7123.

[39] N. H. Evans, P. D. Beer, Advances in anion supramolecular chemistry: From recognition to chemical applications, *Angew. Chem., Int. Ed.*, **2014**, *53*, 11716-11754.

[40] P. A. Gale, N. Busschaert, C. J. E. Haynes, L. E. Karagiannidis and I. L. Kirby, Anion receptor chemistry: Highlights from 2011 and 2012, *Chem. Soc. Rev.*, **2014**, *43*, 205-241.

[41] D. T. Quang and J. S. Kim, Fluoro- and chromogenic chemodosimeters for heavy metal ion detection in solution and biospecimens, *Chem. Rev.*, **2010**, *110*, 6280-6301.

[42] Y. Zhou, Z. Xu and J. Yoon, Fluorescent and colorimetric chemosensors for detection of nucleotides, FAD and NADH: Highlighted research during 2004-2010, *Chem. Soc. Rev.*, **2011**, *40*, 2222-2235.

[43] J. F. Zhang, Y. Zhou, J. Yoon and J. S. Kim, Recent progress in fluorescent and colorimetric chemosensors for detection of precious metal ions (silver, gold and platinum ions), *Chem. Soc. Rev.*, **2011**, *40*, 3416-3429.

[44] H. N. Kim, W. X. Ren, J. S. Kim and J. Yoon, Fluorescent and colorimetric sensors for detection of lead, cadmium, and mercury ions, *Chem. Soc. Rev.*, **2012**, *41*, 3210-3244.

[45] Y. Hu, S. Long, H. Fu, Y. She, Z. Xu and J. Yoon, Revisiting imidazolium receptors for the recognition of anions: Highlighted research during 2010-2019, *Chem. Soc. Rev.*, **2021**, *50*, 589-618.

[46] M. K. Goshisht and N. Tripathi, Fluorescence-based sensors as an emerging tool for anion detection: Mechanism, sensory materials and applications, *J. Mater. Chem. C*, **2021**, *9*, 9820-9850.

[47] M. Cametti and K. Rissanen, Highlights on contemporary recognition and sensing of fluoride anion in solution and in the solid state, *Chem. Soc. Rev.*, **2013**, *42*, 2016-2038.

[48] Y. Zhou, J. F. Zhang and J. Yoon, Fluorescence and colorimetric chemosensors for fluoride-ion detection, *Chem. Rev.*, **2014**, *114*, 5511-5571.

[49] L. Gai, J. Mack, H. Lu, T. Nyokong, Z. Li, N. Kobayashi and Z. Shen, Organosilicon compounds as fluorescent chemosensors for fluoride anion recognition, *Coord. Chem. Rev.*, **2015**, *285*, 24-51.

[50] A. Dhillon, M. Nair and D. Kumar, Analytical methods for determination and sensing of fluoride in biotic and abiotic sources: A review, *Anal. Methods*, **2016**, *8*, 5338-5352.

[51] P. Chen, W. Bai and Y. Bao, Fluorescent chemodosimeters for fluoride ions via silicon-fluorine chemistry: 20 years of progress, *J. Mater. Chem. C*, **2019**, *7*, 11731-11746.

[52] S. Dhiman, M. Ahmad, N. Singla, G. Kumar, P. Singh, V. Luxami, N. Kaur and S. Kumar, Chemodosimeters for optical detection of fluoride anion, *Coord. Chem. Rev.*, **2020**, *405*, 213138.

[53] S. Xiong, M. V. N. Kishore, W. Zhou and Q. He, Recent advances in selective recognition of fluoride with macrocyclic receptors, *Coord. Chem. Rev.*, **2022**, *461*, 214480.

[54] M. Mansha, S. A. Khan, M. A. Aziz, A. Z. Khan, S. Ali and M. Khan, Optical chemical sensing of iodide ions: A comprehensive review for the synthetic strategies of iodide sensing probes, challenges, and future aspects, *The Chemical Record*, **2022**, *22*, e202200059.

[55] D. Wu, L. Chen, Q. Xu, X. Chen and J. Yoon, Design principles, sensing mechanisms, and applications of highly specific fluorescent probes for HOCl/OCl$^-$, *Acc. Chem. Res.*, **2019**, *52*, 2158-2168.

[56] F. Wang, L. Wang, X. Chen and J. Yoon, Recent progress in the development of fluorometric and colorimetric chemosensors for detection of cyanide ions, *Chem. Soc. Rev.*, **2014**, *43*, 4312-4324.

[57] S. Panja, A. Panja and K. Ghosh, Supramolecular gels in cyanide sensing: A review, *Mater. Chem. Front.*, **2021**, *5*, 584-602.

[58] M. V. R. Raju, S. M. Harris and V. C. Pierre, Design and applications of metal-based molecular receptors and probes for inorganic phosphate, *Chem. Soc. Rev.*, **2020**, *49*, 1090-1108.

[59] S. Pal, T. K. Ghosh, R. Ghosh, S. Mondal and P. Ghosh, Recent advances in recognition, sensing and extraction of phosphates: 2015 onwards, *Coord. Chem. Rev.*, **2020**, *405*, 213128.

[60] D. Zhang, J. R. Cochrane, A. Martinez and G. Gao, Recent advances in $H_2PO_4^-$ fluorescent sensors, *RSC Adv.*, **2014**, *4*, 29735-29749.

[61] S. K. Kim, D. H. Lee, J. -I. Hong and J. Yoon, Chemosensors for pyrophosphate, *Acc. Chem. Res.*, **2009**, *42*, 23-31.

[62] S. Anbu, A. Paul, G. J. Stasiuk, A. J. L. Pombeiro, Recent developments in molecular sensor designs for inorganic pyrophosphate detection and biological imaging, *Coord. Chem. Rev.*, **2021**, *431*, 213744.

[63] I. Ravikumar and P. Ghosh, Recognition and separation of sulfate anions, *Chem. Soc. Rev.*, **2012**, *41*, 3077-3098.

[64] R. Dutta and P. Ghosh, Artificial receptors for nitrate: a comprehensive overview, *Chem. Commun.*, **2015**, *51*, 9070-9084.

[65] Q. Li and S.-J. Shao, Progress on optical probes for hydrogen sulfate anion sensing, *Chin. J. Anal. Chem.*, **2017**, *45*, 1248-1257.

[66] S. Paul, T. Majumdar and A. Mallick, Hydrogen bond regulated hydrogen sulfate ion recognition: an overview, *Dalton Trans.*, **2021**, *50*, 1531-1549.

[67] P. Ebbesen, Deae-dextran and polybrene cation enhancement and dextran sulfate anion inhibition of immune cytolysis, *J. Immunol.*, **1972**, *109*, 1296-1299.

[68] H. Weingartner, E. U. Franck, G. Wiegand, N. Dahmen, G. Schwedt, F. H. Frimmel, B. C. Gordalla, K. Johannsen, R. S. Summers, W. Holl, M. Jekel, R. Gimbel, R. Rautenbach and W. H. Glaze, Ullman's Encyclopedia of Industrial Chemistry, Wiley-VCH Verlag GmbH & Co., **2000**.

[69] B. A. Moyer, L. H. Delmau, C. J. Fowler, A. Ruas, D. A. Bostick, J. L. Sessler, E. Katayeu, G. D. Pantos, J. M. Llinares, M. A. Hossain, S. O. Kang and K. Bowman-James, in Advances in Inorganic Chemistry, ed. R. V. Eldik and K. Bowman-James, Academic Press, New York, **2006**, pp. 175-204.

[70] T. J. Grahame and R. B. Schlesinger, Evaluating the health risk from secondary sulfates in eastern North American regional ambient air particulate matter, *Inhalation Toxicol.*, **2005**, *17*, 15-27.

[71] P. I. Jalava, R. O. Salonen, A. S. Pennanen, M. S. Happo, P. Penttinen, A. I. Halinen, M. Sillanpaa, R. Hillamo and M. -R. Hirvonen, Effects of solubility of urban air fine and coarse particles on cytotoxic and inflammatory responses in RAW 264.7 macrophage cell line, *Toxicol. Appl. Pharmacol.*, **2008**, *229*, 146-160.

[72] H. von Plessen, Sodium sulfates, Ullmann's encyclopedia of industrial chemistry, 2000, Wiley-VCH Verlag GmbH & Co. KGaA. https://doi.org/10.1002/14356007.a24_355.

[73] J. K. Spears, C. M. Grieshop and G. C. Fahey Jr., Evaluation of sodium bisulphate and phosphoric acid as urine acidifiers for cats, *Arch. Anim. Nutr.*, **2003**, *57*, 389-398. https://doi.org/10.1080/00039420310001607743.

[74] S. Kubik, Anion Recognition in Water, *Chem. Soc. Rev.*, **2010**, *39*, 3648-3663.

[75] Y. Marcus, Thermodynamics of solvation of ions. Part 5.-Gibbs free energy of hydration at 298.15 K, *J. Chem. Soc., Faraday Trans.*, **1991**, *87*, 2995-2999.

[76] W. Kohn, A. D. Becke and R. G. Parr, Density Functional Theory of electronic structure, *J. Phys. Chem.*, **1996**, *100*, 12974-12980. https://doi.org/10.1021/jp960669l.

[77] J. B. Foresman and A. Frisch, Exploring Chemistry with Electronic Structure Methods, 2nd ed.; Gaussian, Inc: Pittsburgh, PA, **1996**.

[78] The Nobel Prize in Chemistry 1998. NobelPrize.org. https://www.nobelprize.org/prizes/chemistry/1998/summary/

[79] M. J. Frisch, G. W. Trucks, H. B. Schlegel, G. E. Scuseria, M. A. Robb, J. R. Cheeseman, J. A. Montgomery, Jr., T. Vreven, K. N. Kudin, J. C. Burant, J. M. Millam, S. S. Iyengar, J. Tomasi, V.

Barone, B. Mennucci, M. Cossi, G. Scalmani, N. Rega, G. A. Petersson, H. Nakatsuji, M. Hada, M. Ehara, K. Toyota, R. Fukuda, J. Hasegawa, M. Ishida, T. Nakajima, Y. Honda, O. Kitao, H. Nakai, M. Klene, X. Li, J. E. Knox, H. P. Hratchian, J. B. Cross, V. Bakken, C. Adamo, J. Jaramillo, R. Gomperts, R. E. Stratmann, O. Yazyev, A. J. Austin, R. Cammi, C. Pomelli, J. Ochterski, P. Y. Ayala, K. Morokuma, G. A. Voth, P. Salvador, J. J. Dannenberg, V. G. Zakrzewski, S. Dapprich, A. D. Daniels, M. C. Strain, O. Farkas, D. K. Malick, A. D. Rabuck, K. Raghavachari, J. B. Foresman, J. V. Ortiz, Q. Cui, A. G. Baboul, S. Clifford, J. Cioslowski, B. B. Stefanov, G. Liu, A. Liashenko, P. Piskorz, I. Komaromi, R. L. Martin, D. J. Fox, T. Keith, M. A. Al-Laham, C. Y. Peng, A. Nanayakkara, M. Challacombe, P. M. W. Gill, B. G. Johnson, W. Chen, M. W. Wong, C. Gonzalez and J. A. Pople, GAUSSIAN 03 (Revision D.1), Gaussian, Inc., Wallingford, CT, **2004**.

[80] R. Ahlrichs, M. Bar, M. Haser, H. Horn and C. Kolmel, Electronic structure calculations on workstation computers: The program system turbomole, *Chem. Phys. Lett.*, **1989**, *162*, 165-169. https://doi.org/10.1016/0009-2614(89)85118-8.

[81] M. W. Schmidt, K. K. Baldridge, J. A. Boatz, S. T. Elbert, M. S. Gordon, J. H. Jensen, S. Koseki, N. Matsunaga, K. A. Nguyen, S. Su, T. L. Windus, M. Dupuis and J. A. Montgomery, General atomic and molecular electronic structure system, *J. Comput. Chem.*, **1993**, *14*, 1347-1363. https://doi.org/10.1002/jcc.540141112.

[82] M. S. Gordon and M. W. Schmidt, In theory and applications of computational chemistry: The first forty years, ed. C. E. Dykstra, G. Frenking, K. S. Kim and G. E. Scuseria, Elsevier, Amsterdam, **2005**, p. 1167.

[83] F. Neese, ORCA, Universtiy of Bonn, Germany, **2009**.

[84] C. J. Cramer and D. G. Truhlar, Density functional theory for transition metals and transition metal chemistry, *Phys. Chem. Chem. Phys.*, **2009**, *11*, 10757-10816.

[85] D. Wang, W. F. van Gunsteren and Z. Chai, Recent advances in computational actinoid chemistry, Chem. Soc. Rev., 2012,41, 5836-5865.

[86] M. Karar and S. Paul, Effect of substituents on tuning the sensing efficiency of analogous chemosensors: An insight into the mechanism, *J. Lumin.*, **2024**, *269*, 120496. https://doi.org/10.1016/j.jlumin.2024.120496.

[87] S. Paul, Computational justification towards detection of dual anions on a single molecular platform: The role of solvent in the decoration of dual channels, *J. Phys. Org. Chem.*, **2024**, e4666. https://doi.org/10.1002/poc.4666.

[88] Z. Xu, S. K. Kim and J. Yoon, Revisit to imidazolium receptors for the recognition of anions: Highlighted research during 2006-2009, *Chem. Soc. Rev.*, **2010**, *39*, 1457-1466.

[89] M. Boca, R. F. Jameson and W. Linert, Fascinating variability in the chemistry and properties of 2,6-bis-(benzimidazol-2-yl)-pyridine and 2,6-bis-(benzthiazol-2-yl)-pyridine and their complexes, *Coord. Chem. Rev.*, **2011**, *255*, 290-317.

[90] S. K. Manna, T. Das and S. Samanta, Polycyclic benzimidazole: synthesis and photophysical properties, *ChemistrySelect*, **2019**, *4*, 8781-8790.

[91] M. Alfonso, A. Tarraga and P. Molina, A bisferrocene-benzobisimidazole triad as a multichannel ditopic receptor for selective sensing of hydrogen sulfate and mercury ions, *Org. Lett.*, **2011**, *13*, 6432-6435.

[92] P. Saluja, N. Kaur, N. Singh and D. O. Jang, Benzimidazole-based fluorescent sensors for Cr^{3+} and their resultant complexes for sensing HSO_4^- and F^-, *Tetrahedron*, **2012**, *68*, 8551-8556.

[93] D. Zhang, X. Jiang, Z. Dong, H. Yang, A. Martinez and G. Gao, A bifunctional acridine-based fluorescent sensor: Ratiometric sensing of $H_2PO_4^-$ and obvious fluorescence quenching towards

HSO_4^- through a synergistic binding effect of benzimidazolium and urea moieties, *Tetrahedron*, **2013**, *69*, 10457-10462.

[94] M. Mukherjee, S. Pal, B. Sen, S. Lohar, S. Banerjee, S. Banerjee and P. Chattopadhyay, Substituent effect on fluorescence signaling of the cell permeable HSO_4^- receptors through a single point to ratiometric response in a green solvent, *RSC Adv.*, **2014**, *4*, 27665-27673.

[95] B. Sen, M. Mukherjee, S. Pal, S. K. Mandal, M. S. Hundal, A. R. Khuda-Bukhsh and P. Chattopadhyay, Development of a cell permeable ratiometric chemosensor and biomarker for hydrogen sulphate ions in aqueous solution, *RSC Adv.*, **2014**, *4*, 15356-15362.

[96] B. Sen, M. Mukherjee, S. Pal, S. Sen and P. Chattopadhyay, A water-soluble copper(II) complex as a HSO_4^- ion selective turn-on fluorescent sensor applicable in living cell imaging, *RSC Adv.*, **2015**, *5*, 50532-50539.

[97] D. Phapale, A. Kushwaha and D. Das, A simple benzimidazole styryl-based colorimetric chemosensor for dual sensing application, *Spectrochim. Acta, Part A*, **2019**, *214*, 111-118.

[98] D. Bains, G. Singh and N. Singh, A dipodal thiourea-ionic liquid conjugate system for selective ratiometric detection of HSO_4^- ion in purely aqueous medium: Application to real sample analysis, *Tet. Lett.*, **2019**, *60*, 1457-1462.

[99] A. Palta, G. Kumar and V. Luxami, Intramolecular dual hydrogen bonded fluorescent “turn-on” probe for Al^{3+} and HSO_4^- ions: Applications in real water samples and molecular keypad lock, *Spectrochim. Acta, Part A*, **2023**, *300*, 122873.

[100] R. Moral, O. A. Pegu and G. Das, Terminal substituent-induced differential aggregation and sensing properties: A case study of neutral benzimidazole-based urea receptors, *New J. Chem.*, **2023**, *47*, 19625-19632.

[101] F. Yan, J. Sun, Y. Zang, Z. Sun, H. Zhang and X. Wang, Benzothiazole applications as fluorescent probes for analyte detection, *J. Iran. Chem. Soc.*, **2020**, *17*, 3179-3203.

[102] S. Das, H. K. Indurthi, P. Asati, P. Saha and D. K. Sharma, Benzothiazole based fluorescent probes for the detection of biomolecules, physiological conditions, and ions responsible for diseases, *Dyes Pigm.*, **2022**, *199*, 110074.

[103] V. K. Bhardwaj, P. Saluja, G. Hundal, M. S. Hundal, N. Singh and D. O. Jang, Benzthiazole-based multifunctional chemosensor: Fluorescent recognition of Fe^{3+} and chromogenic recognition of HSO_4^-, *Tetrahedron*, **2013**, *69*, 1606-1610.

[104] B.-Y. Kim, H.-S. Kim and A. Helal, A fluorescent chemosensor for sequential recognition of gallium and hydrogen sulfate ions based on a new phenylthiazole derivative, *Sens. Actuators, B*, **2015**, *206*, 430-434.

[105] A. Kumar, K. Prakash, P. R. Sahoo and S. Kumar, Visible light controlled aggregation of a spiropyran-HSO_4^- complex as a strategy for reversible detection in water, *ChemistrySelect*, **2017**, *2*, 8247-8252.

[106] I. Kaur, A. Khajuria, P. Ohri, P. Kaur, K. Singh, Benzothiazole based Schiff-base- A mechanistically discrete sensor for HSO_4^- and I^-: Application to bioimaging and vapour phase sensing of ethyl acetate, *Sens. Actuators, B*, **2018**, *268*, 29-38.

[107] I. Kathuria, A. Datta and S. Kumar, A substituted benzothiazolinic merocyanine derivative as a reversible, selective, colorimetric and fluorescent probe for HSO_4^- in aqueous solution, *J. Mol. Struct.*, **2022**, *1255*, 132471.

[108] I. Kathuria, S. Rani, R. K. Srivastava and S. Kumar, Synthesis and photochemistry of a new benzothiazolinic oxazine salt and its application in the detection of hydrogen sulfate ion, *J. Photochem. Photobiol., A*, **2023**, *445*, 115065.

[109] N. Boens, V. Leena and W. Dehaen, Fluorescent indicators based on BODIPY, *Chem. Soc. Rev.*, **2012**, *41*, 1130-1172.

[110] J. Wang, N. Boens, L. Jiao and E. Hao, Aromatic [b]-fused BODIPY dyes as promising near-infrared dyes, *Org. Biomol. Chem.*, **2020**, *18*, 4135-4156.

[111] H. Lu, J. Mack, Y. Yang and Z. Shen, Structural modification strategies for the rational design of red/NIR region BODIPYs, *Chem. Soc. Rev.*, **2014**, *43*, 4778-4823.

[112] P. Kaur and K. Singh, Recent advances in application of BODIPY in bioimaging and chemosensing, *J. Mater. Chem. C*, **2019**, *7*, 11361-11405.

[113] Z. Shi, X. Han, W. Hu, H. Bai, B. Peng, L. Ji, Q. Fan, L. Li and W. Huang, Bioapplications of small molecule Aza-BODIPY: From rational structural design to *in vivo* investigations, *Chem. Soc. Rev.*, **2020**, *49*, 7533-7567.

[114] M. Poddar and R. Misra, Recent advances of BODIPY based derivatives for optoelectronic applications, *Coord. Chem. Rev.*, **2020**, *421*, 213462.

[115] M. Yan, D. He, L. Zhang, P. Sun, Y. Sun, L. Qu and Z. Li, Explorations into the meso-substituted BODIPY-based fluorescent probes for biomedical sensing and imaging, *TrAC, Trends Anal. Chem.*, **2022**, *157*, 116771.

[116] S. G. Awuah and Y. You, Boron dipyrromethene (BODIPY)-based photosensitizers for photodynamic therapy, *RSC Adv.*, **2012**, *2*, 11169-11183.

[117] I. S. Yadav and R. Misra, Design, synthesis and functionalization of BODIPY dyes: Applications in dye-sensitized solar cells (DSSCs) and photodynamic therapy (PDT), *J. Mater. Chem. C*, **2023**, *11*, 8688-8723.

[118] J. Zhao, K. Xu, W. Yang, Z. Wang and F. Zhong, The triplet excited state of Bodipy: Formation, modulation and application, *Chem. Soc. Rev.*, **2015**, *44*, 8904-8939.

[119] P. Lu, K.-Y. Chung, A. Stafford, M. Kiker, K. Kafle and Z. A. Page, Boron dipyrromethene (BODIPY) in polymer chemistry, *Polym. Chem.*, **2021**, *12*, 327-348.

[120] Q. Li, Y. Guoa and S. Shao, A BODIPY derivative as a highly selective ‘‘Off-On’’ fluorescent chemosensor for hydrogen sulfate anion, *Analyst*, **2012**, *137*, 4497-4501.

[121] Q. Li, Y. Yue, Y. Guo and S. Shao, Fluoride anions triggered “OFF-ON” fluorescent sensor for hydrogen sulfate anions based on a BODIPY scaffold that works as a molecular keypad lock, *Sens. Actuators, B*, **2012**, *173*, 797-801.

[122] L. Wang, J. Ou, G. Fang and D. Cao, A fluorescent turn-on probe for detection of HSO_4^- ion based on hydrolysis of BODIPY-derived Schiff base with chromogenic and fluorogenic dual signals, *Sens. Actuators, B*, **2016**, *222*, 1184-1192.

[123] G. Kesan, B. Topaloglu, E. Ozcan, H. H. Kazan, E. T. Ecik, E. Senkuytu, I. F. Sengul, H. Kandemir and B. Cosut, Azaindole-BODIPYs: Synthesis, fluorescent recognition of hydrogen sulfate anion and biological evaluation, *Spectrochim. Acta, Part A*, **2019**, *213*, 73-82.

[124] D. Cao, Z. Liu, P. Verwilst, S. Koo, P. Jangjili, J. S. Kim and W. Lin, Coumarin-based small-molecule fluorescent chemosensors, *Chem. Rev.*, **2019**, *119*, 10403-10519.

[125] A. Mondal, S. Nag and P. Banerjee, Coumarin functionalized molecular scaffolds for the effectual detection of hazardous fluoride and cyanide, *Dalton Trans.*, **2021**, 50, 429-451.

[126] D. Khan and Shaily, Coumarin-based fluorescent sensors, *Appl. Organomet. Chem.*, **2023**, *37*, e7138.

[127] H. J. Kim, S. Bhuniya, R. K. Mahajan, R. Puri, H. Liu, K. C. Ko, J. Y. Lee and J. S. Kim, Fluorescence turn-on sensors for HSO_4^-, *Chem. Commun.*, **2009**, 7128-7130.

[128] V. Kumar, A. Kumar, U. Diwan and K. K. Upadhyay, Uncovering the true mechanism of optical

detection of HSO_4^- in water by Schiff-base receptors-hydrolysis vs. hydrogen bonding, *Chem. Commun.*, **2012**, *48*, 9540-9542.

[129] D. Sarkar, A. K. Pramanik and T. K. Mondal, Coumarin based dual switching fluorescent ‘turn on’ chemosensor for selective detection of Zn^{2+} and HSO_4^-: An experimental and theoretical study, *RSC Adv.*, **2014**, *4*, 25341-25347.

[130] R. R. Nair, M. Raju, S. Bhai, I. H. Raval, S. Haldar, B. Ganguly and P. B. Chatterjee, Estimation of bisulfate in edible plant foods, dog urine, and drug: Picomolar level detection and bioimaging in living organisms, *Analyst*, **2019**, *144*, 5724-5737.

[131] Z.-P. Deng, B. Zhao, L.-L. Gao, B.-T. Ji, J.-G. Li, Y.-X. Sun, J. Li and Y. Sun, Coumarin-derived Schiff base as a colorimetric and fluorescent dual-channel chemosensor for detecting HSO_4^- and bioimaging & biosensing in Zebrafish, *J. Mol. Struct.,* **2024**, *1299*, 137203.

[132] Y. Shimazaki, T. Yajima, M. Takani and O. Yamauchi, Metal complexes involving indole rings: Structures and effects of metal-indole interactions, *Coord. Chem. Rev.*, **2009**, *253*, 479-492.

[133] A. Dorababu, Indole-a promising pharmacophore in recent antiviral drug discovery, *RSC Med. Chem.*, **2020**, *11*, 1335-1353.

[134] A. Mallick, T. Katayama, Y. Ishibasi, M. Yasuda and H. Miyasaka, Norharmane: Old yet highly selective dual channel ratiometric fluoride and hydrogen sulfate ion sensor, *Analyst*, **2011**, *136*, 275-277.

[135] S. Paul, M. Karar, S. Mitra, S. A. Sher Shah, T. Majumdar and A. Mallick, A molecular lock with hydrogen sulfate as “Key” and fluoride as “Hand”: Computing based insights on the functioning mechanism, *ChemistrySelect*, **2016**, *1*, 5547-5553.

[136] S. Paul, M. Karar, P. Paul, A. Mallick and T. Majumdar, Dual mode nitro explosive detection under crowded condition: Conceptual development of a sensing device, *J. Photochem. Photobiol. A,* **2019**, 379, 123-129.

[137] J. Chang, Y. Lu, S. He, C. Liu, L. Zhao and X. Zeng, Efficient fluorescent chemosensors for HSO_4^- based on a strategy of anion-induced rotation-displaced H-aggregates, *Chem. Commun.*, **2013**, *49*, 6259-6261.

[138] S. Bayindir and N. Saracoglu, A facile one-pot method to synthesis of 2-alkylated indole and 2,2'-bis(indolyl)methane derivatives using ketones as electrophile and its anion sensing ability, *RSC Adv.*, **2016**, *6*, 72959-72967.

[139] D. Sain, C. Kumari, A. Kumar and S. Dey, Colorimetric ‘turn on TBET’ sensors for ‘on the spot’ visual detection of HSO_4^- in semi-aqueous medium: Experimental and quantum chemical (DFT) studies, *Sens. Actuators, B*, **2015**, *221*, 849-856.

[140] D. Sain, C. Kumari, A. Kumar and S. Dey, Indole-based distinctive chemosensors for ‘naked eye’ detection of CN and HSO_4^-, associated with hydrogen-bonded complex and their DFT study, *Supra. Chem.*, **2016**, *28*, 239-248.

[141] S. Samanta, P. Dey, A. Ramesh and G. Das, A solo fluorogenic probe for real-time sensing of SO_3^{2-} and SO_4^{2-}/HSO_4^- in aqueous medium and live cells by distinct turn-on emission signals, *Chem. Commun.*, **2016**, *52*, 10381-10384.

[142] T. Yu, G. Yin, T. Niu, P. Yin, H. Li, Y. Zhang, H. Chen, Y. Zeng and S. Yao, A novel colorimetric and fluorescent probe for simultaneous detection of SO_3^{2-}/HSO_3^- and HSO_4^- by different emission channels and its bioimaging in living cells, *Talanta*, **2018**, *176*, 1-7.

[143] T. Majumdar, B. Haldar and A. Mallick, A strategic design of an opto-chemical security device with resettable and reconfigurable password based upon dual channel two-in-one chemosensor molecule, *Sci. Rep.*, **2017**, *7*, 42811.

[144] S. Bayindir and F. Lafzi, A simple oxindole-based colorimetric HSO_4^- sensor: Naked-eye detection and spectroscopic analysis, *J. Photochem. Photobiol. A*, **2019**, *376*, 146-154.

[145] S. Paul, R. S. Fernandes and N. Dey, Ppb-level, dual channel sensing of cyanide and bisulfate ions in an aqueous medium: computational rationalization of the ion-dependent ICT mechanism, *New J. Chem.*, **2022**, *46*, 18973-18983.

[146] T. Chatterjee, A. Srinivasan, M. Ravikanth and T. K. Chandrashekar, Smaragdyrins and sapphyrins analogues, *Chem. Rev.*, **2017**, *117*, 3329-3376.

[147] Y. Ding, Y. Tang, W. Zhu and Y. Xie, Fluorescent and colorimetric ion probes based on conjugated oligopyrroles, *Chem. Soc. Rev.*, **2015**, *44*, 1101-1112.

[148] Y. Ding, W.-H. Zhu and Y. Xie, Development of ion chemosensors based on porphyrin analogues, *Chem. Rev.*, **2017**, *117*, 2203-2256.

[149] J. K.-H. Wong, M. H. Todd and P. J. Rutledge, Recent advances in macrocyclic fluorescent probes for ion sensing, *Molecules*, **2017**, *22*, 200.

[150] Y. Qin, X. Liu, P.-P. Jia, L. Xu and H.-B. Yang, BODIPY-based macrocycles, *Chem. Soc. Rev.*, **2020**, *49*, 5678-5703.

[151] S. J. Barrow, S. Kasera, M. J. Rowland, J. del Barrio and O. A. Scherman, Cucurbituril-based molecular recognition, *Chem. Rev.*, **2015**, *115*, 12320-12406.

[152] C. Jiang, Z. Song, L. Yu, S. Ye and H. He, Fluorescent probes based on macrocyclic hosts: Construction, mechanism and analytical applications, *TrAC, Trends Anal. Chem.*, **2020**, *133*, 116086.

[153] H. M. Taya and P. Beer, Optical sensing of anions by macrocyclic and interlocked hosts, *Org. Biomol. Chem.*, **2021**, *19*, 4652-4677.

[154] D. Xia, P. Wang, X. Ji, N. M. Khashab, J. L. Sessler and F. Huang, Functional supramolecular polymeric networks: The marriage of covalent polymers and macrocycle-based host-guest interactions, *Chem. Rev.*, **2020**, *120*, 6070-6123.

[155] K. Kato, S. Fa, S. Ohtani, T.-Hao Shi, A. M. Brouwer and T. Ogoshi, Noncovalently bound and mechanically interlocked systems using pillar[n]arenes, *Chem. Soc. Rev.*, **2022**, *51*, 3648-3687.

[156] B. Wang, Z.-A. Nan, Q. Li, J. Liu, Z.-X. Lu, W. Wang, Z. Zhuo, G.-L. Li, and Y.-G. Huang, Trapping an ester hydrate intermediate in a -stacked macrocycle with multiple hydrogen bonds, *Molecules*, **2023**, *28*, 5705; https://doi.org/10.3390/molecules28155705.

[157] W.-L. Guan, J.-F. Chen, J. Liu, B. Shi, H. Yao, Y.-M. Zhang, T.-B. Wei, and Q. Lin, Macrocycles-assembled AIE supramolecular polymer networks, *Coord. Chem. Rev.*, **2024**, *507*, 215717. https://doi.org/10.1016/j.ccr.2024.215717.

[158] R. Shen, X. Pan, H. Wang, L. Yao, J. Wu and N. Tang, Selective colorimetric and fluorescent detection of HSO_4^- with sodium(I), magnesium(II) and aluminium(III) xanthone-crown ether complexes, *Dalton Trans.*, **2008**, 3574-3581.

[159] A. Tripathi and P. S. Pandey, Hydrogen sulfate-induced organogelation of a bile acid based anion-receptor, *Tet. Lett.*, **2011**, *52*, 3558-3560.

[160] S.-T. Yang, D.-J. Liao, S.-J. Chen, C.-H. Hu and A.-T. Wu, A fluorescence enhancement-based sensor for hydrogen sulfate ion, *Analyst*, **2012**, *137*, 1553-1555.

[161] X.-M. Liu, Y.-P. Li, W.-C. Song, Q. Zhao and X.-H. Bu, A new ion pair receptor fulfilling a dual function as a chromogenic molecular switch for F^- and ratiometric selective recognition of HSO_4^- , *Talanta*, **2012**, *97*, 111-117.

[162] N. R. Song, J. H. Moon, J. Choi, E. J. Jun, Y. Kim, S.-J. Kim, J. Y. Lee and J. Yoon, Cyclic benzobisimidazolium derivative for the selective fluorescent recognition of HSO_4^- via a

combination of C-H hydrogen bonds and charge interactions, *Chem. Sci.*, **2013**, *4*, 1765-1771.

[163] T. Chatterjee, A. Ghosh, S. Madhu and M. Ravikanth, Stable core-modified calixsmaragdyrins: Synthesis, structure and specific sensing of the hydrogen sulfate ion, *Dalton Trans.*, **2014**, *43*, 6050-6058.

[164] S. Erdemir, B. Tabakci and M. Tabakci, A highly selective fluorescent sensor based on calix[4]arene appended benzothiazole units for Cu^{2+}, S^{2-} and HSO_4^- ions in aqueous solution, *Sens. Actuators, B*, **2016**, *228*, 109-116.

[165] E. M. Fatila, E. B. Twum, J. A. Karty and A. H. Flood, Ion-pairing and co-facial stacking drive high-fidelity bisulfate assembly with cyanostar macrocyclic hosts, *Chem. -Eur. J.*, **2017**, *23*, 10652-10662.

[166] J.-H. Shin, J.-H. Hong, M.-S. Ko and D.-G. Cho, Fluorescent and cooperative ion pair receptor based on tolan for Na^+ (or Li^+) and HSO_4^-: Logic AND gate, *Chem. Commun.*, **2017**, *53*, 11414-11417.

[167] M.-S. Ko, A. S. Aslam and D.-G. Cho, Cooperative ion pair receptor based on tolan as a Li^+/HSO_4^- selective extractor and fluorescent indicator, *Tet. Lett.*, **2018**, *59*, 4475-4478.

[168] Q. Liu, H. Wu, Z. Zhao and D. Wei, Macrometallocycle binuclear NHC silver(I) complex with bridging azobenzene: Synthesis, structure and recognition for hydrogen sulfate, *Tetrahedron*, **2019**, *75*, 3128-3134.

[169] M. Sethupathi, G. Muthusankar, V. Thamilarasan, N. Sengottuvelan, G. Gopu, N. M. Vinita, P. Kumar and F. Perdih, Macrocyclic “tet a” derived colorimetric sensor for the detection of mercury cations and hydrogen sulfate anions and its bio-imaging in living cells, *J. Photochem. Photobiol. B*, **2020**, *203*, 111739.

[170] J. Cho, R. Parida, C. Lim, J. Y. Lee, J. S. Kim and S. Kim, A pyrene-calix[4]triazolium conjugate for fluorescence recognition of hydrogen sulfate, *Org. Chem. Front.*, **2024**, *11*, 4258-4263, https://doi.org/10.1039/D4QO00704B.

[171] A. I. Reza, K. Iwai and N. Nishiwaki, Recent advances in synthesis of multiply arylated/alkylated pyridines, *Chem. Rec.*, **2022**, *22*, e202200099.

[172] D. M. Peloquin and T. A. Schmedake, Recent advances in hexacoordinate silicon with pyridine-containing ligands: Chemistry and emerging applications, *Coord. Chem. Rev.*, **2016**, *323*, 107-119.

[173] D. Devadiga and T. N. Ahipa, Recent synthetic advances in pyridine-based thermotropic mesogens, *RSC Adv.*, **2019**, *9*, 23161-23228.

[174] S. De, A. Kumar S K, S. K. Shah, S. Kazi, N. Sarkar, S. Banerjee and S. Dey, Pyridine: the scaffolds with significant clinical diversity, *RSC Adv.*, **2022**, *12*, 15385-15406.

[175] M. Sheokand, Y. Rout and R. Misra, Recent development of pyridine based charge transporting materials for organic light-emitting diodes and perovskite solar cells, *J. Mater. Chem. C*, **2022**, *10*, 6992-7017.

[176] M. Rezaeivala and H. Keypour, Schiff base and non-Schiff base macrocyclic ligands and complexes incorporating the pyridine moiety-The first 50 years, *Coord. Chem. Rev.*, **2014**, *280*, 203-253.

[177] R. D. Hancock, The pyridyl group in ligand design for selective metal ion complexation and sensing, *Chem. Soc. Rev.*, **2013**, *42*, 1500-1524.

[178] W. Xue, L. Li, Q. Li and A. Wu, Novel furo[2,3-d] pyrimidine derivative as fluorescent chemosensor for HSO_4^-, *Talanta*, **2012**, *88*, 734-738.

[179] U. Fegade, S. K. Sahoo, A. Singh, P. Mahulikar, S. Attarde, N. Singh and A. Kuwar, A selective and discriminating noncyclic receptor for HSO_4^- ion recognition, *RSC Adv.*, **2014**, *4*, 15288-15292.

[180] S. Chopra, J. Singh, N. Singh and N. Kaur, Fluorescent organic nanoparticles of tripodal receptor as sensors for HSO_4^- in aqueous medium: Application to real sample analysis, *Anal. Methods*, **2014**, *6*, 9030-9036.

[181] Q. Wan, J.-B. Zhuo, X.-X. Wang, C.-X. Lin and Y.-F. Yuan, A simple and highly selective 2,2-diferrocenylpropane-based multi-channel ion pair receptor for Pb^{2+} and HSO_4^-, *Dalton Trans.*, **2015**, *44*, 5790-5796.

[182] K. Tayade, B. Bondhopadhyay, K. Keshav, S. K. Sahoo, A. Basu, J. Singh, N. Singh, D. T. Nehete and A. Kuwar, A novel zinc(II) and hydrogen sulphate selective fluorescent “turn-on” chemosensor based on isonicotiamide: INHIBIT type's logic gate and application in cancer cell imaging, *Analyst*, **2016**, *141*, 1814-1821.

[183] J. A. O. Granados, J. G. Hernandez, C. A. Huerta-Aguilar and P. Thangarasu, Exploration of ruthenium complex of (E)-2-((pyridine-2-yl)methyleneamino) benzoic acid as chemosensor for simultaneous recognition of acetate and HSO_4^- ions in cell bio-imaging: Experimental and theoretical studies, *Sens. Actuators, B*, **2018**, *270*, 570-581.

[184] R. S. Fernandes and N. Dey, A combinatorial effect of TICT and AIE on bisulfate detection using a pyrenylated charge-transfer Luminogen, *Mater. Res. Bull.*, **2023**, *163*, 112192.

[185] R. S. Fernandes, S. Paul and N. Dey, Sequence-specific relay recognition of multiple anions: An interplay between proton donors and acceptors, *ChemPhysChem*, **2023**, *24*, e202300434. https://doi.org/10.1002/cphc.202300434.

[186] R. S. Fernandes, S. Paul, J. Tydlitat, F. Bures and N. Dey, Triphenylamine based push-pull dyes for chromogenic detection of HSO_4^- ion in water: Role of anion in the formation of fluorescent organic nanoparticles, *J. Org. Chem.*, **2024**, *89*, 17926-17933. https://doi.org/10.1021/acs.joc.4c01124.

[187] V. Alagarsamy, K. Chitra, G. Saravanan, V. R. Solomon, M. T. Sulthana and B. Narendhar, An overview of quinazolines: Pharmacological significance and recent developments, *Eur. J. Med. Chem.*, **2018**, *151*, 628-685.

[188] S. N. M. Boddapati, H. B. Bollikolla, K. G. Bhavani, H. S. Saini, N. Ramesh and S. B. Jonnalagadda, Advances in synthesis and biological activities of quinazoline scaffold analogues: A review, *Arabian J. Chem.*, **2023**, *16*, 105190.

[189] J. Chen, Y. Wang, X. Luo and Y. Chen, Recent research progress and outlook in agricultural chemical discovery based on quinazoline scaffold, *Pestic. Biochem. Physiol.*, **2022**, *184*, 105122.

[190] M. Alfonso, A. Espinosa, A. Tarraga and P. Molina, Multichannel HSO_4^- recognition promoted by a bound cation within a ferrocene-based ion pair receptor, *Chem. Commun.*, **2012**, *48*, 6848-6850.

[191] P. Kaur, H. Kaur and K. Singh, A *‘turn-off’* emission based chemosensor for HSO_4^- formation of a hydrogen-bonded complex, *Analyst*, **2013**, *138*, 425-428.

[192] M. Mukherjee, B. Sen, S. Pal, S. Banerjee, S. Lohar, E. Zangrando and P. Chattopadhyay, A bio-attuned ratiometric hydrogen sulfate ion selective receptor in aqueous solvent: structural proof of the H-bonded adduct, *RSC Adv.*, **2015**, *5*, 4468-4474.

[193] H. Jia, S. Pu, C. Fan, G. Liu and C. Zheng, A highly selective ratiometric fluorescent Cu^{2+} and HSO_4^- probe based on a new photochromic diarylethene with a 6-aryl[1,2-c]quinazoline unit, *Dyes Pigm.*, **2015**, *121*, 211-220.

[194] S. Sahu, Y. Sikdar, R. Bag, D. K. Maiti, J. P. Ceron-Carrasco and S. Goswami, A novel quinoxaline-rhodamine conjugate for a simple and efficient detection of hydrogen sulphate ion, *Compounds*, **2021**, *1*, 29-40.

[195] P. P. Mohanta, A. P. Devi, B. P. Bag, H. N. Pati and A. K. Behera, A new class of fluorogenic

thiazolo[2,3-b] quinazolinone receptor: selective detection towards mercury and hydrogen bisulfate ions in aqueous medium, *RSC Adv.*, **2021**, *11*, 33288-33293.

[196] N. Bar and P. Chowdhury, A Brief Review on Advances in Rhodamine B Based Chromic Materials and Their Prospects, *ACS Appl. Electron. Mater.*, **2022**, *4*, 3749-3771.

[197] P. Ghosh, Review on metal ion recognition by bis-rhodamine probes with a future in artificial intelligence and machine learning, *J. Mol. Struct.*, **2024**, *1304*, 137597.

[198] M. Rajasekar, P. Baskaran, J. Mary, S. Meenambigai and M. Selvam, Review of current developments in rhodamine derivatives-based photoresponsive chemosensors for ion detection, *Inorg. Chem. Commun.*, **2024**, *162*, 112143.

[199] P. Yang, A. L. Tang, S. Tan, G. -Y. Wang, H. -Y. Huang, W. Niu, S. -T. Liu, M. -H. Ge, L. -L. Yang, F. Gao, X. Zhou, L. -W. Liu and S. Yang, Recent progress and outlooks in rhodamine-based fluorescent probes for detection and imaging of reactive oxygen, nitrogen, and sulfur species, *Talanta*, **2024**, *274*, 126004.

[200] R. Kaur, J. Singh, A. Saini, N. Singh and N. Kaur, Fluorometric appraisal of HSO_4^- in aqueous media and daily utilities using organic-inorganic nanohybrids, *RSC Adv.*, **2014**, *4*, 48004-48011.

[201] J. Rull-Barrull, M. d'Halluin, E. L. Grognec, F. -X. Felpin, Chemically-modified cellulose paper as smart sensor device for colorimetric and optical detection of hydrogen sulfate in water, *Chem. Commun.*, **2016**, *52*, 2525-2528.

[202] Y. Upadhyay, S. Bothra, R. Kumar, H. -J. Choi and S. K Sahoo, Optical sensing of hydrogen sulphate using rhodamine 6G hydrazide from aqueous medium, *Spectrochim. Acta, Part A*, **2017**, *180*, 44-50.

[203] J. Wang, Q. Meng, Y. Yang, S. Zhong, R. Zhang, Y. Fang, Y. Gao and X. Cui, Schiff Base Aggregation-Induced Emission Luminogens for Sensing Applications: A Review, *ACS Sens.*, **2022**, *7*, 2521–2536.

[204] M. K. Goshisht, G. K. Patra and N. Tripathi, Fluorescent Schiff base sensors as a versatile tool for metal ion detection: strategies, mechanistic insights, and applications, *Mater. Adv.*, **2022**, *3*, 2612-2669.

[205] A. Afrin and P. Chinna Ayya Swamy, Novel Schiff base derivatives for the detection of one-to-multi metal ions and tracking the live cell imaging, *Coord. Chem. Rev.*, **2023**, *494*, 215327.

[206] P. Li, Y.-M. Zhang, Q. Lin, J.-Q. Li and T.-B. Wei, A novel colorimetric HSO_4^- sensor in aqueous media, *Spectrochim. Acta, Part A*, **2012**, *90*, 152-157.

[207] A. Kumar, V. Kumar and K. K. Upadhyay, An Al^{3+} and $H_2PO_4^-$/HSO_4^- selective conformational arrest and bail to a pyrimidine-naphthalene anchored molecular switch, *Analyst*, **2013**, *138*, 1891-1897.

[208] C.-Y. Lin, K.-F. Huang and Y.-P. Yen, A new selective colorimetric and fluorescent chemodosimeter for HSO_4^- based on hydrolysis of Schiff base, *Spectrochim. Acta, Part A*, **2013**, *115*, 552-558.

[209] S. Goswami, S. Das, K. Aich, D. Sarkar and T. K. Mondal, Colorimetric as well as dual switching fluorescence 'turn on' chemosensors for exclusive recognition of Zn^{2+} and HSO_4^- in aqueous solution: Experimental and theoretical studies, *Tet. Lett.*, **2013**, *54*, 6892-6896.

[210] L. Wang, L. Yang, L. Huang and D. Cao, Diketopyrrolopyrrole-derived Schiff base as colorimetric and fluoromertic probe for sequential detection of $HSO_4^-$and Fe^{3+} with "off-on-off" response, *Sens. Actuators, B*, **2015**, *209*, 536-544.

[211] L. Wang, L. Yang and D. Cao, Detection of HSO_4^- ion based on the hydrolysis of diketopyrrolopyrrole-derived Schiff base with chromogenic and fluorogenic dual signals, *J. Fluoresc.*, **2014**, *24*, 1347-1355.

[212] U. Fegade, J. Bhosale, H. Sharma, N. Singh, R. Bendre and A. Kuwar, Fluorescence chemosensor for HSO_4^- ion based on pyrrole-substituted salicylimine Zn^{2+} complex: Nanomolar detection, *J Fluoresc.*, **2015**, *25*, 819-824. https://doi.org/10.1007/s10895-015-1599-9.

[213] Z. Luo, K. Yin, Z. Yu, M. Chen, Y. Li and J. Ren, A fluorescence turn-on chemosensor for hydrogen sulfate anion based on quinoline and naphthalimide, *Spectrochim. Acta, Part A*, **2016**, *169*, 38-44.

[214] R. Goel, S. Sharma, K. Paul and V. Luxami, Naphthalimide based chromofluorescent sensor and DNA intercalator: Triggered by Hg^{2+}/HSO_4^- cleavage reaction, *Sens. Actuators, B*, **2017**, *246*, 776-782.

[215] Z. M. Dong, J. N. Wang, W. Wang, J. B. Chao and Y. Wang, Selective optical detection of HSO_4^- via hydrolysis of a simple Schiff Base, *Res. Chem. Intermed.*, **2018**, *44*, 4001-4013.

[216] M. Orojloo and S. Amani, colorimetric detection of pollutant trivalent cations and HSO_4^- in aqueous media using a new Schiff-base probe: An experimental and DFT studies, *Polycyclic Aromat. Compd.*, **2021**, *41*, 33-46.

[217] S. Roy, P. Paul, M. Karar, M. Joshi, S. Paul, A. R. Choudhury and B. Biswas, Cascade detection of fluoride and bisulphate ions by newly developed hydrazine functionalised Schiff bases, *J. Mol. Liq.*, **2021**, *326*, 115293.

[218] Y. Liu, X. Wang, E. Feng, C. Fan and S. Pu, A highly selective sequential recognition probe for Zn^{2+} and HSO_4^-/$H_2PO_4^-$ based on a diarylethene chemosensor, *Spectrochim. Acta, Part A*, **2021**, *246*, 119052.

[219] Y.-D. Peng, Y.-F. Ding, Y.-R. Zheng, Z.-L. Chai, Y.-X. Wei, L. Wang, H.-T. Zhang and W.-K. Dong, Spectroscopic and theoretical studies on a rare and rigid bis(salamo)-like fluorescent probe for the sequential recognition of Cu^{2+} and HSO_4^- ions, *Inorg. Chem. Commun.*, **2023**, *158*, 111598.